

EPIDEMIOLOGICAL SURVEILLANCE OF FELINE MORBILLIVIRUS INFECTION IN THE  
ASPECTS OF POLYMERASE CHAIN REACTION, INDIRECT ELISA AND  
IMMUNOHISTOCHEMISTRY



A Dissertation Submitted in Partial Fulfillment of the Requirements  
for the Degree of Doctor of Philosophy in Veterinary Pathobiology

Department of Veterinary Pathology

FACULTY OF VETERINARY SCIENCE

Chulalongkorn University

Academic Year 2019

Copyright of Chulalongkorn University

การสำรวจทางระบาดวิทยาของการติดเชื้อออร์บิทัลไวรัสในแมว โดยการศึกษาทางปฏิกิริยาลูกโซ่โพลี  
เมอเรส อินไดเร็กอีไลซ่า และเทคนิคทางอิมมูโนฮิสโตเคมี



วิทยานิพนธ์นี้เป็นส่วนหนึ่งของการศึกษาตามหลักสูตรปริญญาวิทยาศาสตรดุษฎีบัณฑิต  
สาขาวิชาพยาธิชีววิทยาทางสัตวแพทย์ ภาควิชาพยาธิวิทยา  
คณะสัตวแพทยศาสตร์ จุฬาลงกรณ์มหาวิทยาลัย  
ปีการศึกษา 2562  
ลิขสิทธิ์ของจุฬาลงกรณ์มหาวิทยาลัย



สุรางคนางค์ ไชยศักดิ์ : การสำรวจทางระบาดวิทยาของการติดเชื้อมอร์บิลลิไวรัสในแมว โดยการศึกษาทางปฏิกิริยา  
ลูกโซ่โพลีเมอเรส อินไดเร็กต์ไอโซซา และเทคนิคทางอิมมูโนฮิสโตเคมี. ( EPIDEMIOLOGICAL SURVEILLANCE OF  
FELINE MORBILLIVIRUS INFECTION IN THE ASPECTS OF POLYMERASE CHAIN REACTION, INDIRECT  
ELISA AND IMMUNOHISTOCHEMISTRY) อ.ที่ปรึกษาหลัก : รศ. ส.พญ.ดร.สมพร เตชะงามสุวรรณ, อ.ที่ปรึกษาร่วม  
: รศ. น.สพ.ดร.อนุเทพ รังสีพิพัฒน์

เชื้อมอร์บิลลิไวรัสในแมวเป็นเชื้อใหม่ที่ถูกค้นพบในแมว โดยอาจมีความเกี่ยวข้องกับโรคไตในแมวเมื่อปี ค.ศ. 2012 ที่ฮ่องกง เชื้อ  
มอร์บิลลิไวรัสในแมวถูกค้นพบในหลายประเทศทั่วโลกโดยยังไม่สามารถหาข้อสรุปทางพยาธิกำเนิดของโรคติดเชื้อนี้ในแมวได้ การศึกษาในครั้งนี้มี  
วัตถุประสงค์เพื่อเพิ่มองค์ความรู้ของเชื้อมอร์บิลลิไวรัส โดยการตรวจหาลักษณะทางพันธุกรรมของตัวเชื้อ การตรวจหาแอนติบอดีด้วยวิธีเซรัม  
วิทยา และการศึกษาพยาธิวิทยาในแมวไทยที่ติดเชื้อมอร์บิลลิไวรัสในแมว นอกจากนี้ยังพัฒนาวิธีไอโซซาและแอนติบอดีต่อโปรตีนเมทริกซ์  
สำหรับการตรวจหาแอนติบอดีด้วยวิธีเซรัมวิทยาและการระบุตำแหน่งที่อยู่ของเชื้อในเนื้อเยื่อแมวที่ติดเชื้อด้วยวิธีอิมมูโนฮิสโตเคมีตามลำดับ ผล  
การศึกษาพบว่าประเทศไทยมีความชุกของเชื้อมอร์บิลลิไวรัสในแมวชนิดอารีเอ็นเอเท่ากับร้อยละ 11.9 และมีความชุกของภูมิคุ้มกันต่อโปรตีนเม  
ทริกซ์ของเชื้อมอร์บิลลิไวรัสในซีรัมแมวเท่ากับร้อยละ 66.9 ในแมวที่มาจากสถานที่พักพิงสัตว์และแมวที่เลี้ยงในบ้าน โดยเชื้อที่พบในไทยเป็นจี  
โนไทป์ 1A โดยไม่พบการเกิดไวรัสลูกผสมของเชื้อมอร์บิลลิไวรัสในแมวในไทย ทั้งนี้การตรวจหาเชื้อมักตรวจพบได้ในปัสสาวะมากกว่าการตรวจ  
พบในเลือด แต่อย่างไรก็ตาม ยังไม่ทราบความสัมพันธ์อย่างชัดเจนของการตรวจพบเชื้อมอร์บิลลิไวรัสกับค่าเคมีหรือลักษณะทางกายภาพของ  
ปัสสาวะในแมว สำหรับการระบุตำแหน่งเป้าหมายของเชื้อมอร์บิลลิไวรัสและการแพร่กระจายของเชื้อในแมวที่เสียชีวิตโดยธรรมชาติจำนวน 2 ตัว  
โดยพบว่ามีประวัติอาการที่ชัดเจนคือกระเพาะปัสสาวะอักเสบเฉียบพลันและมีเลือดออก จึงได้ทำการตรวจทางจุลพยาธิวิทยา อิมมูโนฮิสโตเคมี  
และการใช้กล้องจุลทรรศน์อิเล็กตรอนแบบส่องผ่านในการศึกษาร่วมกัน จากกระบวนการทางจุลพยาธิวิทยาพบอินคลูชันบอดี ดิสดีนดงในไซโต  
พลาสซึมของเซลล์เยื่อหุ้มไตโดยเฉพาะในส่วนเชื่อมต่อของเนื้อเยื่อชั้นนอกและชั้นในของไต และกรวยไต จึงทำการตรวจหาเชื้อไวรัสด้วยการใช้  
กล้องจุลทรรศน์อิเล็กตรอนแบบส่องผ่าน พบการรวมกลุ่มของชิ้นส่วนของสายพันธุกรรมไวรัสที่เรียกว่านิวคลีโอแคปซิด ลักษณะแบบพื้นปลา  
รวมอยู่กับอนุภาคไวรัสในไซโตพลาสซึมของเซลล์ ซึ่งเป็นตำแหน่งเดียวกับบริเวณที่ย้อมติดสีด้วยวิธีอิมมูโนฮิสโตเคมี นอกจากนี้ยังพบการย้อม  
ติดสีในเซลล์และอวัยวะต่างๆ ได้แก่ เซลล์เยื่อหุ้มไต เซลล์เยื่อในหลอดลม เซลล์เยื่อในหลอดลมฝอย ลิมโฟไซต์และฮิสติโอไซต์ในม้ามและ  
เนื้อเยื่อต่อมน้ำเหลืองมีเซนเทอร์รี และเซลล์เกลียในชั้นสีขาวของสมอง ซึ่งเป็นการบ่งชี้ถึงการติดเชื้อทั้งระบบร่างกาย ที่สำคัญ เราเสนอว่าเซลล์  
เยื่อหุ้มไตคือเป้าหมายของเชื้อมอร์บิลลิไวรัสในแมวเช่นเดียวกับเชื้อมอร์บิลลิไวรัสชนิดอื่นๆ โดยพบการมีอยู่ของอินคลูชันบอดีโดยปราศจากการ  
เปลี่ยนแปลงทางพยาธิสภาพของเนื้อเยื่อไต มากไปกว่านั้นเรายังพบว่าเลือดวีสิตา 2 ตัว สามารถติดเชื้อมอร์บิลลิไวรัสในแมว จีโนไทป์ 1A ได้  
โดยมีความสัมพันธ์กับการเกิดโรคไตวายเรื้อรัง โดยสรุป เราจึงชี้ให้เห็นว่าสัตว์ตระกูลแมวทั้งแมวบ้านและไม่ใช่แมวบ้านสามารถติดและรับเชื้อ  
นี้ได้ อย่างไรก็ตามการหาความสัมพันธ์ของเชื้อมอร์บิลลิไวรัสในแมวและโรคไตตลอดจนพยาธิกำเนิดของโรคยังคงมีความจำเป็นอย่างมากใน  
อนาคต

จุฬาลงกรณ์มหาวิทยาลัย  
CHULALONGKORN UNIVERSITY

สาขาวิชา พยาธิชีววิทยาทางสัตวแพทย์

ปีการศึกษา 2562

ลายมือชื่อนิสิต .....

ลายมือชื่อ อ.ที่ปรึกษาหลัก .....

ลายมือชื่อ อ.ที่ปรึกษาร่วม .....

# # 5875513131 : MAJOR VETERINARY PATHOBIOLOGY

KEYWORD: Feline morbillivirus RT-PCR Matrix protein ELISA Immunohistochemistry

Surangkanang Chaiyasak : EPIDEMIOLOGICAL SURVEILLANCE OF FELINE MORBILLIVIRUS INFECTION IN THE ASPECTS OF POLYMERASE CHAIN REACTION, INDIRECT ELISA AND IMMUNOHISTOCHEMISTRY. Advisor: Assoc. Prof. SOMPORN TECHANGAMSUWAN, DVM, MSc, PhD, DTBVP Co-advisor: Assoc. Prof. ANUDEP RUNGSIPIPAT, DVM, PhD, DTVBP

Feline morbillivirus (FeMV), a relatively new virus, has been discovered in domestic cats and associated with kidney diseases since 2012 in Hong Kong. The FeMV study gained widely attentions in many countries whereas the pathogenesis remains elusive. These studies aimed to provide the FeMV knowledge in Thai domestic cat by performing the genetic-based, serological-based and pathological-based studies of FeMV-infected in Thai cats. Additionally, the indirect enzyme linked immunosorbent assay (ELISA) and rabbit polyclonal antibody against FeMV matrix (FeMV-M) protein was produced for seroprevalence and viral localization by immunohistochemistry (IHC) techniques, respectively. Our results revealed the FeMV RNA prevalence at 11.9% and seroprevalence at 66.9% in cats derived from shelters and households. The FeMV Thai strains were clustered in FeMV-1A genotype without evidence of viral recombination. Urine sample provided more FeMV positivity rate when compared with blood sample, however the significant correlation between FeMV positive urine and urine characteristics was not observed. To study the localization and distribution of FeMV in two moribund FeMV-positive-PCR cats with history of acute hematuria and, grossly, acute hemorrhagic cystitis, histopathology, IHC, and transmission electron microscopy (TEM) were performed. Microscopically, the prominent lesions revealed scattering intracytoplasmic eosinophilic inclusion bodies (ICIB) in renal epithelial cells locating at corticomedullary junction and renal pelvis. By TEM, the ultrastructural morphology demonstrated the aggregation of electron-dense ribonucleocapsid herringbone-like structure in the cytoplasm of renal tubular epithelial cells, where the inclusion materials were found. Moreover, the immunoreactive signals were also visualized in the ICIB of renal epithelial cells, cytoplasm of tracheal, bronchial, and bronchiolar epitheliums, circulating lymphocytes and infiltrating histiocytes in spleen and mesenteric lymph node, and neuroglial cells in the white matter of brain, suggesting systemic viral infection. Importantly, we proposed that FeMV is a renal epitheliotropic virus, similarly to other morbilliviruses, by existing viral inclusions without integral pathological changes of kidney disease. Furthermore, we have reported the two black leopards (*Panthera pardus*) which were positive to FeMV-1A genotype and associated with chronic kidney disease. In conclusion, we suggested that domestic and non-domestic felids are susceptible to FeMV infection. However, the association between FeMV and kidney diseases throughout its pathogenesis is needed further investigations.

Field of Study: Veterinary Pathobiology

Academic Year: 2019

Student's Signature .....

Advisor's Signature .....

Co-advisor's Signature .....

## ACKNOWLEDGEMENTS

I am overwhelmed in all humbleness and gratefulness to acknowledge my depth to my principal advisor Assoc. Prof. Dr. Somporn Techangamsuwan, who gave me the golden opportunity to do this wonderful project and my co-advisor Assoc. prof. Dr. Anudep Rungsipipat for valuable guidance, support and encouragement to help me achieve my educational goal. I would like to express my appreciation to committee members, Assoc. Prof. Dr. Morakot Kaewthamasorn, Assoc. Prof. Dr. Theerayuth Kaewamatawong, Assoc. Prof. Dr. Rosama Pusoonthornthum, Dr. Navapon Techakriengkrai and Asst. Prof. Dr. Tassanee Jaroensong, who provided valuable advices in this research project.

This project could not be completed without excellent assistance from Dr. Jadsada Ratthanophart, National Institute of Animal Health (NIAH), Department of Livestock Development, Thailand for assistance in Pab-His-rFeMV-M and PAb-FeMV-M construction and serology guidance. I also thankful to Ms. Prukswan Chetanachan, a senior medical scientist, National Institute of Health (NIH), Department of Medical Sciences, Ministry of Public Health and Mr. Poowadon Chai-in, National Nanotechnology Center (NANOTEC) for performing TEM procedure. With necessarily, I also appreciate to thank Dr. Chutchai Piewbang, Senior Postdoctoral fellowship, Department of Pathology, Faculty of Veterinary science, Chulalongkorn University, who have been accompany contributed in this studies especially the topic of FeMV in black leopard. However, from those I was indebted, I could not regard all things they have advocated me to complete in doing a lot of research and I came to know about so many new things I am really thankful to them.

I also deeply extend my thanks to the animal shelters (CHSATHai stray animal shelter) and Small Animal Teaching Hospital, Faculty of Veterinary Science, Chulalongkorn University for providing samples and Dr. Nawin Manachai for statistical analysis.

I would also like to thank my parents and beloved friends who helped me a lot in finalizing this project within the limited time frame.

Last but not least, I would like to thank Chulalongkorn University for financial support through The 100th year Anniversary of Chulalongkorn University Fund for Doctoral Scholarship, The 90th Anniversary of Chulalongkorn University Fund (Ratchadaphiseksomphot Endowment Fund) and oversea presentation scholarship during my PhD course.

Surangkanang Chaiyasak

## TABLE OF CONTENTS

	<b>Page</b>
ABSTRACT (THAI).....	iii
ABSTRACT (ENGLISH).....	iv
ACKNOWLEDGEMENTS.....	v
TABLE OF CONTENTS.....	vi
LIST OF TABLES.....	xi
LIST OF FIGURES.....	xii
ABBREVIATIONS.....	1
CHAPTER I INTRODUCTION.....	2
Outline of the thesis.....	2
Importance and rationale.....	4
Literature review.....	7
Objectives of the study.....	24
Hypothesis.....	24
Conceptual framework.....	25
Advantages of the study.....	25
CHAPTER II Molecular Epidemiology and Genome Analysis of Feline Morbillivirus in Household and Shelter Cats in Thailand.....	27
Abstract.....	28
Background.....	29
Results.....	31
Detection of FeMV in the urine and blood of Thai cats.....	31

Association between the FeMV infection status, urine characteristics, urologic diseases and feline retrovirus detection .....	34
Phylogenetic analysis and genome organization of the full-length FeMV-Thai strains .....	34
Unique deduced amino acid residues of the F and H genes among the FeMV genotype and clade.....	36
Recombination and selective pressure analysis.....	37
Discussion .....	38
Conclusions.....	42
Methods.....	42
Animals and sample collection.....	42
Urinalysis and feline retrovirus infection screening .....	43
Two-stage real-time reverse transcription polymerase chain reaction (RT-qPCR) .....	43
Amplification and sequencing of the complete F and H genes, and full-length genome of Thai FeMV .....	44
Genetic characterization and phylogenetic analysis of the FeMV Thai strains..	44
Recombination and selective pressure analyses .....	45
Statistical analysis.....	46
CHAPTER III Detection of Antibody against Feline Morbillivirus by using Recombinant Matrix Enzyme-Linked Immunosorbant assay .....	48
Abstract.....	49
Introduction.....	50
Materials and methods.....	51
Sample collection .....	51



Expression, purification and identification of the recombinant FeMV-M protein .....	51
Western blot analysis for the serum samples .....	52
Indirect ELISA assay .....	53
Realtime reverse transcription PCR (RT-qPCR) of the L gene of FeMV.....	54
Statistical analysis.....	55
Results.....	55
Expression and identification of His-rFeMV-M protein and serum immunoblotting.....	55
Development of the His-rFeMV-M i-ELISA .....	56
Detection of FeMV in the blood samples .....	57
Discussion .....	57
CHAPTER IV Localization and Viral Distribution of Feline Morbillivirus-1 in Non-Kidney Diseased Cats.....	61
Abstract.....	63
Introduction.....	65
Materials and Methods.....	67
Animals and clinical history.....	67
Molecular detection of FeMV in urine and fresh tissue samples.....	67
Phylogenetic analysis of FeMV-F and H genes .....	68
Immunohistochemistry (IHC) for FeMV localization .....	69
Results.....	69
Pathological findings of necropsied cats .....	69
Ultrastructural finding of FeMV particles .....	73

Molecular detection, sequencing, and phylogenetic analysis of FeMV-1A genotype .....	73
Cellular tropism and tissue localization of FeMV .....	75
Discussion .....	75
CHAPTER V Feline morbillivirus infection associated with tubulointerstitial nephritis in black leopards ( <i>Panthera pardus</i> ) .....	79
Abstract .....	81
Materials and Methods .....	84
Cases and samples .....	84
Virologic investigation .....	84
Molecular analysis of the FeMV L gene .....	85
Antibody production and analysis of FeMV-M protein .....	87
Construction of the recombinant (r)FEMV-M encoding plasmid .....	87
Expression and enrichment of His-rFeMV-M .....	88
Western blot analysis .....	88
Production of polyclonal antibody against the His-rFeMV-M protein .....	89
In-situ FeMV antigen detection by IHC and IF .....	89
Retrospective study of FeMV in other wild felids .....	91
Results .....	91
Pathological changes .....	91
Virology investigation and identification of FeMV .....	92
Molecular analysis of the FeMV L gene .....	94
Tissue localization of FeMV .....	94
Retrospective study of FeMV in other wild felids .....	95

Discussion .....	97
CHAPTER VI DISCUSSION AND CONCLUSION .....	101
General discussion .....	101
Genetic-based surveillance of FeMV infection in Thai domestic cats .....	101
FeMV antibody against matrix protein in Thai domestic cat .....	103
Localization of FeMV antigen in cats with active FeMV infection .....	105
Molecular and pathological aspect in non-domestic cat.....	107
Limitation of the study .....	109
Suggestion of the study .....	110
Conclusions .....	110
APPENDIX.....	111
REFERENCES .....	140
VITA.....	152

## LIST OF TABLES

	Page
Table I-1 Comparison of pathological findings in hosts resulted from related morbillivirus infection .....	15
Table I-2 Total length of gene products of morbilliviruses (modified from Woo et al., 2012).....	16
Table I-3 Vector type.....	19
Table I-4 Example of frequently used restriction enzyme in rDNA technology .....	20
Table I-5 Recombinant DNA/Protein using in veterinary diagnosis (Balamurugan et al., 2010).....	23
Table II-1 Positivity rate of FeMV detection by RT-PCR.....	31
Table II-2 Biological data of cats with FeMV-positive results.....	32
Table II-3 Differences in start codon peptides and deduced amino acid residues of the FeMV F gene.....	39
Table II-4 Differences in the deduced amino acid residues of the FeMV H gene .....	39
Table III-1 Comparison of i-ELISA and western blot analysis .....	58
Table III-2 Comparison of real-time RT-PCR (RT-qPCR) and western blot analysis .....	59
Table III-3 Statistical analysis between shelter and household cats.....	59

## LIST OF FIGURES

	Page
Figure I-1 Morbillivirus phylogeny based on P gene analysis (Barrett et al., 1993) .....	8
Figure I-2 Morphology of morbillivirus (Tatsuo et al., 2001).....	9
Figure I-3 Comparison of morbillivirus genome (Woo et al., 2012) .....	12
Figure I-4 Schematic of recombinant DNA or protein construction.....	18
Figure I-5 The concept of cloning the recombinant DNA.....	22
Figure II-1 Phylogenetic analysis of the full-length genome sequence of FeMV strains.....	36
Figure III-1 (1A) Purified protein elutions (E1-E3).....	56
Figure III-2 Receiver operating characteristic (ROC) curve analysis.....	58
Figure IV-1 Feline morbillivirus infection, cat. Urinary bladder, case no. 1 and 2. Severe distension of urinary bladder with red urine, and hemorrhage at mucosal and serosal surface.....	71
Figure IV-2 Lung, case no.1. Pulmonary edema with tracheal froth.....	71
Figure IV-3 Brain, case no. 2. Congestion.....	71
Figure IV-4 Kidney, case no. 2. Moderate congestion at corticomedullary junction...	71
Figure IV-5 Feline morbillivirus infection, cat. Kidney, case no. 2 (HE).....	72
Figure IV-6 Feline morbillivirus infection, cat. Kidney, case no. 2 (IHC). .....	72
Figure IV-7 Feline morbillivirus infection, cat. Kidney, case no. 2 (TEM).....	72
Figure IV-8 Feline morbillivirus infection, cat. Kidney, case no. 2 (TEM).....	72
Figure IV-9 Feline morbillivirus infection, cat. Urinary bladder, case no. 2 (IHC). .....	74
Figure IV-10 Respiratory airway, case no.1 (IHC).....	74
Figure IV-11 Central nervous system, case no.1 (IHC).....	74

Figure IV-12 Lymph node, case no.1 (IHC).....	74
Figure IV-13 Phylograms of FeMV-F and H genes.....	77
Figure V-1 Feline morbillivirus infection, kidney, black leopard, case 2.....	93
Figure V-2 Locally diffuse lymphoplasmacytic tubulointerstitial nephritis (HE).....	93
Figure V-3 Moderate renal tubular necrosis (HE).....	93
Figure V-4 Feline morbillivirus infection, spleen, black leopard, case 2 (HE).....	93
Figure V-5 Phylogeny of feline morbillivirus genome sequences compared with reference FeMV viruses in the NCBI database.....	95
Figure V-6 Feline morbillivirus infection, kidney, black leopard. Case 1 (IHC).....	96
Figure V-7 Kidney. black leopard. Case 2 (IHC).....	96
Figure V-8 Kidney. Black leopard. Case 1 (IF).....	97
Figure V-9 Spleen, black leopard, case 2 (IF).....	97

## ABBREVIATIONS



BIC:	Bayesian information criterion
cDNA:	complementary DNA
DAB:	3,3'-diaminobenzidine
dN/dS:	ratio value between nonsynonymous and synonymous
F:	Fusion
FeL:	Fixed-effects likelihood
FeLV:	Feline leukemia virus
FeMV:	Feline morbillivirus
FFPE:	Formalin-fixed paraffin-embedded
FIV:	Feline immunodeficiency virus
FUBAR:	Fast, Unconstrained Bayesian AppRoximation
GTR:	General-time reversible model
H:	Hemagglutinin
IF:	Immunofluorescence analyses
IHC:	Immunohistochemistry
IP TG:	Isopropyl- $\beta$ -D-thiogalactopyranoside
L:	RNA polymerase
M:	Matrix
MEME:	Mixed Effect Model Evolution
N:	Nucleocapsid
NPV:	Negative predictive value
P/V/C:	Phosphoprotein
PPV:	Positive predictive value
PVDF:	Polyvinylidene-fluoride membrane
QCES:	The QIAxcel capillary electrophoresis
RT-qPCR:	Real-time reverse transcription polymerase chain reaction
SDS-PAGE:	Sodium dodecyl sulfate–polyacrylamide gel electrophoresis
TEM:	Transmission electron microscope
TIN:	Tubulointerstitial nephritis
TMB:	3,3,5,5-tetramethylbenzidine substrate
UTD:	Urinary tract disease
UTIs:	Urinary tract infections
<b>K</b> coefficient:	The Kappa, quantify interrater agreement

## CHAPTER I INTRODUCTION

### Outline of the thesis

The thesis was divided into six chapters. The first chapter is an overview of the thesis which provide general introduction, rationale, objectives of the studies, review literatures and advantages of the studies. All studies in the thesis were provided in chapter two to chapter five. Firstly, before reaching along these studies. I am appreciated to tell in brief. Various animal species of carnivores, herbivores and aquatic mammals are susceptible to genus Morbillivirus (Rima and Duprex, 2006). Morbilliviruses are the virus members that severely affected the health impacts in whom has infected. Along to canine distemper virus (CDV) that infected mainly in order Canivora (Appel and Summers, 1995), Feline morbillivirus (FeMV) has just discovered for almost a decade ago, infection in domestic felid in the world associating with tubulointerstitial nephritis (Woo et al., 2012). Since Asia was the first continent comprehensively studying FeMV associating with kidney disease (Woo et al., 2012; Furuya et al., 2014), then other countries around the world have attended to imply the pathogenesis of this novel virus (Choi et al., 2020; Crisi et al., 2020) which is the sixth member of animal morbilliviruses (Takeda et al., 2020).

As first sight in Thailand, we have attended to approach and investigate FeMV in both antigen and antibody detection assays. First study of antigen detection. Molecular study using specific primers for FeMV detection were performed, FeMV Thai strains were detected in 2016 and revealed high genetic homology accounting in genotype 1 which is the most genotype founding around the world. In our study, urine source was the mainly sample detectable higher than blood sample. Nevertheless, various urine characterizations were play the insignificant role associated with urine sample that positive to FeMV (Chaiyasak et al., 2020). FeMV Thai strains were so far detectable and



found actively of infection stage of this virus. Interestingly that viral inclusions were found globular eosinophilic hyaline material in proximal renal epithelium without pathological changes especially at renal corticomedullary junction in two cats which were initially suffering with severe hemorrhagic cystitis and severe cardiomyopathy. This study primarily concluded that renal epithelial cell is at least the cell tropism of FeMV. We have attended that FeMV genotype 1 can be concealed in non-kidney disease cat like in previous research (Choi et al., 2020). Moreover, for the investigation of virus localization, other epithelial cells such as in trachea and lung parenchyma were positive immunostaining to in-house polyclonal antibody anti-FeMV matrix protein (Pab-FeMV\_M). Reticuloendothelial cells such as lymphocyte and macrophage in lymphoid tissues and glial cells in central nervous system were also infected with FeMV genotype 1 clarified by immunohistochemistry assay (Chaiyasak et al., 2020). To raise the serological study of FeMV, we attempted to use in-house recombinant matrix protein as an antigen in indirect-ELISA (i-ELISA). After optimizing the diagnosis protocol, sensitivity and specificity were 90.1% and 75.6%, respectively with acceptable 95% confidence interval (Chaiyasak et al., 2020). Our in-house antibody detection assay was reliable when compare to other protein such as nucleocapsid (N) and phosphoprotein (P) in previous study. Beyond of domestic cat, large cats from a zoo in Thailand was consistently reported existing of FeMV genotype 1 in melanistic leopard (*Panthera pardus*). Their renal epithelium was positively stained of in-house Pab-FeMV\_M (Piewbang et al., 2020a)

These are inestimable insight of FeMV studies in Thailand we have performed. We raised the knowledges of both molecular, pathology and epidemiology implications in domestic and zoo felids. The comprehensive studies mention above were disclosed and described following in each topic in this thesis. Eventually, these studies are restricted some questions such the consistent pathogenesis of FeMV, but

we are hopefully these studies will be high virtue and handy research of coming further FeMV study.

### **Importance and rationale**

The most of a decade ago, the new viral member of Morbillivirus was discovered in stray and household cats. This suspicious virus was named as feline morbillivirus (FeMV) according to the International Committee on Taxonomy of Viruses (ICTV, <https://talk.ictvonline.org>) and still questioned in pathogenesis. Morbillivirus is a member of order Mononegavirales, family Paramyxoviridae and subfamily Paramyxovirinae which accompanied with other genera such are Respirivirus, Rubulavirus, Henipavirus, Avulavirus, Aquaparamyxovirus and Ferlavirus. Recently, Morbillivirus consists of seven species that cause serious host-associated diseases; both in human and animals including Measles virus (MV) in human, Rinderpest virus (RPV) in cattle, Peste des Petits ruminant virus (PPRV) in sheep and goat, canine distemper virus (CDV) in carnivores, phocine distemper virus (PDV) in seals, cetacean morbillivirus (CeMV) in porpoise and dolphins, and feline morbillivirus (FeMV) in cats (Deem et al., 2000; Woo et al., 2012).

The morbillivirus virion possesses a spherical structure about 100-300 nm; its genome contains approximately 15-16 kb in length and is surrounded by a lipid envelope. Morbillivirus has unsegmented single-strand RNA encoding six structural proteins. Two glycoproteins span the membrane and form oligomeric spikes which are visible by electron microscopy; the hemagglutinin (H) protein binds with the cellular receptors, and the fusion (F) protein mediates the entry of virus into permissive cells by fusion of the virion and host plasma membrane. The matrix (M) protein, a hydrophobic viral protein, coats the inside membrane of the virion. It is a multifunctional protein playing a role in virus budding and transcription regulation. Three remaining structural proteins are associated with the genomic RNA and form a helical ribonucleoprotein (RNP) complex; the nucleocapsid (N) protein is the major

component of the RNP, the phospho- (P) and the large (L) proteins function as both transcriptase and replicase (Lamb, 2001; Tatsuo et al., 2001; Lempp et al., 2014).

FeMV was firstly detected in Hong Kong significantly associated with tubulointerstitial nephritis (TIN) (Woo et al., 2012) and its pathogenesis is remained unclear since their recorded (Sakaguchi et al., 2014; Sharp et al., 2016; Darold et al., 2017; Yilmaz et al., 2017; McCallum et al., 2018; Donato et al., 2019; Sieg et al., 2019; Sutummaporn et al., 2019) FeMV incidence was between 0.2-40% from various types of sample including urine, blood, rectal swab,. FeMV can be detected in both antigen-based assays such as RT-PCR, Real-time RT-PCR, Immunohistochemistry (IHC), Immunofluorescence assay (IFA) and antibody-based assays such as indirect ELISA by using Polyclonal anti P and N protein (Park et al., 2016; Arikawa et al., 2017; De Luca et al., 2018; Sutummaporn et al., 2019; De Luca et al., 2020). Recently, FeMV is and fresh and formalin-fixed paraffin-embedded (FFPE) kidney tissue (Woo et al., 2012; Furuya et al., 2014; Sutummaporn et al., 2019) genetically divided into two genotypes including FeMV genotype 1 (FeMV-1) and genotype 2 (FeMV-2) (Sieg et al., 2019). Both genotypes successfully isolated in cell cultured by using urine sample. FeMV-1 was properly isolated in cell lines such as CRFK (feline kidney cell) which were found cell rounding, cell detachment and cell lysis, VERO E6 (African green monkey kidney cell) which was only detected apple green of nucleocapsid protein by Immunofluorescence assay without the trail of cytopathic effect (Woo et al., 2012). FeMV could be finally found the smaller syncytial cell in CRFK cell when compared to CPE in VERO cell which propagating CDV (Sakaguchi et al., 2014). FeMV-2 was able to infect in primary cells of pulmonary epithelial cell, renal epithelial cell, cells of cerebrum and cerebellum and immune cells including CD4+ T cell and CD20+ B cell (Sieg et al., 2019). For viral localization, the nucleocapsid of FeMV is obviously located in renal tubular interstitial cell (FeMV-1,2; (Sharp et al., 2016; Sieg et al., 2019; Sutummaporn et al., 2019; De Luca et al., 2020), macrophage in liver and spleen (FeMV-1; (Woo et al., 2012; Yilmaz et al.,

2017), alveolar macrophage (FeMV-2, (Sieg et al., 2019), urothelial cell (FeMV-2, (Sieg et al., 2019), neuronal cells in brain (FeMV-2, (Sieg et al., 2019) and immune cell such as CD4+ T cell, CD8+ T cell and CD20+ B cells (FeMV-2, (Sieg et al., 2019) For serological test, ELISA based P protein was developed to detect the FeMV antibody in cat serum in Japan with 85% sensitivity and 94% specificity (Arikawa et al., 2017). From these data, we just know some of viral biology such as genetic characterization and cell tropism, but pathogenesis is not well clarified. Thus, the long-term study of clinical and necropsy cases will raise the clinicopathology-fundamental knowledge.

Due to chronic kidney disease (CKD) in cats is frequently the problematic health issue in senior cats and several risk factors had been addressed such as toxic agent, food or water feeding, hypoxia, chronic glomerulonephritis, chronic pyelonephritis, glomerulonephritis, TIN, urinary stone and viral infection (Greene et al., 2014). Thai cats were affected and died with CKD at least 0.6% in cat cases in small animal hospital (Pusoonthornthum et al., 2010). However, FeMV can detect in urine from both non-clinical and CKD cats and found in both stray and household cats. The role of FeMV to those cats remains obscure, this prompts us to further investigate the epidemiology and pathology of FeMV infection in Thai cat population. According the objectives of this study are including 1.) to performed genetic based surveillance of FeMV infection in both shelter and household cats and to characterize FeMV Thai strains compared with the previous known sequences deposited in database, 2.) to develop indirect ELISA assay using the recombinant matrix protein of FeMV (rFeMV-M) as the coating antigen in antiserum from both shelter and household cats and 3.) to localize FeMV antigen in necropsy case of the infected cat by using IHC and trans-electron microscopy (TEM) to literally visualize the virus particle. In addition of molecular study, we developed the rFeMV-M which have protein identity up to 60% with other morbilliviruses especially CDV to enhance the ability of detection in both serological

and viral localizing assays. We hopefully that the multiple aspects of molecular biology in this study will lead us to comprehensively realize in FeMV.

## Literature review

### Morbillivirus

#### Morbillivirus characterization

Morbillivirus is an enveloped negative-sense single strand RNA virus and belongs to subfamily Paramyxovirinae, family Paramyxoviridae, and order Mononegavirales. Currently, morbillivirus consists of seven species that cause serious host-associated diseases; both in human and animals including measles virus (MV) in human (Furuse and Oshitani, 2017), rinderpest virus (RPV) in cattle (Baazizi et al., 2017), peste des petits ruminant virus (PPRV) in small ruminant (Shaila et al., 1996), canine distemper virus (CDV) in carnivores (Lempp et al., 2014; Techangamsuwan et al., 2015), phocine distemper virus (PDV) in seals (Ludes-Wehrmeister et al., 2016), cetacean morbillivirus (CeMV) in whales, porpoise and dolphins (Barrett et al., 1993; Yang et al., 2016), and feline morbillivirus (FeMV) in cats that has been reported in Hong Kong in 2012 (Woo et al., 2012) (Figure I-1).

The morbillivirus virion possesses a spherical structure about 100-300 nm; it contains approximately 15-16 kb genome surrounded by a lipid envelope. This virus has unsegmented single-strand RNA encoding structural proteins; the hemagglutinin (H), the fusion (F), the nucleocapsid (N), the phospho- (P), the large polymerase (L) and the matrix (M) protein, and two other non-structural proteins termed C and V protein (Lamb, 2001). The lipid envelope integrated with H and F surface glycoproteins facilitate the viral attachment and membrane fusion. Surrounded by the envelope, helical nucleocapsid core including P, L and N protein are essential for initial viral replication in host cells. The M protein which connected between the envelope

glycoproteins and nucleocapsid core is important during the viral maturation and assembly (Figure I-2) (Beineke et al., 2009).

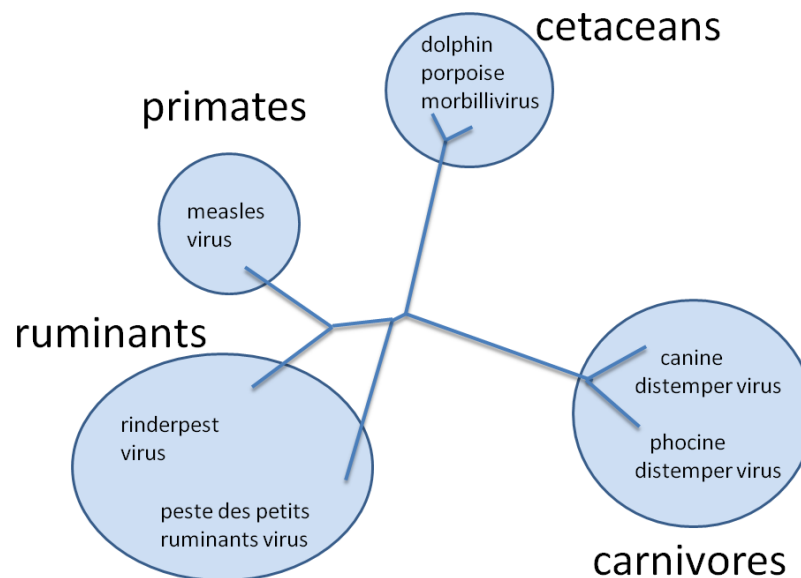


**Figure I-1** Morbillivirus phylogeny based on P gene analysis (Barrett et al., 1993)

The H protein-encoding gene displays the highest genetic variation comparing to other structural proteins, while the F protein-encoding sequence shows variation to a lesser extent (Beineke et al., 2009). However, these two envelope glycoproteins evidently play important roles in host immunity. Both H and F glycoproteins function concomitantly to mediate membrane fusion leading to the entry and the exit of viral particles from the susceptible host cells. The H glycoprotein, a type II integral membrane protein binding to the specific cellular receptor, mediates viral attachment to host cell membrane in the first step of infection. Not only a morbillivirus tropism, but also cytopathogenicity and fusion efficiency in susceptible cell line are contributed by H protein. The F glycoprotein, a type I integral membrane protein, is necessary for fusogenicity between extracellular viral particle and host membrane (von Messling et al., 2001).

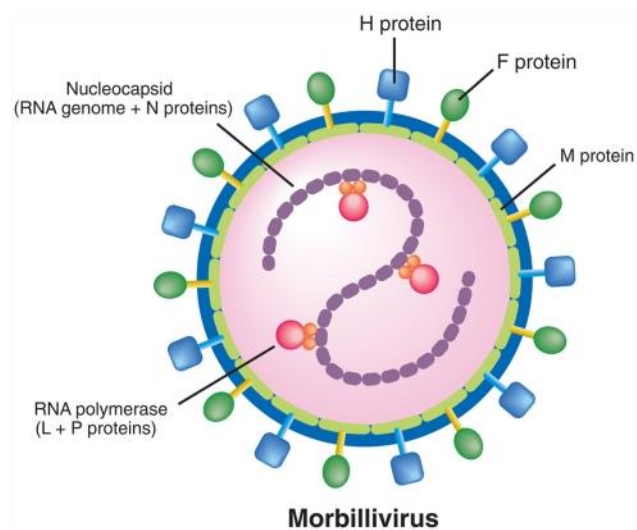


Figure I-2 Morphology of morbillivirus (Tatsuo et al., 2001)

### Pathogenesis and host receptors of genus Morbilliviruses

After virus enters the host cell, the incubation period takes 1 to 4 weeks depending on individual host's immunity. Primary virus replication takes place in lymphoid tissues of respiratory tract. Early clinical signs might be observed such as anorexia, weight loss and oculonasal discharge. During the first viremia phase, the progeny of virus presents in macrophages and monocytes leading to viral dissemination to the distant hematopoietic tissues via hematogenous and lymphatic routes. Viral multiplications in various lymphoid tissues including thymus, spleen, gut-associated lymphoid tissue (GALT) and hepatic Kupffer cells lead to lymphopenia and further severe immunosuppression (Schobesberger et al., 2005; Vandeveldde and Zurbriggen, 2005). Several days later, the second viremic phase occurs associated with the spreading of virus via lymphocytes, platelets as well as free-viral particles. Finally, the virus disseminates to various epithelial cells of organs and the central nervous system (CNS).

Morbillivirus infection typically induces symptoms associated with immunosuppressive condition due to its lymphotropic property that resulted to lymphopenia, lymphoid depletion of lymphoid tissues and increased susceptibility to

opportunistic infection. The principal host's cellular receptor for morbillivirus is signaling lymphocyte activation molecule (SLAM; also called CD150), a membrane glycoprotein molecule. SLAM is expressed on immune cells including immature thymocytes, activated lymphocytes, macrophages and dendritic cells which regularly produce interleukin-4 (IL-4) and IL-13 by CD4+ T cells as well as produce IL-12, tumor necrotic factor alpha (TNF $\alpha$ ) and nitric oxide (NO) by macrophages (Yanagi et al., 2006). Recently, amino acid sequences of SLAM have been compared in various carnivores to explore the variation and expand the host range of CDV infection (Ohishi et al., 2014). Thirty-four amino acid residues are found for the candidates binding to CDV on the interface of the carnivore SLAMs. SLAM of the domestic dog (*Canis lupus familiaris*) are similar to those of other members of the suborder Caniformia, indicating that the animals in this group have probably similar sensitivity to dog's CDV. However, dog SLAM contains 9 amino acid positions differently from those of felid counterpart. Among these 9 residues, four of domestic cat (*Felis catus*) SLAM (at 72, 76, 82, and 129) and three of lion (*Panthera leopardsica*) SLAM (at 72, 82, and 129) are associated with charge alterations, suggesting that the felid interfaces possess relatively lower affinities to dog CDV. Only the residue 76 is different between domestic cat and lion SLAM interfaces. The domestic cat SLAM has threonine at 76, whereas the lion SLAM has arginine, a positively charged residue like that of the dog SLAM. The cat SLAM with threonine is likely to have lower affinity to CDV-H and to confer higher resistance against dog CDV. Thus, the 4 residues (72, 76, 82, and 129) on carnivore SLAMs are important for the determination of affinity and sensitivity with CDV. Nonetheless, this study is applicable to animals that have no information about morbillivirus infection. In addition, there is no study regarding reaction between cat SLAM and FeMV infection in cats so far.

Moreover, morbillivirus could infect epithelial cells including pneumocytes, vascular endothelial cells, gastrointestinal mucosa, and transitional cells of urinary



bladder as well as neuronal cells; all of which are SLAM-negative, indicating other cellular receptors might be involved. Nectin-4 is a cell adhesion molecule (CAM), a member of nectin family consisting of 4 members (nectin-1, -2, -3 and -4). Nectin-1 and -2 are originally identified as poliovirus receptor-related protein (PRRs; PRR-1 and PRR-2 respectively). Nectin-4 is discovered to play role in morbillivirus pathogenesis and involved in neurovirulence (Pratakpiriya et al., 2012; Delpeut et al., 2014; Pratakpiriya et al., 2017). CD9, a tetraspan transmembrane-protein is found associated with cell-to-cell fusion, but not virus-to-cell fusion. This membrane protein takes part in the regulation of H protein binding to the unknown cellular receptor. So CD9 is mentioned as a cofactor for CDV induced syncytial cell formation by controlling the access of the fusion machinery to cell contact areas (Singethan et al., 2006; Singethan et al., 2008).

#### **Pathological morphology of morbillivirus infection**

Pathological findings of morbillivirus infection occur both in nervous and non-nervous tissues. CDV, particularly, frequently associates with characteristic eosinophilic intracytoplasmic and intranuclear inclusion bodies. Respiratory lesions include serous to mucopurulent rhinitis, interstitial pneumonia, necrotizing bronchiolitis which is often complicated by secondary bacterial pneumonia in infected animals. Gastrointestinal manifestations result in gastroenteritis associated with the depletion of Peyer's patches. Generalized lymphocytic depletion of lymphoid organs is commonly found and is associated with an impairment of the immune response. Skin infection displays variable features, including pustular dermatitis of the thighs and ventral abdomen, and hyperkeratosis of the footpads and nasal planum. Furthermore, CDV-associated bone lesions have been shown in young dogs with systemic distemper infection. Metaphyseal osteosclerosis develops due to persistence of the primary spongiosa and atrophy as well as necrosis of osteoclasts and bone marrow cells (Beineke et al., 2009; Radtanakantikanon et al., 2013). The comparison between various morbillivirus infection induced pathological lesions is summarized in table I-1. However, there is no

information in this aspect in FeMV-induced pathological findings, except for the association with tubulointerstitial nephritis (TIN) in chronic kidney disease (CKD) cats (Woo et al., 2012).

### Genome characterization of feline morbillivirus (FeMV)

Woo et al. (2012) discovered the feline morbillivirus (FeMV) firstly which is classified in genus morbillivirus. The genome length of FeMV is 16,050 bp and consists of six genes which are N, P/V/C(P), P/V/C(V), P/V/C(C), M, F, H and L (Figure I-3). In comparison with other morbillivirus, FeMV contains a 55-nt the 3' leader and a 400-nt at 5' trailer sequence while the others have only a 40-nt or 41-nt at 5' trailer sequence; this results in the largest genome sequence of FeMV (Table I-2).

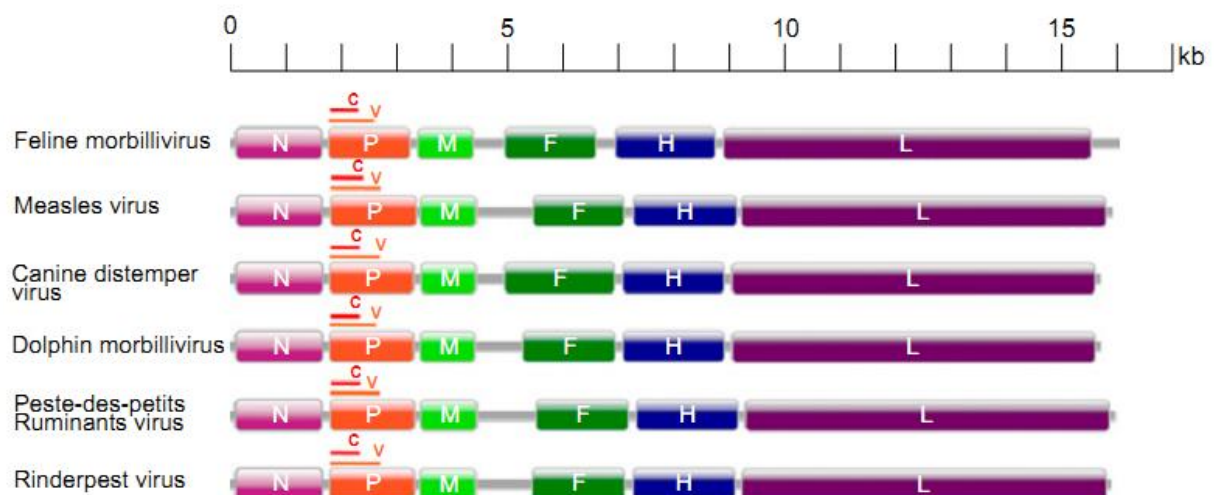


**Figure I-3** Comparison of morbillivirus genome (Woo et al., 2012)

Genome characteristic data of FeMVs have been sequenced and deposited in bio-database such the GenBank which are Chinese strain: 761U, 776U, M252A (JQ411014, JQ411015, JQ411016) isolated from feces and urine, respectively; Japanese strain: OtJP001, MiJP003 and ChJP073 (AB924120, AB924121, AB924122); USA strain:

US1 (KR014147) and Italian strain: Piuma/2015 (KT825132). The coding region of the first gene, nucleocapsid gene (N) of FeMV, starts with MSSLL residues while CDV, PDV and RPV start with MASLL residues; and MV, PPRV and DMV start with MATLL residues.

### **Diagnostic assay of morbilliviruses**

Virus isolation in appropriate tissue culture system serves as the standard diagnostic method; this method is highly accurate for virus detection even though it is laborious and time consuming. It is preferable for basic viral biology study in vitro, but not suitable for clinical diagnosis. Recently, FeMV characteristics were clarified by inoculation in various cell lines. The results showed that FeMV strain SS1 from Japan could reach a plateau phase of infection at day 5<sup>th</sup> and the end point at day 7<sup>th</sup> post inoculation. For the effect of temperature on FeMV, freeze-and-thaw did not affect virus titers and the virus could survive at 4 °C at least 12 days. FeMV caused the cytopathic effects (CPE) with syncytia formation as same as other paramyxoviruses did at 3–4 days post infection (d.p.i) (Koide et al., 2015).

Molecular platform such as reverse transcription-polymerase chain reaction (RT-PCR) technique has been used for detection of various infectious pathogens (Piewbang et al., 2017). This technique provides several advantages including the rapidity, relatively high sensitivity and specificity, and requirement of low amount of sample. For FeMV detection, it is initially discovered by RT-PCR assay by applying blood and urine samples from stray cats in Hong Kong since 2012 (Woo et al., 2012). Afterwards, real-time RT-PCR is utilized for FeMV detection in formalin-fixed paraffin-embedded (FFPE) kidney tissues (Furuya et al., 2014). The down-stream application of PCR platform such as sequencing and phylogenetic tree analysis has been performed to verify the accuracy of synthesized PCR product and to clarify the relationship among morbilliviruses.

Currently, genetic-based detection of virus is widely done by molecular assays (PCR or RT-PCR); however, serological tests such as enzyme-linked immunosorbent assay (ELISA) or immunochromatography are easier to perform at veterinary hospital and do not require special equipment. Moreover, such tests are more suitable for epidemiological surveillance, because they can detect past virus infection. For FeMV antibodies detection, only anti-N and P proteins have been reported with similar positive percentage (21-28%) and studies are limited only in Japan and Hong Kong (Woo et al., 2012; Sakaguchi et al., 2014; Park et al., 2016; Arikawa et al., 2017). Future investigation comparing antibody responses between other proteins from FeMV genes will be useful to elucidate possible differences in their immune responses.

In Thailand, we performed a preliminary study of FeMV detection from sheltered cats located in Saraburi province in 2016 and found that FeMV was positive for 20% from blood and urine samples by RT-PCR assay (Chaiyasak and Techangamsuwan, 2017). This result indicated the existence of FeMV in Thai cat population.

Table I-1 Comparison of pathological findings in hosts resulted from related morbillivirus infection

Morbilliviruses <sup>a</sup>	MV	CDV	PPRV	CeMV
Host	Human	Dog and related carnivores	Small ruminant	Dolphin and porpoises
Central nervous system (brain)	- Acute demyelinating encephalomyelitis (ADEM) - Measles inclusion body encephalitis (MIBE) - Subacute sclerosingpanencephalitis (SSPE) Pneumonia	Demyelinating leukoencephalitis	-	Encephalitis with "Warthin-Finkeldey" type syncytia (hallmark of CeMV infection)
Respiratory tract	Pneumonia	Pneumonia	- Pneumonia - Severe broncho-interstitial pneumonia	- Pneumonia - Bronchopneumonia - Broncho-interstitial pneumonia
Lymphoid tissue	Lymphoid depletion	Lymphoid depletion	- Lymphoid depletion - Engorge spleen - Edematous lymph nodes	Lymphoid depletion
Gastrointestinal tract	Enteritis	Rare	Congestion and severe enteritis	-
Skin	Maculopapular rash	Hyperkeratosis of hard pad and planum	-	-
Blood profile	- Lymphopenia - Thrombocytopenia	- Lymphopenia	-	-

<sup>a</sup> measles virus (MV), canine distemper virus (CDV), peste des petits ruminant virus (PPRV), cetacean morbillivirus (CeMV)

Table I-2 Total length of gene products of morbilliviruses (modified from Woo et al., 2012)

Virus <sup>a</sup> Gene <sup>b</sup>	Total length (bp)						Amino acid Identity (%)
	FeMV	MV	CDV	DMV	PPRV	RPV	
Leader	55	55	55	55	55	55	-
N	1,659	1,689	1,683	1,683	1,683	1,683	54.3-56.8
PV/C(P)	1,637	1,655	1,655	1,655	1,655	1,655	25.6-31.7
PV/C(V)	1,638	1,656	1,656	1,656	1,656	1,656	20.7-25.7
PV/C(C)	1,637	1,655	1,655	1,655	1,655	1,655	18.3-25.4
M	1,378	1,466	1,447	1,453	1,483	1,460	57.6-60.0
F	2,191	2,373	2,206	2,212	2,411	2,367	35.8-45.1
H	1,934	1,958	1,946	1,946	1,957	1,958	20.4-28.1
L	6,781	6,643	6,642	6,643	6,643	6,643	55.2-57.3
Trailer	400	40	41	40	40	40	-

<sup>a</sup>feline morbillivirus (FeMV), measles virus (MV), canine distemper virus (CDV), dolphin morbillivirus (DMV), peste des petits ruminant virus (PPRV), rinderpest virus (RPV)

<sup>b</sup>nucleocapsid (N), phospho- (P), matrix (M), fusion (F), hemagglutinin (H), large (L) gene

## Recombinant DNA (rDNA) and applications

### Recombinant DNA/Protein technology

The rDNA means a re-combination of interested gene with the different host living cell that known as cloning. DNA cloning is a method for identifying and purifying a particular DNA fragment of interest from a complex mixture of DNA fragments and subsequent producing a large amount of the gene fragment (clone). The rDNA has developed since 1972 in Stanford University and they deserved the patent of their technology about the development of recombining the gene from different host (Overton, 2014). From the efficient technology, the year of 1982, worldwide has approved of pharmaceutical use of human insulin recombinant gene which produced by bacterial expression system, E.coli, to produce the effective clone instead of using pork insulin that has previously used (Gualandi-Signorini and Giorgi, 2001). Nowadays, the rDNA technology is widely applied in both research and medicine.

In the past, virulent diseases had to be controlled or eradicated by using efficient diagnostic and systematic management of epidemiology. The infectious disease especially the virus can be diagnosed from two fundamental techniques: antigenic- and antibody-based methods. Most antigenic-based diagnosis earns high accuracy as well as high investment of diagnostic instruments. The antibody-based technique gains the evidence of infection history. The rDNA technology is presently widely used for antibody-based diagnosis because of its safe, non-handling directly with virulent pathogen, high efficiency, inexpensive tools, non-expertise requirement. Moreover, the rDNA-based technique can prevent the false positive result due to the selectively preserved gene of interest without biological interferences from host protein (Balamurugan et al., 2010).

The construction of rDNA composes of 5 important parts: gene fragment or whole gene of interest, restriction endonuclease, expression vector, expression system and cloning technique (Figure I-4).

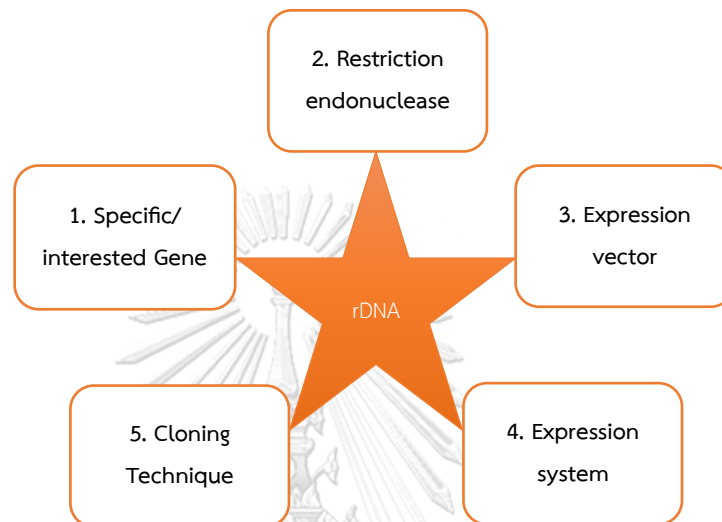


*Figure I-4 Schematic of recombinant DNA or protein construction*

Expression system

Bacterial system

Among several developing expression systems, the bacterial system is globally used because of its easy manipulation. The *E. coli* usually take part of cloning the gene due to rapid replication and efficient production of the recombinant gene with the usual media within a brief time. However, there are some disadvantages of this system such as the limited size of cloned gene, toxic protein or endotoxin production, insoluble inclusion bodies, and unsuitable system for non-phosphorylation gene.



Besides, there are mammalian system, transgenic plant system, yeast system, baculovirus expression system, insect cell system and silkworm larvae system. These expression systems are accepted for cloning the gene and show higher expression level than the bacterial system has limit. After selected the suitable expression system, the vector type will be subsequently considered for the proper gene expression.

### Vector

Vector that acts as a carrier vehicle of DNA, is composed of 5-type; Plasmid DNA, Bacteriophage DNA, Yeast DNA, Bacterial DNA and Viral DNA (Table I-3). Each vector has limited capacity for harvesting the interested DNA length. Usually, plasmid vector has many advantages such as its small size which could be handled easily, its circular DNA is more stable, large replication and easy to select the clone from the culture system. However, the limitation of plasmid is restricted by which the DNA insertion size should be less than 20-kb length for the efficient transformation step.

**Table I-3 Vector type**

Vector type	DNA base length for proper ligation (Kb)
Plasmid (Plasmid DNA)	20
Lambda Phage (Bacteriophage)	25
Cosmid (Plasmid with bacteriophage)	45
P1 Phage (Bacteriophage)	100
BAC (bacterial artificial chromosome)	300
YAC (yeast artificial chromosome)	1000
Lentivirus (Viral plasmid)	8
$\Psi$ -Retrovirus (Viral plasmid)	8

## Restriction endonuclease

The restriction endonuclease is used for digestion of the DNA product and expression vector before the recombining of different gene in ligation step with ligase activity. The final product of digestion has two forms such as sticky end and blunt end. Table I-4 shows the example of frequently used restriction enzymes in this step.

**Table I-4 Example of frequently used restriction enzyme in rDNA technology**

Enzyme*	Microbial	Digestion site	End of product
EcoRI	Escherichia coli	5'...GAATTC...3' 3'...CTTAAG...5'	Sticky end
BamHI	Bacillus amyloliquefaciens	5'...GGATCC...3' 3'...CCTAGG...5'	Sticky end
HindIII	Haemophilus influenza	5'...AAGCTT...3' 3'...TTCGAA...5'	Sticky end
SmaI	Serratiamarcesens	5'...CCCGGG...3' 3'...GGGCC...5'	blunt end

**\*Nomenclature:** EcoRI stands for E: genus (Eschericea), co: species (coli), R: strain, I: number of enzymes

### Construction of rDNA in bacterial system

The principles are the construction of rDNA by ligation into the competent cell or using the expression vector. Subsequently, the transformation of the transformants into the host living cells is done. After culturing in media, the host cells divide that resulting in the clone. Finally, the clone is selected for sequencing and/or is purified for further applications in any diagnostic assay.

Firstly, the construction of rDNA is started from amplification the PCR product of selected gene. Then the ligation step is done by cutting the selected gene using restriction endonuclease and ligating it into the plasmid vector. The pGEM®-T Easy vector system (Promega Corporation, USA), the commercial plasmid vector, facilitates the replication in a high copy number and greatly improves the efficiency of

ligation and transformation the target gene into competent cell (DH5a). Subsequently, culturing the plasmid vector in ampicillin-containing media allows the presence of blue/white colony as a screening selection. Then the colony is picked up, checking for DNA target replication by plasmid extraction and digestion with specific restriction enzyme in each selected colony. Briefly with blue/white system, when the ampicillin containing plate is prepared and cultured the competent cell, the Isopropyl  $\beta$ -D-1-thiogalactopyranoside (IPTG), playing role in trigger the transcription of the lac operon and X-gal(organic compound of galactose), are added to promote the screening system of blue white selection. At first, the DNA would insert in the lac operon region which produce the inactive beta galactosidase, then the lactose (X-gal) will be added. The successful ligation is indicated by the presence of white colonies, while the abortive ligation is illustrated by the presence of blue colony.

When the DNA yield is at the satisfactory quantity, subcloning into the expression vector and transformation into the host bacterial cell like BL21 competent cell (New England Biolab: NEB, USA) will be done to replicate the clone. For the transformation step, it composes of two methods. The first method is chemical transformation by using the optimal temperature; also called heat shock, to introduce the plasmid vector into the bacterial cell. The transformation will be performed at 42°C in water bath for 30-60 seconds. The time of incubation depends on the used competent cell. The second method is electroporation by using electric shock. Finally, the multiplication of plasmid vector will be done by incubation at 37 °C with shaking overnight. The selected colony will be shown on the plate containing kanamycin-rich media as a screening method.

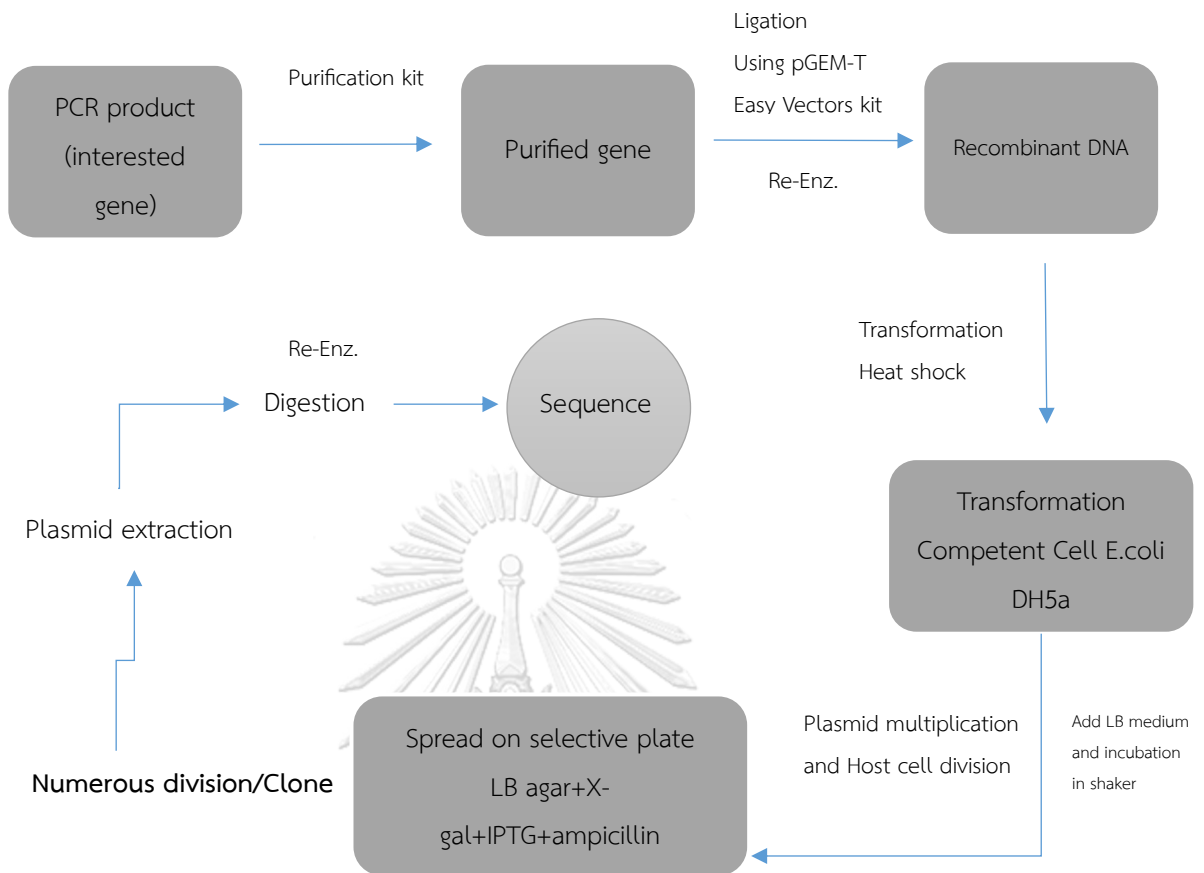


**Figure I-5** The concept of cloning the recombinant DNA

### Application of rDNA technique

The rDNA application in veterinary science is used widely in diagnostic viral disease, the vaccination technology that combining gene for decreasing allergy reaction and increasing immunization in animals. The enzyme-linked immunosorbent assay (ELISA) is the basic platform of using rDNA by inoculation the rDNA or protein into mice or rabbits to produce monoclonal antibody or polyclonal antibody. Table I-5 represents the example of using the recombinant DNA/protein in veterinary diagnosis (Balamurugan et al., 2010; Overton, 2014).

Table I-5 Recombinant DNA/Protein using in veterinary diagnosis (Balamurugan et al., 2010)

Viral diseases	Recombinant protein/expression system	Diagnostic assay
<b>Livestocks</b>	Glycoproteins-gp48, p80, gp62/E.coli,	I-ELISA
Foot and mouth disease virus	insect cells Glycoproteins-E0, E2 and NS-3/Insect cells E2 glycoprotein/Drosophila melanogaster	
Peste des petits ruminant virus	NP / E.coli HA protein/ Insect cells (glycosylate protein) M protein/ E.coli	Sandwich-ELISA, C-ELISA, B-ELISA, IFA
Equine encephalitis virus (Eastern/Western)	Glycoprotein E1 and E2 /E.coli, Recombinant Sindbis virus	I-ELISA, Epitope-blocking assay
<b>Poultry</b>		
Avian influenza virus	NP/E.coli, Insect cells HA protein/E.coli	I-ELISA, C-ELISA, B-ELISA, indirect sandwich-ELISA
<b>Companion pet</b>		
Canine distemper virus	NP/E.coli, Insect cells	Capture sandwich ELISA, IgG/IgM-Elisa, Dot blot assay
<b>Wildlife</b>		
Aleutian mink disease virus	Capsid proteins (VP1 and VP2)/ Vaccinia virus insect cell NSP-1 and NSP-2/ Vaccinia virus insect cell	ELISA

B-ELISA: Blocking ELISA, C-ELISA: Competitive ELISA, I-ELISA: Indirect ELISA

### Objectives of the study

1) To perform genetic-based surveillance of FeMV infection in Thai cats and characterize FeMV Thai strains compared with the previous known sequences deposited in database

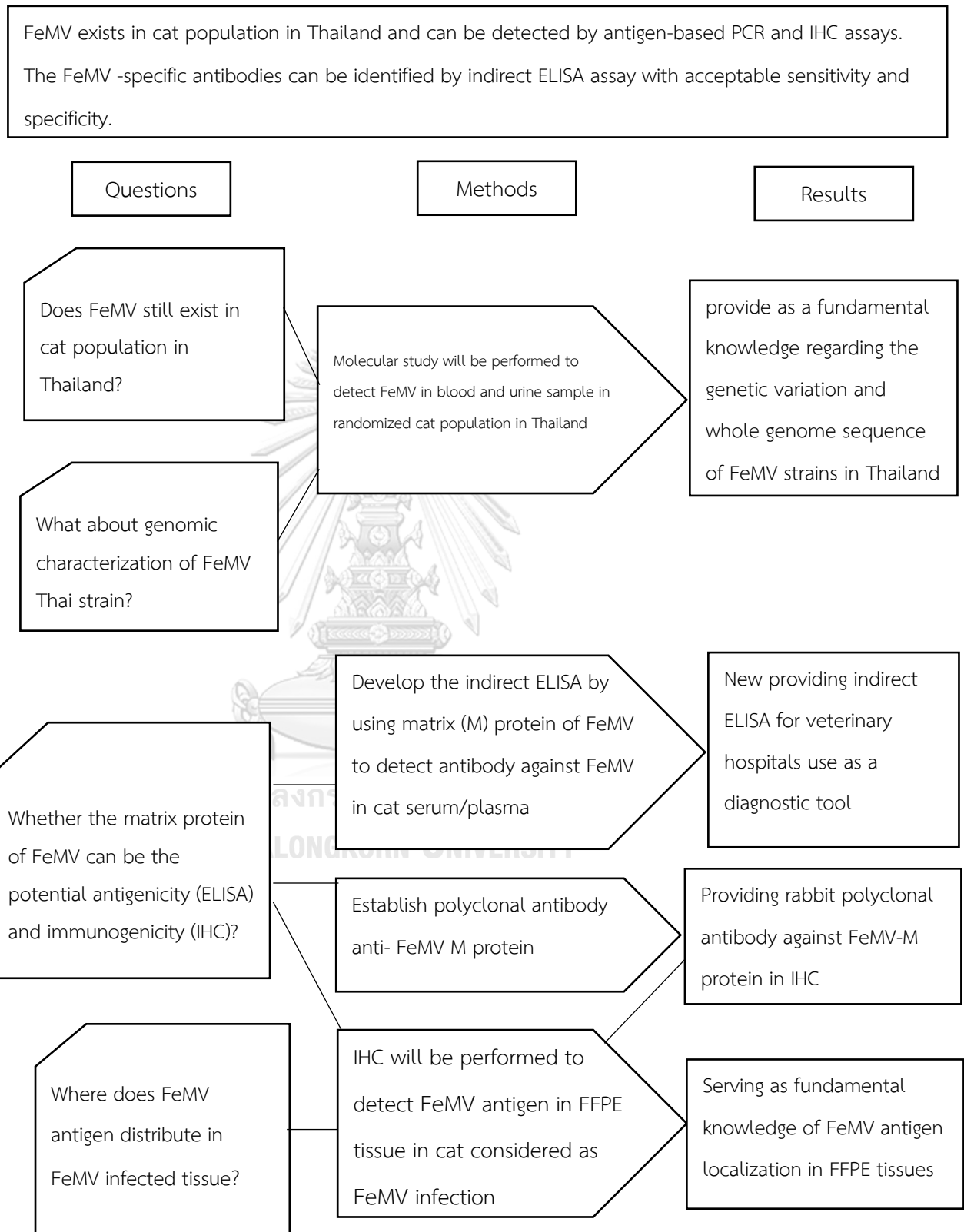
2) To develop an in-house indirect ELISA assay for anti-FeMV matrix (M) protein and investigate FeMV-specific antibody prevalence in large scale gaining the database of FeMV infection in Thai cat population

3) To define the distribution of FeMV antigen in various organs of suspected FeMV infected cats by immunohistochemistry

### Hypothesis

FeMV exists in cat population in Thailand and can be detected by antigen-based PCR and IHC assays. The FeMV-specific antibodies can be identified by indirect ELISA assay with acceptable sensitivity and specificity.

### Conceptual framework



### Advantages of the study

1. Establishment the diagnostic tools both pathogen detection using RT-PCR assay and antibody detection using indirect in-house ELISA.
2. Confirmation of natural FeMV infection and supporting epidemiological data of FeMV infection among Thai cats in large scale screening
3. Serving as a fundamental knowledge regarding the genetic variation and whole genome sequence of FeMV isolates in Thailand.
4. Providing indirect in-house ELISA for veterinary hospitals use as a diagnostic tool.
5. Providing in-house established rabbit anti-M polyclonal antibody for future research.
6. Preference new information of FeMV information and outbreak prevention as well as to provoke awareness of potential transmission of zoonosis of emerging paramyxoviruses to humans.



CHAPTER II  
Molecular Epidemiology and Genome Analysis of Feline Morbillivirus in  
Household and Shelter Cats in Thailand

**Authors**

Surangkanang Chaiyasak, Chutchai Piewbang and Somporn Techangamsuwan

Department of Pathology, Faculty of Veterinary Science, Chulalongkorn University,  
Bangkok 10330, Thailand and Animal Virome and Diagnostic Development Research  
Group, Faculty of Veterinary Science, Chulalongkorn University, Bangkok 10330,  
Thailand

Anudep Rungsipipat

Department of Pathology, Faculty of Veterinary Science, Chulalongkorn University,  
Bangkok 10330, Thailand



**Publication status:** published in “BMC Veterinary Research” 2020, DOI: [10.1186/s12917-020-02467-4](https://doi.org/10.1186/s12917-020-02467-4) (Q1, Impact Factor 1.86)

**Abstract**

**Background:** Feline morbillivirus (FeMV) has been discovered in domestic cats associated with tubulointerstitial nephritis, but FeMV is also detected in healthy cats. This research aimed to identify and characterize the FeMV strains detected in a Thai cat population.

**Results:** Two-hundred and ninety-two samples (131 urine and 161 blood) derived from 261 cats (61 sheltered and 200 household cats) were included for investigating the FeMV prevalence using real-time reverse transcription PCR. The overall prevalence of FeMV detection was 11.9% (31/261) among both samples, which accounted for 14.5% (19/131) and 7.5% (12/161) of the urine and blood samples, respectively. Among the FeMV-PCR positive cats, the FeMV-detected prevalence was insignificantly associated with healthy cats (58.1%; 18/31) or urologic cats (41.9%; 13/31). Full-length genome analysis of these FeMV-Thai strains revealed that their genomes clustered together in the FeMV-1A clade with up to 98.5% nucleotide identity. Selective pressure analysis showed that overall FeMV-1 has undergone negative selection, while positive selection sites were more frequently observed in the phosphoprotein gene.

**Conclusions:** The detected FeMV infections in the Thai cat population were not correlated with urologic disorders, although the virus was more detectable in urine samples. The genetic patterns among the FeMV-1 Thai strains were more consistent. A large-scale study of FeMV in Thai cat samples is needed for further elucidation.

**Keywords:** Feline morbillivirus; Fusion, Hemagglutinin; Phosphoprotein; Selective pressure analysis; Urine

## Background

Feline morbillivirus (FeMV), belonging to genus Morbillivirus, family Paramyxoviridae, is a 16,050-bp length, non-segmented, enveloped, single-stranded, negative-sense RNA virus, that encodes for six genes; nucleocapsid (N), phosphoprotein (P/V/C), matrix (M), fusion (F), hemagglutinin (H), and RNA polymerase (L) (Woo et al., 2012). Among the functional proteins, the H and F glycoproteins on the viral membrane play a key role for attaching and fusing the host cells membrane, respectively (Fukuhara et al., 2019). Additionally, the diversity of H gene characterization is potentially affected the host range and virulence (von Messling et al., 2001; McCarthy et al., 2007; Denzin et al., 2013; Ke et al., 2015). Since the first identification of FeMV in domestic cats showing tubulointerstitial nephritis in Hong Kong in 2012 [(Woo et al., 2012), the virus has been investigated in both clinically healthy and ill cats in many countries, such as Japan, Turkey, Germany, Italy, USA, Brazil, and Malaysia (Furuya et al., 2014; Sakaguchi et al., 2014; Sieg et al., 2015; Marcacci et al., 2016; Sharp et al., 2016; Darold et al., 2017; Yilmaz et al., 2017; McCallum et al., 2018; Mohd Isa et al., 2019; De Luca et al., 2020). The prevalence of FeMV detection ranges from 0.2–40% based on the tested samples, comprised such as blood, urine, rectal swab, fresh tissues, and formalin-fixed paraffin-embedded tissues (Furuya et al., 2014; Sieg et al., 2015; Marcacci et al., 2016; Sharp et al., 2016; Darold et al., 2017; Yilmaz et al., 2017; Mohd Isa et al., 2019; De Luca et al., 2020). Because the first emergence of FeMV was associating with renal disease, the initial studies on FeMV identification were conducted in urine samples, while comparison of FeMV detection in urine and other derived samples was also reported (Woo et al., 2012; Furuya et al., 2014). Geographically, the prevalence of FeMV-positive samples is seemingly inconsistent, with a higher detection rate in Japan (ranging from 6.1–23.1%) (Furuya et al., 2014; Park et al., 2014; Sakaguchi et al., 2014), Italy (ranging from 1.2–31.8%) (Stranieri et al., 2019; De Luca et al., 2020), and Malaysia (50.8%) (Mohd Isa et al., 2019), while a lower detection rate was reported

in the USA, Germany, Brazil, and Turkey (Sieg et al., 2015; Sharp et al., 2016; Darold et al., 2017; Yilmaz et al., 2017; Stranieri et al., 2019).

Currently, full-length genome analysis of FeMV has categorized this virus into the two genotypes of FeMV-1 (former FeMV) (Donato et al., 2019; Sieg et al., 2019) and FeMV-2 (former FeMV-GT2), the latter of which was recently detected in cats showing urinary tract disease (UTD) in Germany (Sieg et al., 2019). The FeMV-1 genotype was subsequently clustered based on the partial L gene sequence into the FeMV-1A, -1B and -1C subgroups (Park et al., 2016). However, neither the FeMV-1 nor FeMV-2 genotype is able to clarify the association with nephropathy in cats (Sakaguchi et al., 2014; Sharp et al., 2016; Darold et al., 2017; Yilmaz et al., 2017; McCallum et al., 2018; Sieg et al., 2019). Therefore, the genetic characteristics of FeMV in many regions remain to be elucidated for studying viral pathogenesis, such as different cellular tropism (Sakaguchi et al., 2015; Sieg et al., 2019).

Since most RNA viruses are prone to mutation, due to the lack of an internal proof-reading mechanism during replication that results in a high rate of variant nucleotide substitutions, the identification of local strains would be beneficial for the further future management of disease control and monitoring. The genetic characterization of the newly identified FeMV in Thailand would contribute to the basic knowledge of not only the identification of FeMV but also on its evolution. Thus, this study aimed to establish the identification of FeMV Thai strains with viral genetic characterizations. Molecular genetic recombination and selective pressure analysis for evolutionary evaluation of the FeMV were also investigated. This fundamental data on the molecular epidemiology of FeMV strains might contribute to a more comprehensive understanding of FeMV evolution.

## Results

### Detection of FeMV in the urine and blood of Thai cats

The presence of FeMV in all the samples was 11.9% (31/261), as detected by the RT-qPCR assay. Among the samples, the FeMV was detected at a two-fold higher rate in the urine (19/131, 14.5%; as six shelter and 13 household cats) than in the blood (12/161, 7.5%; all were shelter cats). However, from the 61 shelter cats examined, although 18/61 (29.5%) showed FeMV in either the blood or the urine, no any cat showed FeMV-positive results in both sample types at the same time (Tables II-1 and II-2).

Considering the category of tested cats, the presence of FeMV detection in the shelter cats (18/61, 29.5%) was 4.5-fold higher than in the household cats (13/200, 6.5%). For the FeMV-positive urine samples, FeMV infection was found in cats with UTD (11/19, 57.9%; all were household cats), followed by no clinical significance or apparently healthy (6/19, 31.6%; all were shelter cats) and chronic kidney disease (CKD) (2/19, 10.5%; both were household cats) (Table II-2).

**Table II-1 Positivity rate of FeMV detection by RT-PCR.**

		Shelter cats (n = 61)		Group A Household cats (n = 100)		Group B Household cats (n = 100)		Total cats (n = 261)	
		Urine (n = 31)	Blood (n = 61)	Urine (n = 100)	Blood (n = 100)	Urine (n = 131)	Blood (n = 161)		
FeMV- PCR positive	Individual sample type	6 <sup>a</sup>	12 <sup>a</sup>	13 <sup>b</sup>	0	19/131 (14.5%)	12/161 (7.5%)		
Average		18/61 (29.5%)		13/200 (6.5%)		31/261 (11.9%)			

<sup>a</sup> There was no positive FeMV-PCR result in the same shelter cat.

<sup>b</sup> All FeMV-PCR positive cats showed abnormal urinalysis results, representing urologic disorders.

Table II-2 Biological data of cats with FeMV-positive results.

Sample type	Sample No. <sup>a</sup>	Sex <sup>b</sup>	Clinical sign <sup>c</sup>	Rapid test <sup>d</sup>	
				FeLV Ag	FIV Ab
Urine	U16	F (n)	CI	-	-
	U36	M (n)	CI	-	-
	U44	F (n)	CI	-	-
	U48	M (n)	CI	-	-
	U50	F (n)	CI	-	-
	U55	F (n)	CI	-	-
	CTL-8	M (n)	UTD	n/a	n/a
	CTL-15	M (n)	UTD	n/a	n/a
	CTL-16	M (n)	UTD	n/a	n/a
	CTL-25	n/a	UTD	n/a	n/a
	CTL-32	M	UTD	n/a	n/a
	CTL-43	M	UTD	n/a	n/a
	CTL-58	M	UTD	n/a	n/a
	CTL-60	M	CKD+DM	n/a	n/a
	CTL-63	M	UTD	n/a	n/a
	CTL-70	n/a	UTD	n/a	n/a
	CTL-89	n/a	UTD	n/a	n/a
	CTL-90	M	UTD	n/a	n/a
	CTL-100	n/a	CKD	n/a	n/a

Blood	E11	F (n)	CI	-	-
	E20	F (n)	CI	-	-
	E23	F (n)	CI	-	-
	E25	M (n)	CI	-	-
	E27	F (n)	CI	-	-
	E29	M (n)	CI	+	-
	E32	F (n)	CI	-	-
	E49	M (n)	CI	-	-
	E51	M (n)	CI	-	-
	E53	M (n)	CI	-	-
	E56	F (n)	CI	-	-
	E61	F (n)	CI	-	+

<sup>a</sup> U = urine from shelter cat, CTL = urine from household cat, E = blood from shelter cat

<sup>b</sup> F = female, M = male, (n) = neutered, n/a = no data available

<sup>c</sup> CI = clinically insignificant, CKD = chronic kidney disease, DM = diabetes mellitus, UTD = urinary tract disease.

<sup>d</sup> FeLV Ag = feline leukemia virus antigen, FIV Ab = feline immunodeficiency virus antibody, - = negative, + = positive

### **Association between the FeMV infection status, urine characteristics, urologic diseases and feline retrovirus detection**

The urinalysis of the group A household cats was determined in terms of the physical, chemical, and microscopic features and tabulated according to the FeMV-PCR positive results. Even though there were no statistical significances between the presence of FeMV in the urine and the urine characteristics ( $P>0.05$ ), some features, such as hematuric, pyuric, proteinuric, and aciduric urines, had a higher numerical tendency to be positive with FeMV detection. Among the 91 urine samples with urologic conditions from 100 household cats examined, the positive FeMV in the urine was evidenced at a six-fold lower rate (13/91, 14.3%), without significance, than the negative FeMV counterpart (78/91, 85.7%) ( $P>0.05$ , Supplementary Table S2). Moreover, among the FeMV-PCR positive cats, only one shelter cat each revealed a positive FeLV antigen (no. E27) and a FIV antibody (no. E61) (Table II-2).

### **Phylogenetic analysis and genome organization of the full-length FeMV-Thai strains**

Three full-length FeMV-Thai strains were obtained and have been submitted to GenBank as U16-2016 (MF627832; 16,050 nt length), CTL16-2018 (MN164531; 15,946 nt length), and CTL43-2018 (MN164532; 15,949 nt length). After nucleotide alignment and analysis, all three FeMV-Thai strains displayed the six consecutive gene sequences (N-P-M-F-H-L), comprised of the N (1,560 nt), P (1,476 nt), M (1,014 nt), F (1,632 nt), H (1,788 nt), and L (6,609 nt) genes, which encoded for 520, 492, 338, 544, 596, and 2,203 deduced amino acids, respectively. The different genome lengths among these three FeMV-Thai strains were due to the incomplete nucleotide sequence at the 5' end of CTL16-2018 and CTL43-2018.

Phylogenetic analysis of the full-length genome of the three FeMV-Thai strains revealed that they shared the same monophyletic topology of the FeMV-1 genotype



and segregated into the FeMV-1A clade, clustered with the FeMV strains reported from Hong Kong (M252A) and Japan (strain ChJP073, MiJP003, SS2, and SS3) (Fig. II-1). Pairwise nucleotide identity analyses revealed that these FeMV-Thai strains had the highest nucleotide identity to the FeMV-1A strain SS3 (97.8–98.5%), and to a lesser extent, to the FeMV-1A strain M252A (97.5–98.3%). Likewise, comparisons of nucleotide identities between three FeMV-1A Thai strains and the other FeMV clades displayed relatively high percentage similarities with the strains from FeMV-1B (91.3–92.0%), FeMV-1C (87.7–88.3%), FeMV-1D (86.9–87.4%), and FeMV-2 (81.6–81.9%) (Supplementary Table S3).

For the individual nucleotide and deduced amino acid analysis between these three FeMV-1A Thai strains and the FeMV-2 genotype (Gordon strain), the result showed that the P segment contained the most divergent nucleotide and amino acid identity at 80.4–80.6% and 69.2–74.5%, respectively, while the L segment revealed the most conserved nucleotide and amino acid identity at 82.4–82.5% and 90.6–90.8%, respectively (Supplementary Table S4). The phylogenetic trees constructed from each gene of FeMV-Thai strains revealed consistent topologies to the tree constructed from the full-length genome, in presenting the homology cluster in FeMV-1A (Supplementary Figs. S1–3).

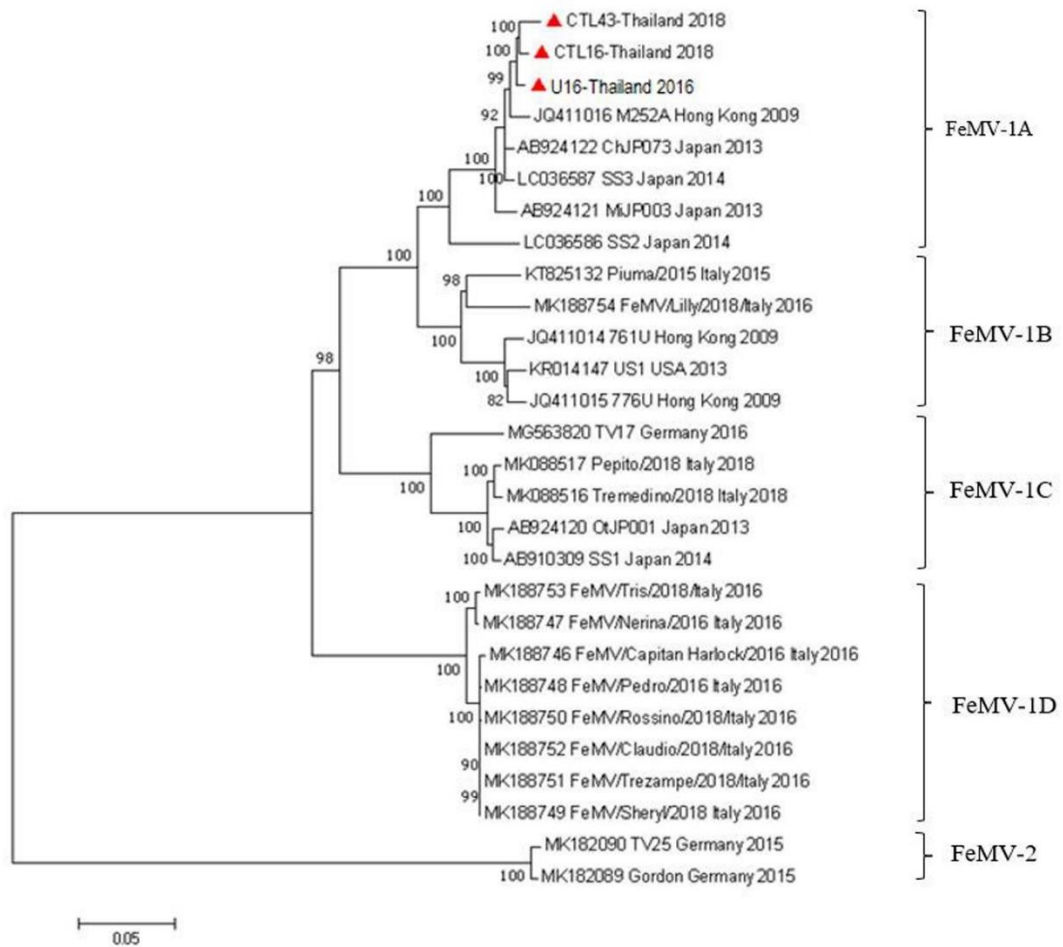


**Figure II-1** Phylogenetic analysis of the full-length genome sequence of FeMV strains. Scale bar is the substitution rate per site. The ML method with GTR model and 1,000 bootstrap replications (shown as % value) were performed in the Mega 7 software. The FeMV strains were grouped into two genotypes and subdivided into four clades of FeMV-1, the same topology as the phylograms from each gene. Red triangles show the three Thai FeMV isolates of this study.

### Unique deduced amino acid residues of the F and H genes among the FeMV genotype and clade

Seven FeMV samples (U16-2016, CTL15-2018, CTL16-2018, CTL25-2018, CTL32-2018, CTL43-2018, and CTL58-2018) were further sequenced for the complete coding region of the F and H genes, and these have been deposited in GenBank with accession

no. MF627832 (full length genome of U16-2016), and MN316616–21 and MN316622–7 for the F and H genes, respectively, of the other six CTL derived samples.

Interestingly, we found that the deduced amino acid residues of the start codon peptides of the F gene were distinguishable among the FeMV genotype and clades. The deduced start codon peptides of the FeMV-1A Thai strains, from this study, presented as MNRIG (U16-2016) and MNRIR (other six CTL derived samples), which were different from the previous FeMV-1A strains from Hong Kong (M252A) and Japan (SS2, SS3, and ChJP073) that were MNRIK. Moreover, the overall deduced amino acids of the F gene for the FeMV-Thai strains were identical to the other FeMV-1 genotype, except for residues 71 and 99 (Table II-3). For the H gene, the amino acid residues of FeMV-1A in this study were identical to other previous FeMV-1 strains at positions that were distinguishable from FeMV-2, such as residues 6, 17, 51, 58, 68, etc. Nevertheless, the residues 75, 82, 129, 500, 542, and 561 were diverse from FeMV-1B to -1D (Table II-4).

### **Recombination and selective pressure analysis**

To further investigate the possible evolution of the FeMV-Thai strains, we performed recombination analysis on the complete genome of the FeMV-Thai strains and, in particular, on the complete F and H gene of FeMV-1, with the other strains available in GenBank using the RDP method. After all models were implemented, no evidence of putative recombination breakpoint was found in our study.

To overcome the selective pressure mediated altered evolution of FeMV, this study explored the selective pressure analysis on each gene of FeMV using various statistical methods. Overall, the FeMV evolution was found to have undergone negative selective pressure, but positive selection sites were presented in the P, N, H, and F genes. Among the six genes of FeMVs, the P gene showed the highest frequency

of potential positive selection sites (9/492 sites using the FEL model) at amino acid sites 58, 64, 80, 88, 132, 154, 156, 218, and 249. This was followed by the H gene (4/596 sites using MEME model) at amino acid sites 62, 86, 104 and 170, N gene (4/520 sites using the MEME model) at amino acid sites 6, 8, 10 and 132, F gene (1/544 site using the MEME model) at amino acid site 503, based upon a  $dN/dS > 1$  and a  $p$ -value of  $< 0.1$ . In contrast, the M and L genes revealed a negative selection pressure with a  $dN/dS < 1$ .

### Discussion

Although FeMV has been recognized in CKD cats since 2012 (Woo et al., 2012) and gained wide attention worldwide, many interesting points, including its pathogenesis, cellular tropism, and association of CKD pathology, through its evolution for viral adaptation are still unclear and in need of further investigation. This study is the first report of the molecular identification and epidemiology of FeMV-1 in Thailand, revealing the existence of FeMV in Thai cats. The prevalence of FeMV in the present study was 11.9%, which was quite similar to that reported from Hong Kong (12.3%) (Woo et al., 2012), but higher than those reported in some other regions, such as Turkey (5.4%) (Yilmaz et al., 2017) and Japan (6.1%) (Furuya et al., 2014), or lower than that in Malaysia (39.4%) (Mohd Isa et al., 2019). This discrepancy in the FeMV prevalence may result from various factors, such as the cat's lifestyle (household/stray/shelter/chance of street access), habitat areas (urban/suburban/rural), and testing groups (Furuya et al., 2014; Yilmaz et al., 2017).

**Table II-3** Differences in start codon peptides and deduced amino acid residues of the FeMV F gene.

FeMV	Start	Amino acid residues											
	codon peptide	10	11	71	99	190	286	372	373	374	491	510	522
FeMV-1A	MNRIR MNRIG MNRIR	S	S	I	V	S	T	L	T	K	L	Y	T
FeMV-1B	MNRIR	S	S	T	A	S	T	L	T	K/E	L	Y	T
FeMV-1C	MGKIK	S	S	M/I	A/T	S	T	L	T	K	L	Y	T
FeMV-1D	MDKIK	S	S	I	T	S	T	L	T	K	L	Y	T
FeMV-2	MYKIK	G	F	A	T	A	V	L	I	N	S	C	A

**Table II-4** Differences in the deduced amino acid residues of the FeMV H gene

FeMVs	Amino acid residues																				
	6	17	51	58	68	75	77	82	129	132	192	257	295	349	420	496	500	542	546	56	595
FeMV-1A	I	G	I	T	T	R	E	Q	V	D	K	V	L	I	A	K	T	L	K	S	K
FeMV-1B	I	G	I	T	T	R	E	Q	V	D	K	V	L	I	A	K	T	V/I	K	S	K/Q
FeMV-1C	I	G	I	T	T	R	E	H	V	D	K/E	V	L	I	A	K	M	I	K	N	K
FeMV-1D	I	G	I	T	T	K	E	Q	M	D	K	V	L	I	A	K	T	I	K	N	K
FeMV-2	N	S	T	I	M	Q	K	K	T	N	N	T	P	M	E	I	L	V	R	A	N

In this study, the urine samples provided an almost two-fold higher FeMV detection rate compared to the blood samples (14.5% and 7.5%, respectively). Furthermore, FeMV RNA was not detected in the blood from cats with FeMV-positive urine. This finding was consistent with a previous report (Yilmaz et al., 2017) and may suggest that FeMV-positive cats probably has the result of an ongoing acute infection as found as in other morbilliviruses (da Fontoura Budaszewski and von Messling, 2016). Thus, the possibility of detectable FeMV in cats might be increased if various biological samples were tested from the same cat. Due to the fact that most FeMV identifications underwent detection of the virus in either the urine, kidney, or both samples, this might underestimate the true FeMV prevalence in regions (Sieg et al., 2015; Park et al.,

2016; Darold et al., 2017; Yilmaz et al., 2017; McCallum et al., 2018; Stranieri et al., 2019). Currently, there have been few studies and minimal case number testing of FeMV RNA in blood samples (Furuya et al., 2014; Yilmaz et al., 2017; De Luca et al., 2018), suggesting a low prevalence of FeMV RNA in blood samples. Conversely, the relative high number of FeMV RNA blood-positive cats (12/61) in our study might be due to the tested cats, which had close contact among other cats in the shelter, leading to persistent viral circulating in the shelter over time.

Since the FeMVs were frequently detected in the urine, previous studies have attempted to figure out the relationship between the presence of FeMV and the pathology of the kidneys (Woo et al., 2012; Sieg et al., 2019; Sutummaporn et al., 2019; De Luca et al., 2020). However, there were few reports about a correlation between FeMV infection (identification) and urinalysis parameters (Sieg et al., 2015; Crisi et al., 2020). Here, we provided another attempt to investigate the correlation of the presence of FeMV and urine parameters, and found that the household cats positive for FeMV in their urine cats were associated with abnormal urine characteristics, such as hematuria, pyuria, proteinuria, and aciduria. Even though this association was not statistically significant, it might raise a note of FeMV infection in cats showing urinary tract infections (UTIs), since a small number of recent publications have demonstrated urinalysis results in cats with FeMV (Darold et al., 2017; Yilmaz et al., 2017; Stranieri et al., 2019). However, other potential pathogens contributing to the feline UTIs, which are bacteria, FIV, leptospirosis and bartonellosis (Jepson, 2016), were not excluded from this study. Therefore, the bacteriology examination or FIV detection should be warrant in future study to evaluate the single FeMV infection or the coinfection with other infectious agents in cats with UTI.

In the present study, the identified Thai FeMV isolates had a genetic homology amongst themselves and were classified as FeMV-1A without any evidence of genetic recombination. This finding may indicate that the local FeMV-1 strain has been

circulating in Thai cat populations. Since the H and F genes of other morbilliviruses, notably the CDV, have played crucial roles associating cellular tropism and host membrane fusion, antigenic and sequence variations may alter the virulence of the virus (von Messling et al., 2001). Furthermore, the antigenic variation of the CDV H gene is used as geographic signature to identify the origin of the CDV, resulting in widely used for lineage classification (Ke et al., 2015; Piewbang et al., 2019b; Piewbang and Techangamsuwan, 2019; Piewbang et al., 2020b). Therefore, the genetic variations of the H and F genes of the FeMVs have been focused and interpreted in this study. Contrast to the CDV, we observed that the F gene of the FeMVs revealed more hypervariable portion than the H gene. The effects of amino acid mutations in the F and H genes, which are hypothesized to be associated with the viral infectivity and virulence, needs further investigation in a future study. In addition, we also proposed distinct deduced amino acid residues in the F and H genes that can potentially differentiate isolates within the FeMV clade.

RNA viruses possess a high mutation rate as a result of viral RNA polymerases lack a proof-reading property, then allowing rapid adaptations to various selection pressures (Yuan et al., 2017; Piewbang and Techangamsuwan, 2019). Moreover, recent studies have shown evidence of other morbilliviruses undergoing selective pressure, such as the negative and positive selective pressure for canine distemper virus and measles virus, respectively (Ke et al., 2015; Piewbang et al., 2019a). In this study, we found that overall the FeMV evolution has undergone a negative selective pressure, but positive selection sites were observed, with the highest frequency in the P gene, followed by in the H, N and F genes. This finding may suggest that these FeMV genes may play a role in FeMV evolution and emphasize the importance of P gene, the non-structural gene of morbillivirus, in the aspect of immunopathogenesis in particular hosts as already mentioned previously in rinderpest virus (RPV) and measles virus (MeV) (Chinnakannan et al., 2013). However, the data used in this study were restricted to

the 23 currently available full-length FeMV genomes. More analyzed sequences would likely allow a more clear understanding of FeMV evolution.

### **Conclusions**

This study presented the first report of FeMV-1 identification in domestic cats in Thailand with a higher detection rate in the urine than in blood samples. The FeMV was detected in both urological-ill and healthy cats without any association, although a higher detection rate was found in healthy cats. Genetic analysis of FeMV-Thai strains revealed a high genetic homology among the Thai strains, which were clustered in the FeMV-1A clade. Without any evidence of genetic recombination, the FeMV has undergone evolution by negative selection but with some positive selection sites in the P, H, N and F genes. Further study of FeMV identification at a larger scale and different sample groups is necessary.

### **Methods**

#### **Animals and sample collection**

Sixty-one cats from shelters locating in Saraburi province and 200 cats from different households in Bangkok (both are located in central Thailand, about 100 km apart) were included in this study. A total of 292 samples, comprised of 131 urine (derived from 31 shelter and 100 household cats) and 161 EDTA anticoagulated blood samples (derived from 61 shelter and 100 household cats) were collected during 2016 to 2018. Of note, the urine and blood samples were parallelly collected from 31 shelter cats, whereas individual urine or blood samples were collected from 100 household cats each (designated as group A and B) (Table II-1). Signalment and clinical presentations were recorded by veterinarians who collected the samples for further analysis.



### **Urinalysis and feline retrovirus infection screening**

Blood samples (where available) were tested for feline immunodeficiency virus (FIV) antibody and feline leukemia virus (FeLV) antigen using a commercial test kit (Bionote, Gyeonggi-do, South Korea). Routine urinalysis, including physical (color and transparency) and chemical (nitrite, pH, glucose, protein, occult blood, ketone, urobilinogen, leukocytes, ascorbic acid, and bilirubin) characteristics, was performed on the 100 urine samples from group A using URIT 11G test strips (URIT<sup>®</sup>, China). The specific gravity of the urine was measured using a refractometer. All samples were then kept at -80 °C until further used.

### **Two-stage real-time reverse transcription polymerase chain reaction (RT-qPCR)**

Viral nucleic acid was extracted from 200 µL of urine or blood samples using a Viral Nucleic Acid Extraction Kit II (GeneAid, Taipei, Taiwan) according to manufacturer's recommendation. The RNA concentration was qualified and quantified using a NanoDrop Lite Spectrophotometer (Thermo Fisher Scientific Inc, Waltham, MA, U.S.A.). For the first stage RT-qPCR, complementary DNA (cDNA) was constructed from 100 ng of extracted RNA using Omniscript Reverse Transcription Kit (Qiagen GmbH, Hilden, Germany), following the manufacturer's protocol. The derived cDNA was kept at -20 °C until further used.

For the second stage RT-qPCR, the presence of FeMV in each sample was detected using a KAPA SYBR fast qPCR master mix (2X) universal (KAPABIOSYSTEMS, Sigma-Aldrich<sup>®</sup>, Modderfontein, South Africa) with specific primer pairs targeting the L gene of FeMV, as previously described (Woo et al., 2012). The qPCR reaction was performed on Rotor-Gene Q real-time PCR cycler (Qiagen GmbH, Manheim, Germany) with 40 cycles of 95 °C for 3 s, 60 °C for 20 s, and 72 °C for 20 s acquiring fluorescence

A green. The software reporting cycling A green and melt A green compared that for the positive control (courtesy of Prof. Furuya) and no template control. Subsequently, selected positive RT- qPCR samples were resolved by 1.5% (w/v) agarose gel electrophoresis, purified using NucleoSpin Extract II kit (Macherey- Nagel, Düren, Germany), and submitted for commercial bidirectional Sanger's sequencing (Macrogen Inc, Incheon, South Korea) to confirm the presence of FeMV.

### **Amplification and sequencing of the complete F and H genes, and full-length genome of Thai FeMV**

The seven FeMV-PCR positive samples (U16-2016, CTL15-2018, CTL16-2018, CTL25-2018, CTL32-2018, CTL43-2018, and CTL58-2018) were further amplified for the complete F and H genes by RT-PCR assays with a set of specific primers targeting the F and H genes. These primers were designed from the alignment of various FeMV strains available in GenBank (Supplementary Table S1). Furthermore, the samples of U16-2016, CTL16-2018, and CTL43-2018 were subjected to full-length genome sequencing using the panel of primers described previously (Park et al., 2014) with some modifications. Positive amplicons were purified and subsequently submitted for Sanger's sequencing as mentioned above. Derived sequences were then aligned to construct the whole genome of these three FeMV-Thai strains.

### **Genetic characterization and phylogenetic analysis of the FeMV Thai strains**

The obtained nucleotide sequences of the FeMV-Thai strains, both the full-length genome and the individual genes, were constructed by BioEdit Sequence Alignment Editor Version 7.2.5 and compared to other previously published FeMV strains retrieved from GenBank. Phylogenetic analyses of detected FeMVs were performed using the maximum likelihood (ML) method implemented in the MEGA7

software package version 7.0. Genetic topology tree was constructed using the general-time reversible model (GTR) as the best-fit model of nucleotide substitution, according to the Bayesian information criterion, with 1,000 bootstrapped replicates. Pairwise distance of the FeMV genome was calculated using the compute pairwise distance in MEGA7. Deduced amino acid sequences analysis of the F and H genes were performed using the BioEdit software.

### **Recombination and selective pressure analyses**

To detect any potential recombination sites in the FeMV-Thai strains, a panel of previously described statistical methods was applied (Piewbang et al., 2019a). Briefly, each recombination analysis, including RDP, GENECONV, BootScan, MaxChi, Chimaera, SiScan, and 3Seq, were run with default settings in the Recombination Detection Program (RDP) package version 4.0, and were performed on the alignment of FeMV sequences. Any potential breakpoint signals detected by at least four models (all with  $P < 0.01$ ) were considered to ensure the positive recombination breakpoints (Martin et al., 2015).

To determine the frequency of selective pressure breakpoints of FeMV-Thai strains, the panel tests were run on six individual genes (N, P, M, F, H, and L). Non-neutral selection of nucleotide substitutions was calculated using the ratio value between nonsynonymous (dN) and synonymous (dS) substitutions with a ML approach, reconstructed using the Datamonkey web server (<http://www.datamonkey.org>). Single-likelihood ancestor counting, Fixed-effects likelihood (FEL), Mixed Effect Model Evolution (MEME), and Fast, Unconstrained Bayesian Approximation (FUBAR) approaches were used, accepting significance at the  $P \leq 0.1$  level in all the methods. The Bayes factor was set at 50 to estimate the rate of dN and dS within an individual

codon (Pond and Frost, 2005). Positive, neutral, and negative selections were defined as  $dN/dS > 1$ ,  $dN/dS = 1$ , and  $dN/dS < 1$ , respectively.

### **Statistical analysis**

The associations between the FeMV status (positive or negative), category of cats (shelter or household), and type of samples (urine or blood) were tested with odds ratio. The presence of FeMV in the urine were analyzed with the urine characteristics from urinalysis, and with the urologic associated diseases using Chi-square test or Fisher's exact test (Prism 6, GraphPad), with a 95% confidence interval and accepting significance at the  $P < 0.05$  level.

### **Declarations**

#### **Ethics approval and consent to participate:**

All experimental protocols were approved by the Chulalongkorn University Animal Care and Use Committee (No. 1631003). All procedures were done in accordance with the relevant guidelines and regulations. The written informed consent was obtained from all cat owners and shelters' owners for sample collection and data publication.

### **Availability of data and materials**

All the data supporting our findings is contained within the manuscript. Sequences from this study have been deposited in NCBI GenBank under accession numbers as followed: three full-length FeMV-Thai strains U16-2016 (MF627832), CTL16-2018 (MN164531), and CTL43-2018 (MN164532); six complete coding region of the F and H genes of FeMV-Thai strains CTL15-2018, CTL16-2018, CTL25-2018, CTL32-2018,

CTL43-2018, and CTL58-2018 with accession no. MN316616–21 and MN316622–7 for the F and H genes, respectively.

### Acknowledgements

We thank the animal shelters and Small Animal Teaching Hospital, Faculty of Veterinary Science, Chulalongkorn University for providing samples and Dr. Nawin Manachai for statistical analysis.



## CHAPTER III

**Detection of Antibody against Feline Morbillivirus by using Recombinant Matrix Enzyme-Linked Immunosorbant assay****Authors**

Surangkanang Chaiyasak, Chutchai Piewbang, and Somporn Techangamsuwan

Department of Pathology, Faculty of Veterinary Science, Chulalongkorn University, Bangkok, 10330, Thailand and Animal Virome and Diagnostic Development Research Group, Faculty of Veterinary Science, Chulalongkorn University, Bangkok 10330, Thailand

Jadsada Ratthanophart

Pathology Laboratory, National Institute Animal Health, Bangkok, 10900, Thailand

Anudep Rungsipipat

Department of Pathology, Faculty of Veterinary Science, Chulalongkorn University, Bangkok, 10330, Thailand

Navapon Techakriengkrai

Department of Virology, Faculty of Veterinary Science, Chulalongkorn University, Bangkok, 10330, Thailand

**Publication status:** in preparation

## Abstract

Feline morbillivirus (FeMV) is a new pathogen that considered being renal epitheliotropic virus even though the pathogenesis remains controversial. Besides the molecular assay, the seroprevalence was performed for epidemiological surveillance of FeMV infection. For FeMV antibody measurement, recombinant matrix (M) protein; the inner viral membrane which plays an important role in the viral assembly and budding process; is constructed to use as an antigen in serological test. Blood samples from 136 cats (56 sheltered and 80 household cats) were included in this study. All blood samples were initially performed real-time reverse transcription polymerase chain reaction (RT-qPCR) to detect FeMV prior the serological test. Later, the antibody level against FeMV was estimated in cat's sera by established indirect ELISA (i-ELISA) and compared with western blotting (WB) as a gold standard validation. The result showed 8.1% (11/136; all from sheltered cats) positive to FeMV by RT-qPCR. Positively serological results were shown by i-ELISA and WB, accounted for 68.4% (93/136) and 66.9% (91/136), respectively. Of noted, there was 6.6% (6/91) of molecular positive samples among the immunopositivity by WB. The sensitivity, specificity, positive predictive value, and negative predictive value of i-ELISA were 90.1%, 75.6%, 88.2% and 79.1%, respectively, with a good agreement between i-ELISA and WB analysis (A K coefficient of 0.664, 95% CI from 0.529 to 0.799). This study provided the first evidence of seroprevalence against FeMV in Thai cats.

**Keywords** Feline morbillivirus, indirect ELISA, recombinant matrix protein

## Introduction

Feline morbillivirus (FeMV), belonging to the genus *Morbillivirus*, family *Paramyxoviridae*, is a non-segmented, enveloped, single-stranded, negative-sense RNA virus. The genome length of FeMV is 16,050 bp and consists of six genes which are nucleocapsid (N), phosphoprotein (P/V/C), matrix (M), fusion (F), hemagglutinin (H) and polymerase (L) (Woo et al., 2012). The pathogenic role of FeMV remains controversial whether the association with feline chronic kidney disease or urinary tract disease (Sieg et al., 2015). Since its discovery in 2012 in stray cats in Hong Kong, several studies have been focused intensively on the viral detection by polymerase chain reaction (PCR) and immunohistochemistry (IHC) with the detection rate ranged from 0.2-40% (Woo et al., 2012; Furuya et al., 2014; Park et al., 2016; Yilmaz et al., 2017; De Luca et al., 2018; Mohd Isa et al., 2019; Stranieri et al., 2019; Chaiyasak et al., 2020; De Luca et al., 2020; Piewbang et al., 2020a). However, the antibody response against FeMV also gained more attention worldwide due to this virus is also detectable in healthy cats.

Previous studies of seroprevalence against FeMV revealed approximately 21-30% of FeMV which cat's serum/plasma derived from Hong Kong, Japan, United Kingdom, and Italy (Woo et al., 2012; Sakaguchi et al., 2014; Park et al., 2016; Arikawa et al., 2017; McCallum et al., 2018; De Luca et al., 2020). So far, there are two proteins; N and P: employing for FeMV serological studies including indirect immunofluorescent assay (IFA) (Park et al., 2016; De Luca et al., 2020), immunoblotting (Woo et al., 2012; Sakaguchi et al., 2014; McCallum et al., 2018), and indirect enzyme-linked immunosorbent assay (i-ELISA) (Arikawa et al., 2017). Recently, our research group performed polyclonal antibody (pAb) production against histidine-tagged recombinant FeMV-M (His-rFeMV-M) protein based on the nucleotide sequence of M gene of the FeMV Thai-U16 strain (Accession no.MF627832) and verified its size and immunogenicity by western blot analysis (Piewbang et al., 2020a).



The established pAb for His-rFeMV-M has been used for identification of viral localization and distribution in histological lesion in FeMV-infected domestic cats (unpublished data) and black leopards (*Panthera pardus*) in Thailand (Piewbang et al., 2020a). However, there is no previous investigation of seroprevalence of FeMV infection in cats in Thailand where the genetic incidence has been recently reported, about 11.9%, derived from both healthy and urologic conditions (Chaiyasak et al., 2020). Thus, this study aimed to evaluate the presence of serum anti-FeMV antibodies in Thai's cats. This fundamental data on the serological epidemiology of FeMV might contribute to a more comprehensive understanding of FeMV pathogenesis.

## **Materials and methods**

### **Sample collection**

Total 136 cats derived from shelters (n=56) locating in Saraburi province and different households (n=80) in Bangkok were included in this study. Anti-coagulated blood and serum (from shelter cats) or plasma (from household cats) samples were collected during 2016-2018. All procedures were approved by the Chulalongkorn University Animal Care and Use Committee (No. 1631003). Essential signalments such as sex, breed and clinical presentations were recorded by attending veterinarians for further analysis (Supplementary table 1). All samples were kept at -80°C until further assayed.

### **Expression, purification and identification of the recombinant FeMV-M protein**

Procedures of the construction of the recombinant (r)FeMV-M encoding plasmid, the expression and purification of histidine (His)-tagged rFeMV-M, and the identification of the His-rFeMV-M protein were described elsewhere (Piewbang et al.,

2020a). Briefly, the full-length of matrix (M) gene (1,014 bp) was amplified which based on accession no. MF627832 (FeMV U16-2016 Thai strain, FeMV-1A clade). The resulting M gene was cloned into the pGEM-T Easy vector (Promega, USA), transformed into *Escherichia coli* (*E. coli*) DH5 $\alpha$  cells (ThermoFisher Scientific, USA), selected and enriched the transformed colonies with ampicillin-containing Luria-Bertani (LB) medium. The derived DNA extracted plasmid was further subcloned into pet24a (+) expression vector (Novagen, Germany), transformed into *E. coli* BL21 (DE3) (Novagen, Germany), selected and enriched the positive colonies with kanamycin-containing LB medium. The resulting rFeMV-M protein was tagged with a six-histidine residue on the C-terminus (named as His-rFeMV-M). After induction, the expression of His-rFeMV-M transformant culture by adding the isopropyl- $\beta$ -D-thiogalactopyranoside (IPTG), the expression of His-rFeMV-M was confirmed by sodium dodecyl sulfate–polyacrylamide gel electrophoresis (SDS-PAGE). Protein purification was performed with the His Bind Kit (Novagen, USA) according to the manufacturer's protocol. Final elution of purified His-rFeMV-M protein concentration was determined with a NanoDrop ND-1000 Spectrophotometer (ThermoFisher scientific, USA) and subjected to antigenicity testing by western blotting.

The derived purified His-rFeMV-M protein was run on SDS-PAGE and transferred onto a polyvinylidene-fluoride (PVDF) membrane with wet-transblot technique (Bio-Rad, USA). After washing and blocking the non-specific reaction, the membrane was probed with Ni-NTA-horseradish peroxidase (HRP) conjugate (Qiagen, Germany) and finally visualized with 3,3'-diaminobenzidine (DAB) (CW BIO, China).

### **Western blot analysis for the serum samples**

Purified His-rFeMV-M protein was separated on 10% SDS-PAGE, and the samples were transferred to PVDF membrane as mentioned above for 3 hours. Subsequently, the completion of protein transfer was checked with Coomassie brilliant blue staining

on transferred SDS-PAGE and with Ponceau S staining on PVDF membrane. The membranes of each transferred samples were separately cut, placed in individual container, triple washed using 0.1% (v/v) Tween-20 in PBS (PBST), and blocked the non-specific reaction with 5% (w/v) skimmed milk powder overnight at 4°C with gentle shaking.

All membranes were then incubated with 136 cat's serum/plasma samples (diluted 1:1000 in 2% (w/v) skimmed milk) overnight at 4°C, and consecutively incubated with goat anti-cat IgG-HRP secondary antibody (diluted 1:8000) (Invitrogen, ThermoFischer Scientific, USA) at room temperature for 1 h. The immunoreactivity was visualized as the positive brown color using DAB. To localize the position of His-rFeMV-M protein on the membrane, the incubation with Ni-NTA-HRP conjugate was parallelly performed as a positive control; while the membranes that omitted protein and omitted cat's serum/plasma were applied as negative controls. The immunopositivity results were semi-quantitatively scored as strong positive, moderate positive, weak positive, and negative.

#### **Indirect ELISA assay**

To optimize the indirect ELISA (i-ELISA) condition, the strong immunopositively blotting samples (n=13) were used with the varied dilutions of His-rFeMV-M protein concentration (0.625-10 µg/ml), cat's serum/plasma (1:100-150), goat anti-cat IgG-HRP secondary antibody (1:2000-8000) and DAB concentration (1:100-800). The results were determined regarding the optimal optical density (OD) value. All trial samples were then double tested for intra-assay evaluation.

Conventional i-ELISA was performed with the following steps. Each well of 96-well plates was coated with 100 µl of optimized purified His-rFeMV-M protein in coating buffer (3.7 g Sodium Bicarbonate (NaHCO<sub>3</sub>), 0.64 g Sodium Carbonate (Na<sub>2</sub>CO<sub>3</sub>) in 1 L of distilled water) as an antigen at 4°C overnight. Afterthat, plates were thrice washes

with PBST and then blocked the non-specific reaction with 100  $\mu$ l 1X ELISA diluent (ELISA assay Diluent (5X), BioLegend®, USA in PBST) on a microplate shaker (Thermo-Shaker PST-60HL-4, BoEco, Germany) at 37°C for 3 h. After plates were washed, 100  $\mu$ l optimized cat's serum/plasma diluted in 1X ELISA diluent was added in each well and incubated at 37°C for 2h. Plates were washed and reacted with 100  $\mu$ l optimized goat anti-cat IgG- HRP secondary antibody (Sigma-Aldrich®, USA) diluted in 1X ELISA diluent at 37°C for 1 h. for detecting IgG against FeMV in cat's samples. Plates were then washed and 100  $\mu$ l 3,3',5,5'-tetramethylbenzidine (TMB) substrate solution (BioLegend®, USA) was added per well for a chromogenic reaction at room temperature for 10 min in complete darkness. The color reaction was stopped by the addition 100  $\mu$ l of 1M H<sub>2</sub>SO<sub>4</sub> to each well. Finally, the OD<sub>450</sub> was measured with ELISA reader (M965, Metertech Inc., Taiwan) and recorded. The wells omitting cat's serum/plasma were used as the average background in each ELISA plate.

#### **Realtime reverse transcription PCR (RT-qPCR) of the L gene of FeMV**

Viral nucleic acid was extracted from blood samples using a Viral Nucleic Acid Extraction Kit II (GeneAid, Taipei, Taiwan) as previously described (Chaiyasak et al., 2020). For complementary DNA (cDNA) construction, 100-ng RNA was employed by Omniscript Reverse Transcription Kit (Qiagen GmbH, Hilden, Germany). Later, cDNA was then used as the template in qPCR reaction using a KAPA SYBR® fast qPCR master mix (2X) universal (KAPA BIOSYSTEMS, Sigma-Aldrich, South Africa) and specific primers targeting the L gene of morbilliviruses (Woo et al., 2012). The qPCR reactions were performed on Rotor-Gene Q real-time PCR cyler (Qiagen GmbH, Germany) as previously mentioned (Chaiyasak et al., 2020). Subsequently, positive samples were randomly selected for bidirectional sequencing to confirm the presence of FeMV (Macrogen Inc, South Korea).

### **Statistical analysis**

To assess the potential of i-ELISA performance compared to immunoblotting, OD values from each sample were average after minus the background. Sensitivity, specificity, positive predictive value (PPV), negative predictive value (NPV) and cutoff value were determined using ROC ANALYSIS (Web-based calculator for ROC Curves) by implemented model JLABROC4, Maximum likelihood estimation of a binormal ROC curve from continuously distributed test results (Metz, 1978). The serological test between i-ELISA and western blot analysis was calculated the Kappa, quantify interrater agreement (**K** coefficient) using GraphPad via online server. Correlations in categorical data were calculated by Fisher's exact and Chi-square test.

## **Results**

### **Expression and identification of His-rFeMV-M protein and serum immunoblotting**

The amplification and construction of recombinant protein of whole M gene of FeMV strain Thai-U16 were showed in supplemental figure (Figure S1-S3)The purified elute protein were confirmed by SDS-PAGE following by Coomassie brilliant blue staining and protein band was confirmed at MW 36 kDa (the predicted size of FeMV-M protein plus 6-His-tagged at 8400 Da) with other products for all 3 elutions. The concentration of the first (E1), second (E2) and the third (E3) were at 420 mg/μl, 360 mg/μl and 260 mg/μl (Figure III-1A). The E1 elution revealed the immunolocalized target band with HRP conjugated Ni-NTA at 36 kDa that corresponding to the expected size and was served as a positive control (Figure III-1B and Figure S4, PTC). To assure completely transferred the FeMV-M protein on PVDF membrane before incubation with cat sera or NI-NTA-HRP conjugated, ponceau S was well red-stained on each row of running protein on the membrane (Figure S5) and no staining of Coomassie brilliant blue left on transferred PAGE. The results from immunoblot assay from cat's samples

revealed 91 positive immunoreactivity samples (66.9%, 91/136) which classified as strong positive (n=16), moderate positive (n=19), and weak positive (n=56), and other 45 samples showed negative immunoreactivity (33.1%, 45/136). The positive samples showed the specific band at 36 kDa of His-rFeMV-M protein, while the negative samples displayed no target band (Figure III-1B).

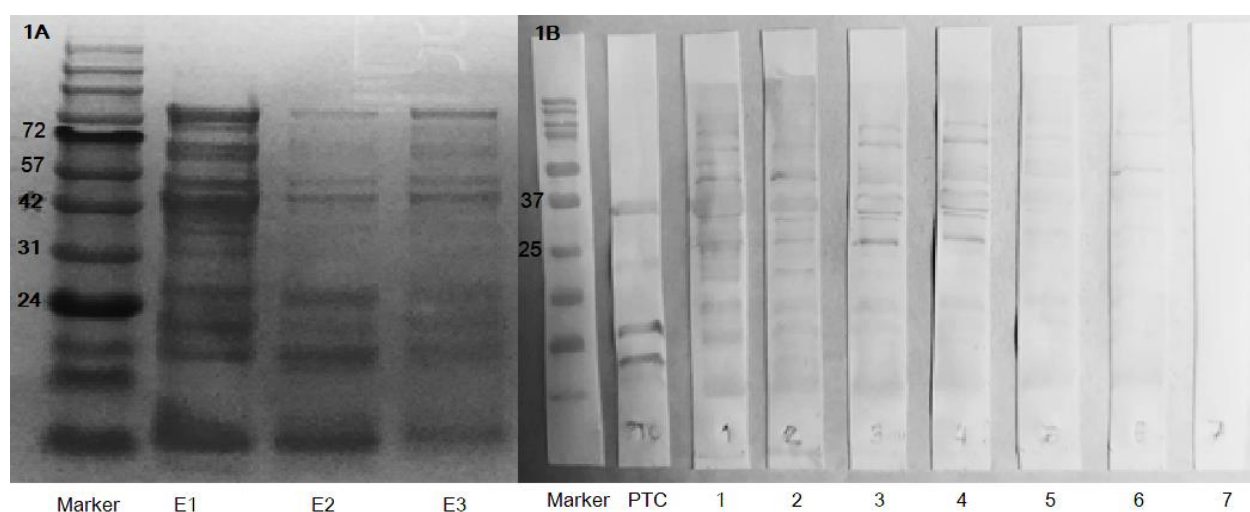


**Figure III-1 (1A)** Purified protein elutions (E1-E3).

**(1B)** The immunoblotting revealed the immunoreactivity at target size 36 kDa, starting from the samples with the highest to lowest  $OD_{450}$  value (lane 1-6). The positive control (PTC) showed marked immunoreactivity at 36 kDa. The negative control showed none of positive band on the membrane (lane 7).

### Development of the His-rFeMV-M i-ELISA

The conditions of i-ELISA were done to determine the optimal coating antigen (His-rFeMV-M) concentration at 0.625  $\mu\text{g}/\text{ml}$ , the optimal dilution of cat serum was 1:150, and the optimal working dilution of goat anti-cat IgG-HRP conjugate was 1:8000. The cutoff (CO) value for the i-ELISA was determined at 0.2505 with 90.1% sensitivity, 75.6% specificity, 88.2% PPV, and 79.1% NPV (Figure 3-2, Table 3-1). Area under fitted curve (Az) was 0.9007 with 0.0320 of estimated standard error (Figure 3-2). A **K**

coefficient of 0.664 (95% CI From 0.529 to 0.799) was calculated, revealing a good agreement between i-ELISA and western blot analysis.

### **Detection of FeMV in the blood samples**

All 136 blood samples were further subjected to detect the conserve L gene of FeMV by RT-qPCR. Among the 91 immunoblot-positive serum samples, 6 blood samples tested positive for the FeMV RNA, while 5 blood samples tested positive for FeMV RNA in the 45 immunoblot-negative serum samples. Therefore, the FeMV infection status is divided into four categories consisted of RNA+/Ab+ (4.4%, 6/136), RNA+/Ab- (3.7%, 5/136), RNA-/Ab+ (62.5%, 85/136), and RNA-/Ab- (29.4%, 40/136) (Table 3-2).

Further analysis on the origin of studied cats showed that all FeMV RNA positive blood samples derived from shelters (11/136), while no evidence in household cats. Among the immunoblot-positive cats, 26 cats derived from shelters while 65 cats derived from household cats (Table 3-3). The clinical status including signs was recorded in Supplementary table 1.



### **Discussion**

This study investigated the prevalence of FeMV infection and antibody response in cats which were from the shelter and household in Thailand. Both sources showed different result of prevalence of FeMV RNA positivity in blood. The shelter cats had significantly higher prevalence (19.6%, 11/56) than the household cats (0%, 0/80) ( $p < 0.001$ ). This finding was in agreement with previous research mentioned that sheltered cats had more circulated FeMV transmission (De Luca et al., 2020). Although, the blood samples from household cats were negative to molecular study, but the

immunoblotting result of the FeMV antibody against M protein were significantly higher than those in shelter cats ( $p < 0.001$ ) during 2016-2018.

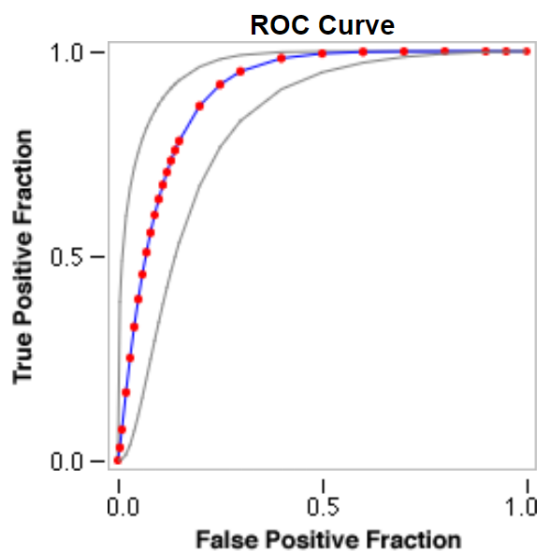


**Figure III-2** Receiver operating characteristic (ROC) curve analysis.

Area under fitted curve ( $A_z$ ) was 0.9007 with 0.0320 of estimated standard error. This analysis contains JROCFIT and JLABROC4 programs for fitting ROC curves using the maximum likelihood fit of a binormal model.

**Table III-1** Comparison of i-ELISA and western blot analysis

ELISA result	Western blot		Total
	Positive	Negative	
Positive	82	11	93
Negative	9	34	43
Total	91	45	136
Total (% coincidence)	90.1% (82/91)	75.6% (34/45)	85.3% (116/136)



Table III-2 Comparison of real-time RT-PCR (RT-qPCR) and western blot analysis

RT-qPCR	Western blot		Total
	Positive	Negative	
Positive	6 (RNA+/Ab+)	5 (RNA+/Ab-)	11
Negative	85 (RNA-/Ab+)	40 (RNA-/Ab-)	125
Total	91	45	136

Table III-3 Statistical analysis between shelter and household cats

Analyzed method	Results	Shelter (n=56)	Household (n=80)	p value
Real-time RT-PCR	Positive	11 <sup>a</sup>	0	< 0.001
	Negative	45	80	
Immunoblotting	Positive	26	65 <sup>a</sup>	< 0.001
	Negative	30	15	

a= significant higher

Comparison between results from RT-qPCR and immunoblotting assays, the positive FeMV RNA blood samples revealed negative correlation to the immunoblot-positive cat sera. Previous study revealed that urine samples might be simultaneously used for FeMV RNA detection for increasing the rate of FeMV positivity (Chaiyasak et al., 2020). Therefore, the rate of FeMV RNA positivity in this study might not reflect the true infectious status in studies cats. Moreover, the unrelatedness between FeMV

viremia and antibody response may be caused by the rather short viremia of FeMV in the host (Mohd Isa et al., 2019).

Our study showed a relatively higher prevalence of FeMV antibody detection than previous studies (Woo et al., 2012; Sakaguchi et al., 2014; Park et al., 2016; Arikawa et al., 2017; De Luca et al., 2020) which might be due to the FeMV-M protein possesses a higher amino acid identity among the FeMV genotypes (Chaiyasak et al., 2020). In addition, the cutoff value in this study (CO=0.244) is lower than previous study (CO=0.43) (Arikawa et al., 2017) that might lead to have more FeMV positive sera. Additionally, the serum cross-reactivity of FeMV-M i-ELISA to other feline pathogens and related morbilliviruses, such as canine distemper (CDV), is not performed in this investigation. Previous studies have been reported the evidence of neutralizing anti-CDV antibodies in cat sera (Appel et al., 1974; Ikeda et al., 2001). Therefore, the cross-reactivity is needed in the next study.

Based on the FeMV infection status, the lower rate of RNA+/Ab+ (4.4%) and highest rate was in RNA-/Ab+ (62.5%), might support that FeMV has a short viremia (Mohd Isa et al., 2019). This established His-rFeMV-M i-ELISA showed a susceptible agreement with corresponding with western blotting assay. However, the viral neutralizing assay is further needed to validate the ELISA test in the future.

In conclusion, the serological test of FeMV implementing this developed i-ELISA is useful to detect the FeMV infected cats. Even though the FeMV-induced pathogenesis remained elusive, the antigen and antibody-based techniques will be useful to monitor the evidence of FeMV infection in Thai cats. The large-scale study in Thai cat population will provide comprehensive understanding of FeMV infection in cats or *Felidae* species.

CHAPTER IV  
Localization and Viral Distribution of Feline Morbillivirus-1 in Non-Kidney  
Diseased Cats

**Authors**

Surangkanang Chaiyasak, Chutchai Piewbang and Somporn Techangamsuwan

Department of Pathology, Faculty of Veterinary Science, Chulalongkorn University, Bangkok, 10330, Thailand and Animal Virome and Diagnostic Development Research Group, Faculty of Veterinary Science, Chulalongkorn University, Bangkok 10330, Thailand

Jakarwan Yostawonkul

Department of Pathology, Faculty of Veterinary Science, Chulalongkorn University, Bangkok, 10330, Thailand and National Nanotechnology Center (NANOTEC), National Science and Technology Development Agency (NSTDA), Thailand Science Park, Pathumthani 12120, Thailand

จุฬาลงกรณ์มหาวิทยาลัย  
CHULALONGKORN UNIVERSITY

Suwimon Boonrungsiman

National Nanotechnology Center (NANOTEC), National Science and Technology Development Agency (NSTDA), Thailand Science Park, Pathumthani 12120, Thailand

Tanit Kasantikul

Department of Preclinic and Applied Science, Faculty of Veterinary Science, Mahidol University, Nakhon Pathom 73170, Thailand (TK)

Anudep Rungsipat

Department of Pathology, Faculty of Veterinary Science, Chulalongkorn University,  
Bangkok, 10330, Thailand

**Publication status:** in preparation



## Abstract

Feline morbillivirus (FeMV) has been discovered with controversial observation whether the association with kidney disease in cats. During routine histopathology examination, we observed the perinuclear eosinophilic hyalinized globular materials in renal tubular epithelial cells deriving from two moribund cats, with antemortem history of severe hematuria. The globular materials were frequently located in the renal tubular epithelial cells at corticomedullary junction and renal pelvis without cellular reaction and tissue inflammation. Ultrastructurally, we observed an aggregation of electron-dense ribonucleocapsid herringbone structure in the cytoplasm of renal tubular epithelial cells, where the hyalinized materials were found. Using immunohistochemistry against FeMV matrix protein revealed the immunopositive signals in the cytoplasm of renal tubular epithelium, particularly in these globular inclusion-like bodies. Moreover, the immunoreactive signals were also visualized in the cytoplasm of tracheal, bronchial, and bronchiolar epitheliums, circulating lymphocytes and infiltrating histiocytes in spleen and mesenteric lymph node, and neuroglial cells in the white matter of brain, suggesting systemic viral infection. Further genetic characterization of fusion and hemagglutinin genes revealed FeMV-1A genotype in both cats. Taken together, these findings strongly indicated the FeMV existence and demonstrated the active FeMV infection. Importantly, we proposed that FeMV is renal epitheliotropic virus, similarly to other morbilliviruses, by existing viral inclusions without inflammatory cellular reactions and integral pathological changes of kidney disease. This study raised another evidence of the FeMV infection in non-kidney diseased cats. Further comprehensive study and larger scale investigation of FeMV in necropsied cats are warranted for understanding of host pathogen interaction in the FeMV infection.

**Keywords:** feline morbillivirus- 1A, inclusion bodies, histopathology, immunohistochemistry, renal epitheliotropism, transmission electron microscopy



## Introduction

Feline morbillivirus (FeMV) is the one of extant morbilliviruses, which was firstly discovered in stray cats in Hong Kong since 2012 (Woo et al., 2012). The FeMV is an enveloped, linear, negative-sense, single-stranded RNA virus, which has genetic material translated into six major proteins following the rule of six of morbillivirus genome organizations including nucleocapsid (N), phosphoprotein (P/V/C), matrix (M), fusion (F), hemagglutinin (H) and polymerase (L) genes (Woo et al., 2012; Chaiyasak et al., 2020). Among the functional proteins, the attachment (H) and fusion (F) glycoproteins on the viral membrane play the major roles for entering and fusing to the host cells in which the genetic characterization of H gene is integral involving the host selection (Fukuhara et al., 2019). The variety of cellular tropisms of morbilliviruses is indicated such as epithelial cells in respiratory, gastrointestinal, urinary tract, integument system, reticuloendothelial cells (lymphoid cells and macrophages), and neuronal and neuroglial cells in central nervous system (Griot et al., 2003; Radtanakantikanon et al., 2013; Techangamsuwan et al., 2015; Pratakpiriya et al., 2017); however, the cellular localization of FeMV is extant that are mostly, but not limit to, renal tubular epithelial cells, an association of FeMV with kidney disease is therefore interesting and need further warrant.

FeMV was initially mentioned to be involved with chronic kidney disease (CKD) in domestic cats (Woo et al., 2012; Sutummaporn et al., 2019) and black leopards (Piewbang et al., 2020a) and, may be associated with feline urinary tract disease (UTD) (Sieg et al., 2015). Pathological examination of FeMV-infected cats mainly revealed tubulointerstitial nephritis (TIN) wherein mononuclear cell infiltrates (Woo et al., 2012; Yilmaz et al., 2017; De Luca et al., 2018; Sutummaporn et al., 2019; De Luca et al., 2020), and to a lesser extent, glomerulosclerosis, tubular atrophy, renal epithelial cell degeneration, urinary casts, and interstitial fibrosis (Sutummaporn et al., 2019). Focusing on the expression of FeMV antigen, the immunopositive signals were presented on

renal tubular epithelial cells (Woo et al., 2012; Park et al., 2016; De Luca et al., 2018; Sutummaporn et al., 2019; De Luca et al., 2020), mononuclear cell infiltrates in renal interstitial area (Woo et al., 2012; Sutummaporn et al., 2019; De Luca et al., 2020), lympho-monocytic cells in spleen (De Luca et al., 2020) and lymph node (Woo et al., 2012; Yilmaz et al., 2017; De Luca et al., 2020) airway epithelial cells (Sieg et al., 2019; De Luca et al., 2020), mucosal layer of urinary bladder (De Luca et al., 2020) and a lesser degree in brain tissue (Sieg et al., 2019; De Luca et al., 2020).

However, the role of FeMV associated with kidney diseased cats was challenged by several studies that showed the FeMV antigens have been detected in healthy cats (Park et al., 2016; Sharp et al., 2016; Chaiyasak et al., 2020). So far, recent studies have reported that the FeMV-infected cats can shed the virus via urine for several months while abnormal clinical signs were yet observed (Sharp et al., 2016; Darold et al., 2017). Thus, the relationship between TIN and presence of FeMV antigen is still questioned (Sakaguchi et al., 2014; Darold et al., 2017; Yilmaz et al., 2017; McCallum et al., 2018; Mohd Isa et al., 2019; Stranieri et al., 2019), and whether FeMV is a pathogenic virus or replicates actively in kidney or other tissues has yet elucidated and needs further investigations.

In this study, we described the FeMV presentation in non-kidney diseased cats, providing further information of the FeMV localization with a special note of active viral replication in renal tubular epithelium using transmission electron microscope (TEM) and immunohistochemistry (IHC). Genetic characterization of the FeMV-F and -H genes revealed that the detected virus belongs to the FeMV-1A genotype as an infective agent. This finding provided evidence of the FeMV infection in cats without clinically relevant kidney disease.



## **Materials and Methods**

### **Animals and clinical history**

Two cats, both 2-year-old, intact male, stray, domestic short hair breed, showed clinical signs of severe hematuria before death and had no previous history of other clinical illnesses. They were raised in different households and died on August and September 2019, respectively. The carcasses were submitted for routine necropsy at Department of Pathology, Faculty of Veterinary Science, Chulalongkorn University, and then designated as 19P244N (case no. 1) and 19P314K (case no. 2), respectively.

### **Pathological and ultrastructural examinations**

After necropsy, macroscopic lesions were recorded and various tissues were collected including brain, trachea, lung, heart, spleen, liver, small intestine, mesenteric lymph node, pancreas, adrenal gland, kidney, and urinary bladder. All tissues were preserved in 10% neutral buffered formalin for 24 hrs., and then continuing processed and embedded in paraffin for histopathological study. Microscopic examination of two cats was systematically evaluated by an American board-certified veterinary pathologist (TK). Urine (from distended urinary bladder) of both cases and fresh tissues of case no. 2 (as mentioned above for histopathology study) were also collected and kept in -80 °C for molecular assays. Furthermore, the formalin-fixed paraffin-embedded (FFPE)-kidney sections of both cases were prepared for ultrastructural examination using TEM. The samples were prepared with the pop-off technique as previously described with minor modifications (Lehmbecker et al., 2014; Piewbang et al., 2018)

### **Molecular detection of FeMV in urine and fresh tissue samples**

Urine samples from both cases and fresh tissue samples from case no. 2 were subjected for viral molecular investigation using pan-morbillivirus PCR (Woo et al., 2012). Viral genetic material was extracted from urine and individually homogenized

tissues employing Viral Nucleic Acid Extraction Kit II (GeneAid, Taiwan) according to manufacturer's recommendation. The quality and quantity of nucleic extraction were evaluated using NanoDrop™ Lite Spectrophotometer (Thermo Fisher Scientific Inc, USA). The nucleic acid was reverse transcribed for complementary DNA (cDNA) construction using Omniscript® Reverse Transcription Kit (Qiagen GmbH, Germany), following manufacturer's suggestion. The PCR condition comprised 40 cycles of denaturation at 95 °C for 30 sec, annealing at 55 °C for 1 min, and extension at 72 °C for 1 min. The PCR products were visualized on 1.5% agarose gel electrophoresis, further purified using NucleoSpin® Extract II kit (Macherey-Nagel, Germany), and then subsequently submitted for Sanger's bidirectional sequencing (Macrogen, Korea).

The pan-morbillivirus PCR-positive samples were then confirmed the presence of FeMV and measured the cycle threshold (Ct) value using reverse transcription real-time polymerase chain reaction (RT-qPCR) (Rotor-Gene Q real-time PCR cycler, Qiagen GmbH, Germany) with specific primers targeting the FeMV-L gene, reagents and protocols as previously described (Woo et al., 2012; Chaiyasak et al., 2020). The positive PCR samples were further purified and submitted for sequencing as described above.

#### **Phylogenetic analysis of FeMV-F and H genes**

To characterize the genotype of FeMV detecting in this study, the FeMV-PCR positive samples were amplified to gain the full-length F and H genes by conventional RT-PCR assays with the set of specific primers targeting F and H genes (Chaiyasak et al., 2020) and submitted for sequencing as mentioned above. Derived nucleotide sequences of both genes of Thai-FeMV strain were constructed using BioEdit Sequence Alignment Editor Version 7.2.5. The complete F and H genome sequences of both cases were phylogenetically analyzed and compared to other previously published FeMV strains available in GenBank database using maximum likelihood (ML) model in MEGA7 software package version 7.0. Genetic topology tree was constructed using the

general-time reversible model (GTR) as a best-fit model of nucleotide substitution according to the Bayesian information criterion with 1,000 bootstrapped replicates.

### **Immunohistochemistry (IHC) for FeMV localization**

To localize FeMV antigen in the FFPE tissues, IHC assay targeting FeMV<sub>matrix</sub> (M) protein was performed using the horseradish peroxidase system (Piewbang et al., 2020a). Briefly, FFPE sections were cut at 4- $\mu$ m thickness, deparaffinized and hydrated. They were then pre-treated with distilled water and autoclaved at 121 °C for 5 min. To block the endogenous peroxidase and non-specific reactions, sections were incubated with 3% (v/v) hydrogen peroxide at room temperature for 15 min and 5% (w/v) skimmed milk in 1% PBS at 37 °C for 60 min, respectively. Subsequently, sections were incubated with generated rabbit polyclonal antibody against histidine-tagged recombinant FeMV-M (Pab-His-rFeMV-M; dilution 1:500) in 5% skimmed milk at 4 °C overnight. After triple washing with 1% PBS, sections were incubated with the EnViSion system according to the manufacturer's instructions before being immersed in 3,3'-diaminobenzidine and counterstained with Mayer's hematoxylin. Omitting primary antibody (replaced with distilled water) slide was served as a negative control, while a CDV-infected dog was used as a positive control. Immunopositive cells were noted for interpretation of cellular tropism and viral distribution. Immunoreactivity was semi-quantitatively scored and analyzed by averaged count in 5 different areas under high-power field (400X) as follows: - (no immunopositive cells); + ( $\leq$  25% immunopositive cells); ++ (26–50% immunopositive cells); +++ (51–75% immunopositive cells); ++++ ( $\geq$  76-100% immunopositive cells).

## **Results**

### **Pathological findings of necropsied cats**

Postmortem examinations of both cases revealed similarly prominent macroscopic findings in urinary bladder by showing severe acute hemorrhagic cystitis with marked accumulation of red urine (Fig. IV-1). Multifocal-to-coalescing hemorrhage

on both mucosal and serosal surfaces of the bladder was found with the urethral plug at the tip of penis of case no. 1. Hypertrophic cardiomyopathy on left ventricle was found in both cats. Moderate frothy exudate in trachea with pulmonary edema (Fig. IV -2), multifocal hemorrhage at right cortical adrenal gland, and mild peritoneal effusion were observed in case no. 1; while mild hemorrhage at mesenteric lymph node was seen in case no. 2. Other organs such as brain, liver, kidneys demonstrated mild to moderate congestion without significant change (Fig. IV -3 and IV -4); Supplementary Table 4-1).

Histologically, both cats revealed diffuse renal tubular vacuolation, mild (case no. 1) to moderate (case no. 2) segmental multifocal membranous glomerulonephropathy. Of noted, occasional renal epithelial cells contained 2-4  $\mu\text{m}$  round to oval intracytoplasmic eosinophilic hyalinized globules, especially in proximal convoluted tubules at corticomedullary junction and renal pelvis in both cats (Fig. IV-5, inset). The sections of urinary bladder illustrated severe locally extensive to multifocal necrotizing hemorrhagic cystitis with marked submucosal hemorrhage and, additionally, marked neutrophil infiltrates through bladder wall and adjacent tissues and multifocal fibrinoid vasculitis (case no. 2). For the heart, both cases showed multifocal myocardial disarray by showing haphazard arrangement of cardiac myofibers. Within the lung section, they revealed multifocal to locally extensive (case no. 1) and diffuse (case no. 2) pulmonary edema, diffuse congestion with alveolar histiocytosis. The brain section disclosed mild to moderate diffuse satellitosis (case no. 1) and focal cerebral rarefaction and vacuolation with multifocal cerebral hemorrhage (case no. 2). The liver of case no. 1 revealed multifocal lobular collapse, central vein fibrosis, moderate sinusoidal leukocytosis, and neutrophilia, while the spleen of case no. 2 showed lymphoid follicular depletion with mild extramedullary hematopoiesis. The small intestine displayed more severity degree of necrotizing enteritis in case no.

2 with mild lymphocytic epitheliotropism. More detail of histopathological findings was included in Supplementary Table 2.

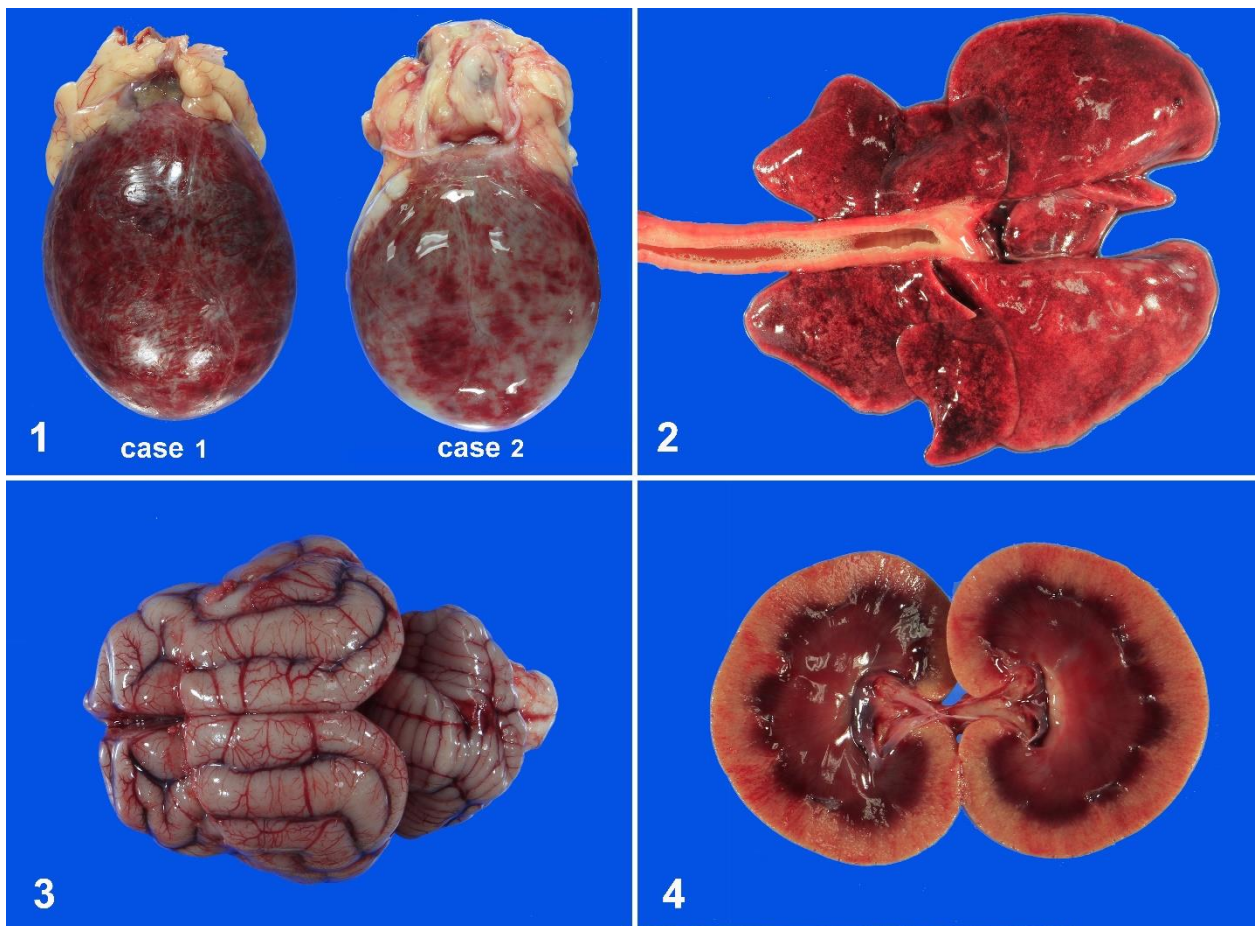


**Figure IV-1** Feline morbillivirus infection, cat. Urinary bladder, case no. 1 and 2.

Severe distension of urinary bladder with red urine, and hemorrhage at mucosal and serosal surface.

**Figure IV-2** Lung, case no.1. Pulmonary edema with tracheal froth.

**Figure IV-3** Brain, case no. 2. Congestion.

**Figure IV-4** Kidney, case no. 2. Moderate congestion at corticomedullary junction.

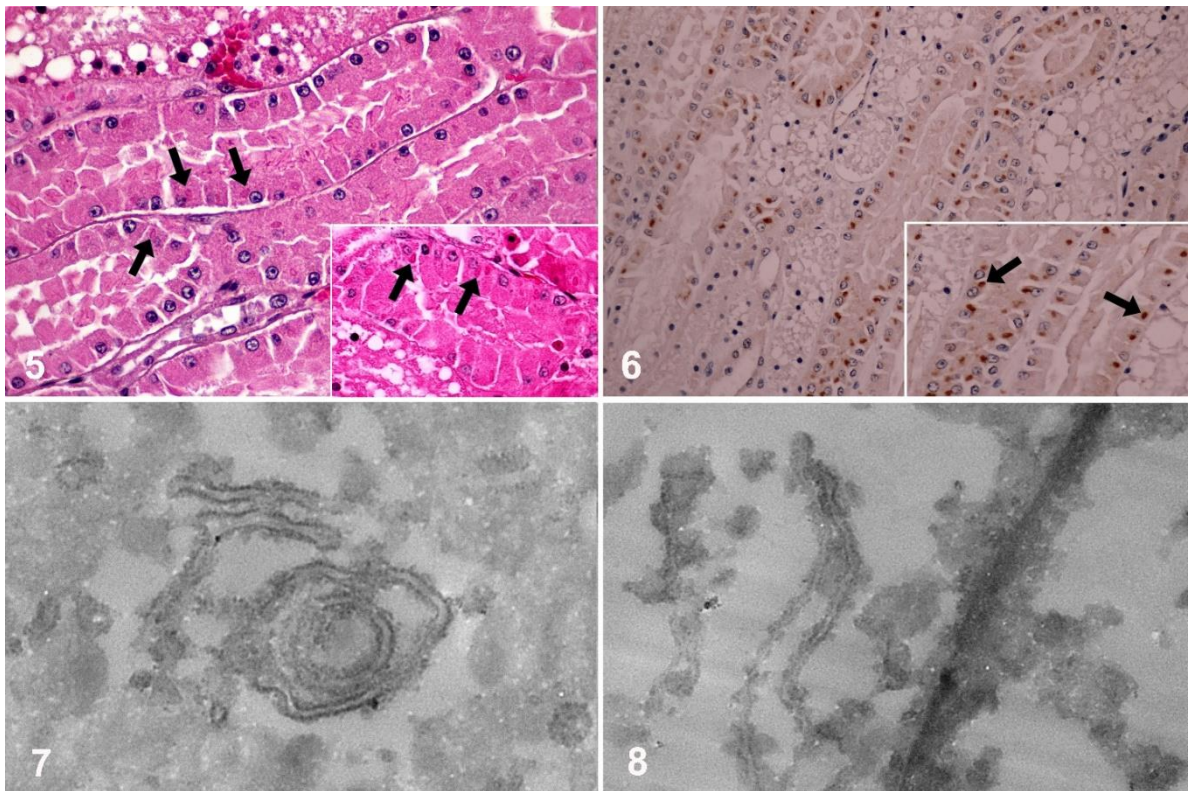


**Figure IV-5** Feline morbillivirus infection, cat. Kidney, case no. 2 (HE).

Renal tubules are degenerate and contain discrete vacuole while some renal tubular epithelial cells are plump cuboidal or tall columnar and contain 2-4  $\mu\text{m}$  round to oval intracytoplasmic eosinophilic hyalinized globule (inset, arrow)

**Figure IV-6** Feline morbillivirus infection, cat. Kidney, case no. 2 (IHC).

The strongly positive immunoreactivity (dark brown) was showed in intracytoplasmic globules within the renal proximal tubular epithelial cells (inset, arrow).

**Figure IV-7** Feline morbillivirus infection, cat. Kidney, case no. 2 (TEM).

The viral ribonucleocapsid particles were about 100-250 nm in diameter, aggregated and localized in adjacent to endoplasmic reticulum of the degenerated renal tubular epithelium. Transmission electron microscope for feline morbillivirus.

**Figure IV-8** Feline morbillivirus infection, cat. Kidney, case no. 2 (TEM).

Free ribonucleocapsid herringbone-like was located at perinucleus.



### **Ultrastructural finding of FeMV particles**

The histological findings of intracytoplasmic eosinophilic hyalinized globules in the renal tubules corresponded to the ultrastructural examination, presented by numerous intracytoplasmic protein aggregations and pleomorphic herringbone-like particles. The viral ribonucleocapsid particles were about 100-250 nm in diameter, aggregated and localized in adjacent to endoplasmic reticulum of the degenerated renal tubular epithelium. The viral particles were also rarely found at the perinucleus area (Fig. IV -7 and IV -8).

### **Molecular detection, sequencing, and phylogenetic analysis of FeMV-1A genotype**

The findings of herringbone-like particles in the renal tubular epithelium prompted us for further identify the causative agent by using pan-morbillivirus PCR in available urine and fresh samples. The positive pan-morbillivirus PCR fragments were identified in urine sample and fresh tissues including kidney, lung, liver, small intestine, urinary bladder, spleen, mesenteric lymph node and brain of case no. 2. The Ct value from RT-qPCR reaction was lowest in urine samples (Ct=24.8), then spleen (Ct=32), kidney and mesenteric lymph node (Ct=34.2), urinary bladder and small intestine (Ct=34.8) and lung (Ct=37.4), respectively, with the melting peak at 79.5-80 °C. However, Ct value could not determine from liver and brain (data not shown).

Subsequently, we analyzed the FeMV lineages by characterizing the full-length F and H genes of both cats. The results revealed the homogeneity among both strains, and they were clustered in FeMV genotype 1A (FeMV-1A) (Figs. IV -13). The nucleotide similarity among them was 98.2% and 98.6% for F and H genes, respectively, while the deduced amino acid counterpart was 97.2% and 97.6%. When compared F and H genes obtained from this study to the former FeMV strains, they revealed the similarity at nucleotide ranging from 92.7-98.9% (FeMV-1A), 90.4-98.7% (FeMV-1B), 89.9-92.5%

(FeMV-1C), 88.9-89.3% (FeMV-1D), and 79.6-80.5% (FeMV-2); while the similarity at deduced amino acid were 95.1-97.6% (FeMV-1A), 93.4-98.9% (FeMV-1B), 93.1-95.1% (FeMV-1C), 92.9-94.1% (FeMV-1D) and 84.1-86.2% (FeMV-2) (Supplementary Figure S1-S2). The obtained FeMV-1A sequences from this study were submitted to GenBank database with accession number MT338572 (case no. 1) and MT338573 (case no. 2).

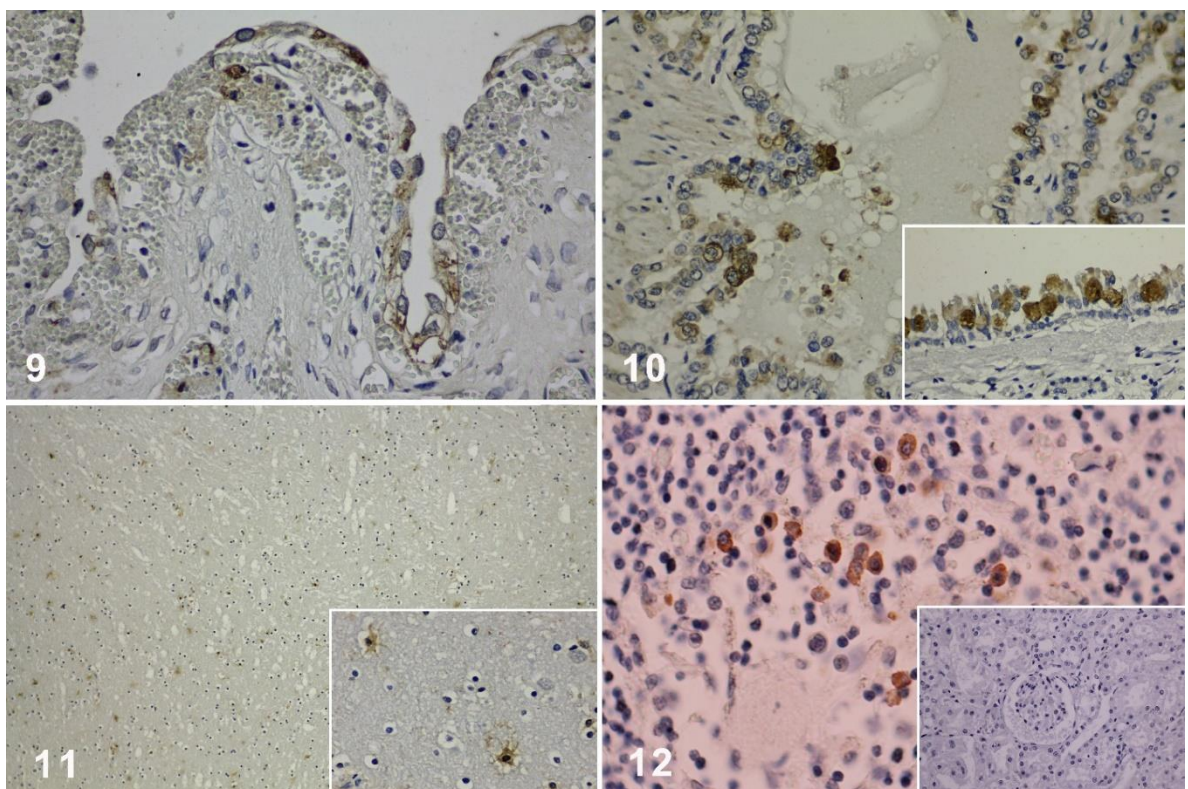


**Figure IV-9** Feline morbillivirus infection, cat. Urinary bladder, case no. 2 (IHC).

The cytoplasm of transitional cell was moderate positive immunolabeling.

**Figure IV-10** Respiratory airway, case no.1 (IHC).

The positive immunoreactivity was strongly represented in cytoplasm of tracheal (inset) and occasional bronchial epithelial cells.

**Figure IV-11** Central nervous system, case no.1 (IHC).

FeMV antigen was detected in the cytoplasm of neuroglial cells (inset).

**Figure IV-12** Lymph node, case no.1 (IHC).



*The positive immunoreactivity was strongly represented in cytoplasm of infiltrating histiocytes. No positive signal was detected in negative control (inset).*

### **Cellular tropism and tissue localization of FeMV**

To confirm the coherent results of the presented herringbone-like viral particles and the positive FeMV genetic materials detected by RT-qPCR, the FFPE kidney sections of both cats were determined the presence of FeMV antigen by IHC assay using Pab-His-rFeMV-M. The prominent FeMV immunoreactivity was localized at the renal tubular epithelial cells where the eosinophilic intracytoplasmic hyalinized globular materials were found (Fig. IV-5, inset). Furthermore, to disclose the FeMV localization in other organs, the remaining FFPE sections were IHC performed. The FeMV immunoreactivity was diffusely localized in the cytoplasm of various epithelial cells including transitional (Fig. IV-9), tracheal, bronchial, and bronchiolar epithelial cells. (Fig. IV-10). For the brain section, the immunopositive signals were observed in the cytoplasm of neuroglial cells in cerebrum and cerebellum (Fig. IV-11, inset), while circulating histiocytes and lymphoid cells of spleen and mesenteric lymph node were occasionally positive. There is no immune reactivity on negative control slides (Fig. IV-12, inset). The IHC scores were evaluated and summarized in Supplemental Table 3.

### **Discussion**

Several factors have been associated with feline CKD which is considered as a complex condition and influenced by non-infectious (aging, genetic, environment, concurrent diseases) and infectious (bacteria, virus) diseases. Cats with CKD gain a higher risk of urinary tract infection (UTI) due to impaired host defense mechanisms (Jepson, 2016). A number of virus causing CKD are documented such as feline immunodeficiency virus (FIV), feline leukemia virus (FeLV), feline infectious peritonitis virus (FIPV) (Brown et al., 2016), feline paramyxovirus (FPaV) (Sieg et al., 2015), and

FeMV (Woo et al., 2012; Sutummaporn et al., 2019; Crisi et al., 2020). However, the association of FeMV with kidney injury remained argumentative.

In this study, two naturally moribund cats suffering from acute hemorrhagic cystitis with unknown previous illness history were infected with FeMV-1A genotype which clarified by ultrastructural, molecular and IHC assays. By pathological study, the lesion of CKD or TIN such as mononuclear interstitial nephritis or renal fibrosis was not evidenced in renal tissues. This implied that both FeMV-infected cats were not involved with kidney inflammation, which in agreement with previous investigations (Sakaguchi et al., 2014; Darold et al., 2017; Yilmaz et al., 2017; McCallum et al., 2018; Mohd Isa et al., 2019; Stranieri et al., 2019).

Since the discovery of FeMV in 2012, the ultrastructural morphology of this virus was displayed only in vitro cell culture system (Woo et al., 2012). Multiple attempts had been conducted to persuade the existence of FeMV in urinary tract system either by genetic detection (Sakaguchi et al., 2014; Sieg et al., 2015; Park et al., 2016; Donato et al., 2019; Sieg et al., 2019; Stranieri et al., 2019; Chaiyasak et al., 2020; De Luca et al., 2020) or immunoreactive reaction (Woo et al., 2012; Park et al., 2016; Sharp et al., 2016; Yilmaz et al., 2017; De Luca et al., 2018; Donato et al., 2019; Sieg et al., 2019; Sutummaporn et al., 2019; De Luca et al., 2020). However, there was no in situ confirmation of FeMV. The round to oval intracytoplasmic eosinophilic hyalinized globules, especially in renal epithelial cells of proximal convoluted tubules at corticomedullary junction and renal pelvis in both cats, prompted us to perform further ultrastructural investigation. We, therefore, reported here as the first evidence of the typical herringbone appearance of viral ribonucleocapsid in paramyxovirus in non-kidney diseased cats. These findings implemented that FeMV could be dormant inside host without stimulating the host immune response. The viral property and pathogenesis of FeMV-induced disease are needed to clarify in future study.

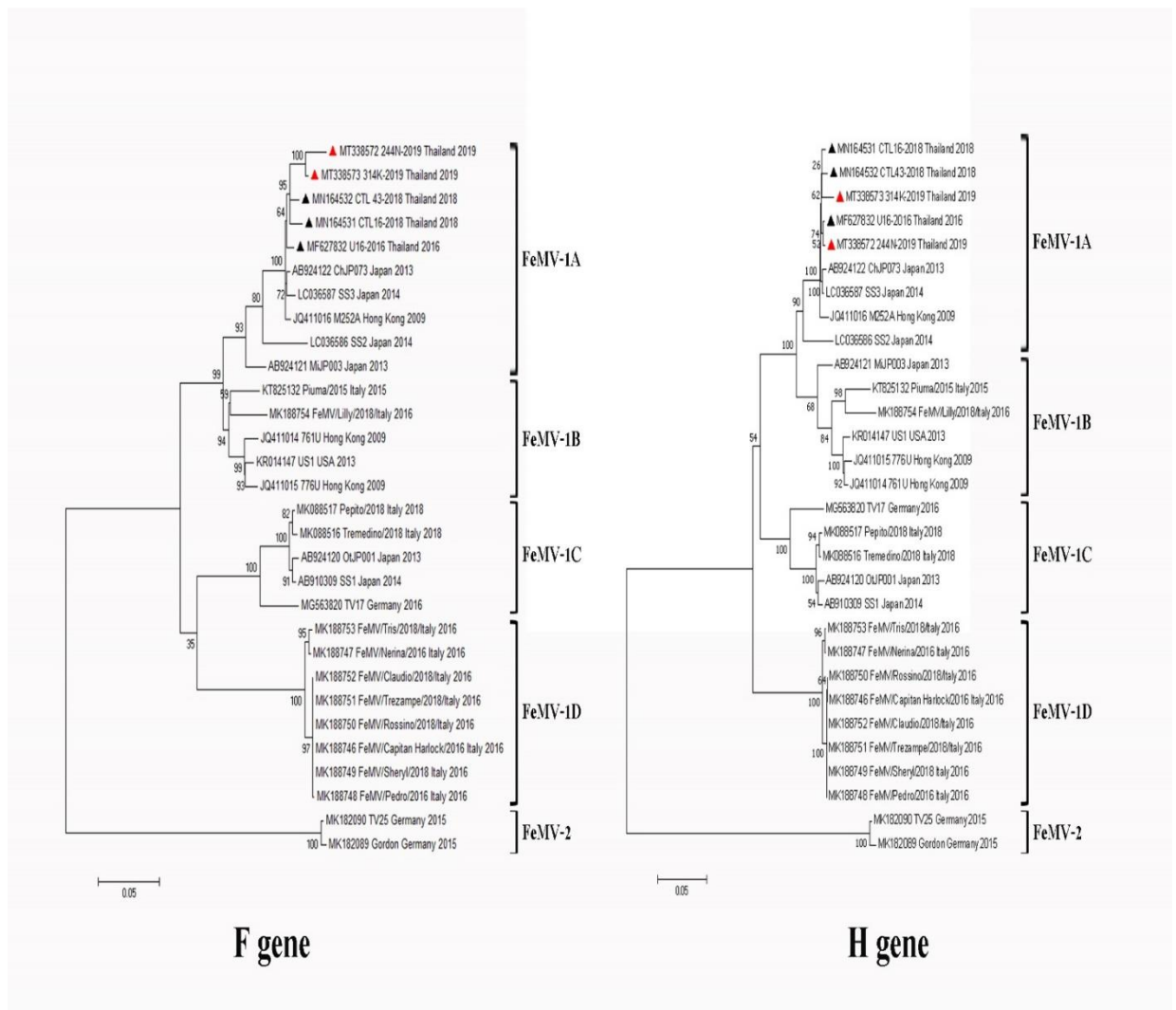


**Figure IV-13** Phylograms of FeMV-F and H genes.

FeMVs from both cats (▲) were clustered in the FeMV-1A lineage. The phylogenetic tree was constructed in MEGA 7.0 using the ML method with 1,000 bootstrap replications. GenBank accession numbers present on the tree. The analysis involved 30 nucleotide sequences. Bar indicates the estimated numbers of nucleotide substitutions per site (previously reported FeMV-Thai strains, ▲).

Morbilliviruses possess the property of lymphotropism and epitheliotropism by invading host cells via specific cellular receptors including signaling lymphocytic activation molecule (SLAM) and nectin-4, respectively (Pratakpiriya et al., 2017). We demonstrated here the cellular localization of FeMV in infected cats by IHC technique,

which are in accordance with previous research (Woo et al., 2012; De Luca et al., 2018; De Luca et al., 2020). FeMV-1A genotype identified in this study also had in vitro tropism for various epithelial cells of trachea, bronchi, bronchioles, kidneys, and urinary bladder, suggesting the epitheliotropic of FeMV, while the FeMV immunoreactivity was also evident in the cytoplasm of lymphoid cells, suggesting the nature of lymphotropic of FeMV that was recently described (Piewbang et al., 2020a). Moreover, the viral infectivity also expanded to residing glial cells in brain and infiltrating mononuclear cells in spleen and lymph node. Even the neither definitive role of FeMV presentation with the association of the cause of death nor the role of hematuria in these cats were summarized, the immunoreactive results were in agreement with the Ct value derived from RT-qPCR assays, suggesting systemic viral infection.

In conclusion, we provided another supportive evidence of FeMV infection in non-kidney diseased cats and indicated the dormant existence of FeMV in kidney in the absence of host immune response and pathological changes but remained the active FeMV infection. Significantly, we proposed that FeMV is renal epitheliotropic virus in cats by existing viral inclusions. Further a large scale of histopathological investigation should be warranted to elucidate the viral inclusion bodies in other organs.

### **Acknowledgements**

We are thankful to Dr. Jadsada Ratthanophart, National Institute of Animal Health (NIAH), Department of Livestock Development, Thailand for assistance in Pab-His-rFeMV-M construction and to Ms. Prukswan Chetanachan, a senior medical scientist, National Institute of Health (NIH), Department of Medical Sciences, Ministry of Public Health and Mr. Poowadon Chai-in, National Nanotechnology Center (NANOTEC) for performing TEM.

## CHAPTER V

Feline morbillivirus infection associated with tubulointerstitial nephritis in  
black leopards (*Panthera pardus*)

**Authors**

Chutchai Piewbang<sup>§</sup>, Surangkanang Chaiyasak<sup>§</sup> and Somporn Techangamsuwan

Department of Pathology, Faculty of Veterinary Science, Chulalongkorn University,  
Bangkok 10330, Thailand, and Animal Virome and Diagnostic Development Research  
Group, Faculty of Veterinary Science, Chulalongkorn University, Bangkok 10330,  
Thailand

<sup>§</sup>These authors contributed equally to this article

Piyaporn Kongmakee, Saowaphang Sanannu and Pornsuda Khotapat,

The Zoological Park Organization under The Royal Patronage of H.M. The King, Bangkok  
10800, Thailand

Jadsada Ratthanophart

National Institute of Animal Health, Department of Livestock Development, Bangkok  
10900, Thailand

Wijit Banlunara

Department of Pathology, Faculty of Veterinary Science, Chulalongkorn University,  
Bangkok 10330, Thailand

**Publication status:** published in “Veterinary Pathology” 2020, DOI:  
10.1177/0300985820948820 (T1, Impact Factor 2.11)



**Abstract**

Feline morbillivirus (FeMV) is an emerging RNA virus in the Paramyxoviridae family that was recently discovered in domestic cats (*Felis catus*). To date, two genotypes (FeMV-1 and FeMV -2) have been detected in cats from various countries and FeMV-1 is recognized as a pathogen associated with nephritis. However, information regarding the pathological roles and potential transmission to other felids is limited. Here, we describe the identification of FeMV in two black leopards (*Panthera pardus*) in Thailand which showed severe azotemia and tubulointerstitial nephritis. Molecular analysis of the partial coding sequence of the L gene revealed that these leopard FeMV strains were genetically close to the FeMV-1 isolate from domestic Thai cats. Immunohistochemistry and immunofluorescence analyses using polyclonal IgG antibodies against the FeMV matrix (M) protein showed FeMV-M antigen in renal tubular epithelial cells. These analyses also showed infiltrating lymphocytes in the renal parenchymal lesions and in the cytoplasm of lymphoid cells residing in the spleen, suggesting viral tropism and a possible pathological role. These findings are the first evidence which indicates that the black leopard could be a possible host for FeMV infection. As for other cats, the role of FeMV as a potential cause of renal disease remains to be established. The pathogenesis of FeMV infection in black leopards, or in other wild felids, through a viral transmission mechanism warrants further investigation.

**Keywords:** Chronic kidney disease, *Felidae*; Feline morbillivirus, Leopard, *Panthera pardus*, Thailand, Tubulointerstitial nephritis

Morbillivirus, a negative-sense single-stranded RNA virus in the *Mononegavirales* order, *Paramyxoviridae* family, contains six core genes that encode for the matrix protein (M), the hemagglutinin (H) and fusion (F) glycoproteins, two RNA-polymerase-associated proteins of phosphoprotein (P) and large protein (L), and a nucleocapsid (N) protein (Sato et al., 2012). This virus family potentially causes serious disease in a wide host range of mammals, such as measles virus in humans, rinderpest virus and peste des petits ruminants virus in ruminants, phocine distemper virus in porpoises, and canine morbillivirus (initially canine distemper virus; CDV) in various species of carnivores (Rima and Duprex, 2006). These viruses preferentially infect the host cells through specific signalling molecules such as the signalling lymphocyte activation molecule (Tatsuo et al., 2001) and nectin-4 (Pratakpiriya et al., 2017), which are common cellular receptors in various mammalian hosts and so suggest the potential for cross-species infection between the different hosts.

As well as from domestic and wild canids, CDV has been identified as a primary cause of fatal illness in wild felids, including tigers lions, and leopards (Appel et al., 1994; Roelke-Parker et al., 1996; Seimon et al., 2013; Martinez-Gutierrez and Ruiz-Saenz, 2016; Sulikhan et al., 2018), while there are no reports of natural CDV infections in domestic cats despite frequent contact with dogs (Beineke et al., 2015). Thus, investigation and monitoring of morbillivirus infection in domestic felids has been widely conducted worldwide, resulting in the identification of a novel morbillivirus, namely feline morbillivirus (FeMV), in cats in Hong Kong in 2012 (Woo et al., 2012). Since then, FeMV has been identified in cats showing tubulointerstitial nephritis and detected in urine samples from cats in various countries throughout Asia, Europe, and the Americas (Furuya et al., 2014; Lorusso et al., 2015; Sharp et al., 2016; Darold et al., 2017; Yilmaz et al., 2017; Sieg et al., 2018; Mohd Isa et al., 2019), suggesting a widespread geographical distribution of the virus.



Even though FeMV is classified as a member of the Morbillivirus genus, it has distinct genetic and biological characteristics, such as a relative phylogenetic distinction, from other morbilliviruses and an association with kidney disease (Woo et al., 2012; Darold et al., 2017; Sutummaporn et al., 2019). Several studies have evaluated the relationship between kidney disease and FeMV infection, but the results are inconclusive (Lorusso et al., 2015; Park et al., 2016; McCallum et al., 2018; Sutummaporn et al., 2019). At present, FeMV biology, including its pathogenicity and the range of susceptible hosts, is still unclear.

Furthermore, genetic analysis of the present FeMV isolates showed a genomic diversity that supports their division into two genotypic lineages, FeMV-1 and FeMV-2 (Sieg et al., 2018; Sieg et al., 2019). The FeMV-2 lineage has been shown to infect a wider cellular target range than FeMV-1, which infects only renal epithelial cells (Sieg et al., 2019). In addition, natural recombination of FeMV-1 has been reported (Park et al., 2014). Together, this raises the possibility that FeMV might be more diverse in its pathogenicity to other hosts.

Due to the fact that morbilliviruses may have a wide host-range, FeMV infection in wild felids, besides domestic cats, needs to be investigated to identify its origin and characterize its genetic background and so give a better understanding of FeMV evolution and pathogenicity. In this study, we identified FeMV infection associated with fatal tubulointerstitial nephritis in two captive black leopards (*Panthera pardus*) in Thailand using reverse transcriptase polymerase chain reaction (RT-PCR), immunohistochemistry (IHC) and immunofluorescence (IF) analyses of the tissues.

## Materials and Methods

### Cases and samples

In November 2016, a 5-year-old male black leopard, designated as case 1, raised in The Zoological Park Organization under The Royal Patronage of H.M. The King, Bangkok, showed clinical signs of anorexia, vomiting, polyuria and polydipsia. The clinical disease worsened with bloody diarrhea, anemia, and markedly elevated serum creatinine and urea levels. Another six-year-old male black leopard, designated as case 2, caged separately, presented similar clinical signs at the beginning of December 2016. After supportive care and treatment, both black leopards died, in late December 2016 (case 1) and at the beginning of January 2017 (case 2).

Initially, renal failure was suggested as a cause of death of these two black leopards, without a specific infection or underlying diseases. They were then subjected to postmortem examinations at the Department of Pathology, Faculty of Veterinary Science, Chulalongkorn University. All vital organs including brain, heart, liver, lung, lymph nodes, kidneys and spleen, were collected and preserved in 10% neutral buffered formalin for two weeks and subsequently embedded in paraffin for histopathology. Microscopic evaluation was performed on hematoxylin and eosin (HE)-stained sections by the veterinary pathologist (WB). Fresh kidney tissues and urine samples were kept at  $-80^{\circ}\text{C}$  for molecular analysis of viral pathogens. Moreover, samples from two other *Felidae* species-- 8 tigers (*Panthera tigris*) and 3 fishing cats (*Prionailurus viverrinus*) were also included in this study.

### Virologic investigation

Viral DNA and RNA were extracted from 200  $\mu\text{L}$  of homogenized renal tissues and urine samples using the Viral Nucleic Acid Extraction Kit II (GeneAid, Taipei, Taiwan) according to the manufacturer's recommendation. The extracted nucleic acid was then

quantified and qualified by spectrophotometric analysis with a Nanodrop® Lite (Thermo Fisher Scientific Inc., MA, USA) and kept at  $-80^{\circ}\text{C}$  until used. Nucleic acids were subjected to routine laboratory viral investigation. One-step Pan-RT-PCR and PCR assays were performed using a separate specific primer set for each of a broad range of morbilliviruses (targeting the 155-bp fragment in the L gene of morbilliviruses) (Woo et al., 2012), parvovirus (Mochizuki et al., 1996), herpesvirus (VanDevanter et al., 1996), feline leukemia virus (FeLV) (Tandon et al., 2005), feline immunodeficiency virus (FIV) (Dandekar et al., 1992), calicivirus (Piewbang et al., 2019a) and coronavirus (Ksiazek et al., 2003), as described previously. Samples previously known to be positive for CDV, feline parvovirus (FPV), feline herpesvirus-1 (FHV-1), FeLV, FIV, feline calicivirus (FCV) and feline coronavirus (FCoV) were used as PCR positive controls while distilled water instead of DNA template was used as a negative control.

In addition, an IHC assay to detect CDV antigens was performed on formalin-fixed paraffin-embedded (FFPE) sections of the above-mentioned tissues using a monoclonal mouse antibody against the CDV envelope protein (Monotope; ViroStat, , ME, USA) as previously described (Techangamsuwan et al., 2015). The lung section was obtained from a CDV-infected dog as a positive control and the primary antibody was omitted as a negative control.

### **Molecular analysis of the FeMV L gene**

Positive samples from the pan-morbillivirus RT-PCR were then subjected to a specific pan-paramyxovirus RT-PCR (PAR-RT-PCR), amplifying the 612-bp fragment of the L gene of paramyxoviruses, as described previously (Tong et al., 2008), with minor modifications by changing the annealing temperature to  $49.6^{\circ}\text{C}$ . Subsequently, PCR products of the partial L gene were run on the QIAxcel capillary electrophoresis (QCES) platform as described previously (Piewbang and Techangamsuwan, 2019). Briefly, the PCR-amplified fragments were analyzed based on high-throughput capillary

electrophoresis using the QIAxcel DNA High Resolution Kit (Qiagen, Hilden, Germany). A custom alignment marker of 15–1,000-bp was simultaneously run with the samples. The QIAxcel DNA size marker (50–800)-bp was used for size estimation. The samples were analyzed using the default OM500 method at 5 kV of separation voltage, 10 s sample injection time and 500 s separation time, using QIAxcel technology. The QCES platform automated the process of detecting and measuring the size and quantity of the PCR-amplified DNA products. The positive PAR-RT-PCR samples were further resolved by 1.5% (w/v) agarose gel electrophoresis and then purified using a NucleoSpin® Extract II kit (Macherey-Nagel, Düren, Germany). The purified amplicons were submitted for commercial Sanger sequencing at Macrogen Inc. (Incheon, South Korea).

The obtained partial FeMV L gene sequences derived from both black leopards were aligned with the FeMV sequences available in GenBank using the MEGA7 software and MAFFT version 7 (<http://maf.cbrc.jp/alignment/server/>). The output alignments were then used as a template for phylogenetic tree construction and pairwise nucleotide distance matrix analysis. The phylogram was constructed using the maximum likelihood (ML) method with the generalized time reversible (GTR) model, as selected by analysis in the ‘find-best-fit’ model algorithm in the Mega 7 software according to the Bayesian information criterion (BIC). The tree was bootstrapped with 1,000 replicates.

To confirm further the presence of FeMV nucleic acids in other tissues derived from the two black leopards, viral nucleic acids were extracted from collected FFPE tissues of both leopards as described previously, using an AllPrep DNA/RNA FFPE kit (Qiagen, Hilden, Germany), following the manufacturer’s recommendations. The extracted nucleic acids were then subjected to the pan-morbillivirus RT-PCR assay as mentioned above.

## Antibody production and analysis of FeMV-M protein

### Construction of the recombinant (r)FEMV-M encoding plasmid

The full-length nucleotide sequence of the FeMV strain Thai-U16 M protein was amplified from the genomic RNA by RT-PCR (accession number: MF627832) using the FeMVMATRIX1011\_F (5'-ATAGAATTCATGACTGAGATATTCACCTCTTGATGAGAGC-3') and FeMVMATRIX1011\_R (5'-TATCTCGAGTTTAATCTTGAAGAGACCATTGGTATTGTCAATAAT-3') primer pair with 5' flanking EcoRI and XhoI restriction sites (underlined), respectively, for cloning. Subsequently, the target M gene (1,014- bp in length) was cloned into the pGEM-T Easy vector (Promega, WI, USA) and transformed into competent Escherichia coli DH5 $\alpha$  cells (Thermo Fisher Scientific, MA, USA). After cloning, transformed colonies were selected from Luria-Bertani (LB) agar plates with ampicillin, enriched in LB medium containing ampicillin (50  $\mu\text{g mL}^{-1}$ ) and then subjected to DNA extraction using an E.Z.N.A.<sup>®</sup> Plasmid mini kit I (Omega Bio-tek, GA, USA). The resulting expression plasmid, named as FeMV-M, was verified by double enzyme digestion and DNA sequence analysis.

Next, FeMV-M was further subcloned into the pet24a(+) expression vector (Novagen, Darmstadt, Germany), transformed into E. coli BL21 (DE3) cells (Novagen, Darmstadt, Germany) and plated on LB agar plates containing kanamycin (50  $\mu\text{g/mL}$ ). After enrichment of the selected colony in kanamycin containing LB medium, the derived pet24\_FeMV-M expression plasmid was verified by EcoRI and XhoI digestions and confirmed by Sanger sequencing. The rFeMV-M protein was tagged with a six-histidine residue on the C-terminus after subcloning in the pet 24a(+) expression vector and was designated as His-rFeMV-M.

### **Expression and enrichment of His-rFeMV-M**

The expression of His-rFeMV-M was induced by adding isopropyl- $\beta$ -D-thiogalactopyranoside (Sigma-Aldrich®, MO, USA) into the selected transformant culture for 10 h at 28 °C with shaking at 250 rpm. After harvesting the E. coli by centrifugation at 5,000g for 15 min at 4 °C, the expression of His-rFeMV-M was analyzed using 12% (v/v) sodium dodecyl sulfate–polyacrylamide gel electrophoresis (SDS-PAGE). The gels were stained with Coomassie brilliant blue to verify the presence of His-rFeMV-M at 36 kDa molecular weight (MW). Induced cells were pelleted, triple-washed with phosphate buffered saline (PBS), then lysed by sonication in an ice–water bath for 30 min at 50% duty cycle. After centrifugation, the lysed-cell suspension was clarified by centrifugation at 10,000g for 30 min at 4 °C and the resulting precipitate was dissolved in 6 mL binding buffer containing 6 M urea on ice and incubated for 1 h to dissolve the protein completely. The residual insoluble materials were discarded by centrifugation at 16,000g for 30 min at 4 °C, while the supernatants were harvested, filtered through a 0.45  $\mu$ m membrane and then enriched through affinity chromatography using a His Bind Kit (Novagen, Darmstadt, Germany) according to the manufacturer’s instructions. The enriched His-rFeMV-M protein was subjected to SDS-PAGE analysis and the final concentration was determined using a Nanodrop ND-1000 spectrophotometer (Thermo Fisher Scientific, MA, USA).

### **Western blot analysis**

The enriched (to apparent homogeneity) His-rFeMV-M protein was mixed with an equal volume of sample loading buffer, boiled at 70 °C for 10 min and separated on a 5% (w/v) stacking/12% (w/v) separating SDS-PAGE apparatus in a Tris–glycine buffer (0.025 M Tris base, 0.25 M glycine, 0.1% (w/v) SDS). The gel was prepared for western blotting as follows. The resolved His-rFeMV-M protein was electrically transferred onto a polyvinylidene fluoride (PVDF) membrane with a Transblot apparatus (Bio-Rad, CA,

USA). After triple-washing, the PVDF membrane with 0.1% (v/v) Tween-20 in PBS (PBST), the membrane was blocked overnight at 4 °C with PBST containing 5% (w/v) skimmed milk powder. The membrane was then incubated overnight at 37 °C with a Ni-NTA-horseradish peroxidase (HRP) conjugate (Qiagen, Hilden, Germany), then washed three times with PBST and the final colour reaction was developed with a solution of 3,3'-diaminobenzidine tetrahydrochloride (DAB) to visualize the specific protein band at 36 kDa MW (His-rFeMV-M). The total lysate of *E. coli* with empty vector was used as a negative control.

### **Production of polyclonal antibody against the His-rFeMV-M protein**

A 3-month old New Zealand White rabbit was used in this study [licence number IACUC EA-010/59 (R)]. Five mL of blood was collected from the middle ear vein of the rabbit on day 0 for preparing pre-immunized serum as a negative control and the rabbit was then inoculated by the subcutaneous route with 150 µg His-rFeMV-M in 1 mL mixed with complete Freund's adjuvant (Sigma-Aldrich<sup>®</sup>, MO, USA) at a 1:1 (v/v) ratio. The rabbit was then injected as above on days 14, 28 and 42, but with incomplete Freund's adjuvant (Sigma-Aldrich<sup>®</sup>, MO, USA) replacing the complete adjuvant. On day 56, the rabbit was humanely euthanized, and then blood was collected from the 7<sup>th</sup>-8<sup>th</sup> left intercostal area of the heart and subjected to serum separation by centrifugation at 3,000g for 15 min at 4 °C. The immunoglobulin G (IgG) fraction in the serum was subsequently purified using an Econo-Pac<sup>®</sup> Protein A Kit (Bio-Rad, CA, USA) and stored at -20 °C until use. Finally, the resulting IgG polyclonal antibody against His-rFeMV-M was verified by western blotting to confirm its size and immunogenicity.

### **In-situ FeMV antigen detection by IHC and IF**

The IHC was performed using the HRP-conjugated envision polymer method to confirm the presence of the FeMV antigen in the FFPE tissues. Sections of collected

tissues were cut at 4  $\mu\text{m}$  thickness and placed on positive slides. After deparaffinization and hydration, the slides were pre-treated with distilled water and autoclaved at 121  $^{\circ}\text{C}$  for 5 min and then endogenous peroxidase and non-specific activities were blocked by incubating first with 3% (v/v) hydrogen peroxide solution at room temperature for 30 min and then with 5% (w/v) skimmed milk powder in PBS at 37  $^{\circ}\text{C}$  for 45 min, respectively. Sections were subsequently incubated overnight at 4  $^{\circ}\text{C}$  with the generated rabbit polyclonal antibody against His-rFeMV-M protein at a dilution of 1:500. After triple-washing, sections were incubated in the anti-rabbit Dako REAL™ EnVision™ Detection system (Dako, Glostrup, Denmark) at room temperature for 45 min. Finally, after washing as above, the positive antigen-antibody reaction was detected by labelling with DAB and counterstained with Mayer's hematoxylin before mounting. A positive signal appeared as a brown colour in the infected cells.

The sets of lung, brain, lymph node and kidney sections from a FeMV-1 infected cat and a CDV-infected dog were immuno-stained in parallel as positive controls. The negative control was kidney sections of case 2 incubated as above except with rabbit polyclonal antibody against herpes simplex virus type 1 (HSV-1; code B 0114, Dako, Glostrup, Denmark) in place of that against the His-rFeMV-M protein.

To confirm further the presence of the FeMV antigen in tissues, 4  $\mu\text{m}$  thick FFPE sections of kidney and spleen of both cases were deparaffinized, rehydrated and pre-treated as mentioned above ready for IHC analyses. For antigen retrieval, the slides were enzymatically treated with 0.05% (w/v) trypsin at 37  $^{\circ}\text{C}$  for 30 min. The endogenous peroxidase and non-specific activities were blocked and then incubated with the generated rabbit polyclonal antibody against His-rFeMV-M as detailed for the IHC analysis. After triple washing with PBS, sections were incubated with FITC-conjugated goat anti-rabbit IgG F(ab')<sub>2</sub> secondary antibody (Invitrogen, CA, USA) at room temperature for 1 h. The slides were counterstained with 4',6-diamidino-2-phenylindole (DAPI; Invitrogen, CA, USA), mounted with a cover slip and visualized



under a fluorescence microscope. A positive signal appeared as a bright green color in infected cells. As a negative control, a kidney section of case 2 was incubated with rabbit polyclonal antibody against HSV-1 (code B 0114).

### **Retrospective study of FeMV in other wild felids**

In order to investigate the potential role of FeMV in other wild felids in the recent past, fresh-frozen tissue samples of kidneys and various organs from eight tigers (*Panthera tigris*) and three fishing cats (*Prionailurus viverrinus*) dating back to 2012 were also included in this study. All animals had been raised in the same zoo as the two black leopards and died without specific conditions. Nucleic acid was extracted from samples and then tested with the pan-morbillivirus RT-PCR and the PAR-RT-PCR assays, as described above.

## **Results**

### **Pathological changes**

Postmortem examination of both black leopards showed moderately poor body condition with evidence of dehydration and pale mucous membranes. Generally, the prominent gross findings of both black leopards were similar with moderately contracted kidneys that were pale brown, and had multifocal areas of light tan discoloration of the renal parenchyma and some areas of cortical depression. There was a greater severity of kidney abnormalities in case 2 (Fig. V-1), which also had mineralization in various organs including the lungs, blood vessels, gastric mucosa, tongue, and muscles.

The histological findings were broadly similar among the two black leopards with moderate infiltration of lymphocytes and plasma cells in the renal tubular interstitium (Fig. V-2). Severe diffuse tubular necrosis and moderate renal tubular degeneration

were also observed (Fig. V-3). These findings were interpreted as chronic tubulointerstitial nephritis, although the severity varied between the two black leopards. Moderate lymphoid depletion, severe splenic congestion, and moderate histiocytic and plasmacytic infiltration were noted in case 2 (Fig. V-4), while case 1 had less severe lesions. The other examined organs were histologically normal.

### **Virology investigation and identification of FeMV**

To identify potential viral causative agents, extracted viral nucleic acids from the urine and kidney samples of these two leopards were screened using several pan-viral PCRs for morbillivirus, parvovirus, herpesvirus, FeLV, FIV, calicivirus and coronavirus, with the same FFPE tissues used for IHC detection of CDV antigen. While the samples showed negative results for all the other tests, the pan-morbillivirus RT-PCR was positive. The 155-bp amplicon obtained from the pan-morbillivirus RT-PCR was sequenced and aligned to the homologous sequences obtained from GenBank (BLASTn search), which showed an approximately 98% RNA (as cDNA) sequence similarity to FeMV-annotated sequences. This prompted us to investigate the presence of FeMV nucleic acid in other extracted FFPE tissues using the pan-morbillivirus RT-PCR. The 155-bp specific FeMV amplicon was detected in the kidneys of both black leopards and in the spleen of black leopard case 2, but the other tissues were negative including brain, heart, liver, lung and lymph node.

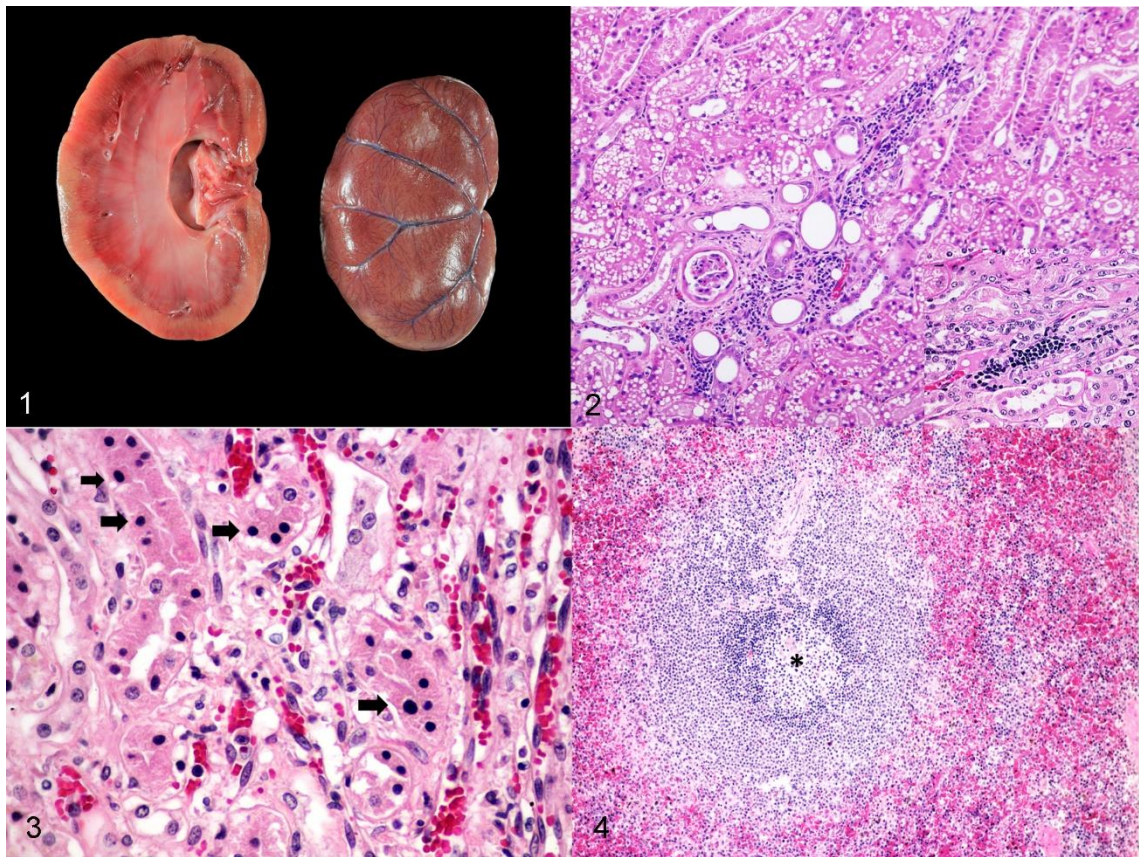


**Figure V-1** Feline morbillivirus infection, kidney, black leopard, case 2.

Contracted kidney. There are variably sized, multifocal areas of light tan discoloration on the external surface of the kidney with some areas of cortical depression. On the cut surface, the parenchyma is light tan.

**Figure V-2** Locally diffuse lymphoplasmacytic tubulointerstitial nephritis (HE).

Characterized by infiltration of lymphocytes and plasma cells in the renal tubular interstitium (inset).

**Figure V-3** Moderate renal tubular necrosis (HE).

Indicated by pyknotic nuclei of tubular epithelial cells (arrows).

**Figure V-4** Feline morbillivirus infection, spleen, black leopard, case 2 (HE).

There is lymphoid depletion (asterisk) indicated by hypocellularity of the splenic white pulp and splenic congestion with infiltration of histiocytes and plasma cells in the red pulp.

### **Molecular analysis of the FeMV L gene**

Since kidney samples of both black leopards showed positive results in the pan-morbillivirus RT-PCR, the presence of FeMV nucleic acid was confirmed using pan-specific RT-PCR for paramyxovirus, targeting the partial L gene of FeMV. The 612-bp FeMV L fragment was amplified, sequenced, and found to share 98.9% genetic similarity among leopard samples and 98.2% genetic similarity to the FeMV-1 strain CTL43 (accession MN164532) derived from the urine of a domestic cat in Thailand (Supplemental Figures S1 and S2). Due to the limitations of fresh tissue samples, we were not able to evaluate viral replication in cell culture nor to amplify the whole genome of the black leopard FeMV. The partial genome sequences of black leopard FeMV were deposited in GenBank with accession numbers MN295672 and MN295673 for cases 1 and 2, respectively. The ML-based phylogenetic analysis of the FeMV L gene showed the black leopard FeMVs grouped in the FeMV-1 genotype and in the Asian FeMV-1 cluster, forming a monophyletic branch close to FeMV strains CTL43, CTL16 and U16, all from Thailand (Fig. V-5).

### **Tissue localization of FeMV**

The presence of the FeMV antigen in the brain, heart, liver, lung, lymph node, kidney and spleen sections were evaluated by IHC analysis using a newly developed rabbit polyclonal antibody against rFeMV-M. The FeMV antigen showed diffuse and strong signals in the cytoplasm of the renal tubular epithelial cells in both cases (Fig. V-6) and in infiltrating lymphocytes in conjunction with tubulointerstitial nephritis of case 2 (Fig. V-7). Furthermore, the FeMV antigen was strongly labelled in the cytoplasm of infiltrating lymphocytes and histiocytes in the spleen of case 2, while case 1 showed weak staining. No FeMV antigen was detected in the other tissue sections examined (i.e., brain, heart, liver, lung, lymph node). To confirm the positive results of the IHC, IF analysis was additionally performed on the kidney and spleen sections using the same polyclonal antibody against rFeMV-M. Strong rFeMV-M signals were evident in the cytoplasm of the renal tubular epithelial cells, similar to that stained with IHC (Fig. V-

8), while the signals were diffusely labelled in mononuclear cells infiltrating the red pulp of the spleen (Fig. V-9).

### Retrospective study of FeMV in other wild felids

Extracted viral nucleic acids from fresh frozen tissues derived from eight captive tigers and three fishing cats were tested with the pan-morbillivirus and PAR-RT-PCR assays. There was no evidence of FeMV nucleic acids in those samples.

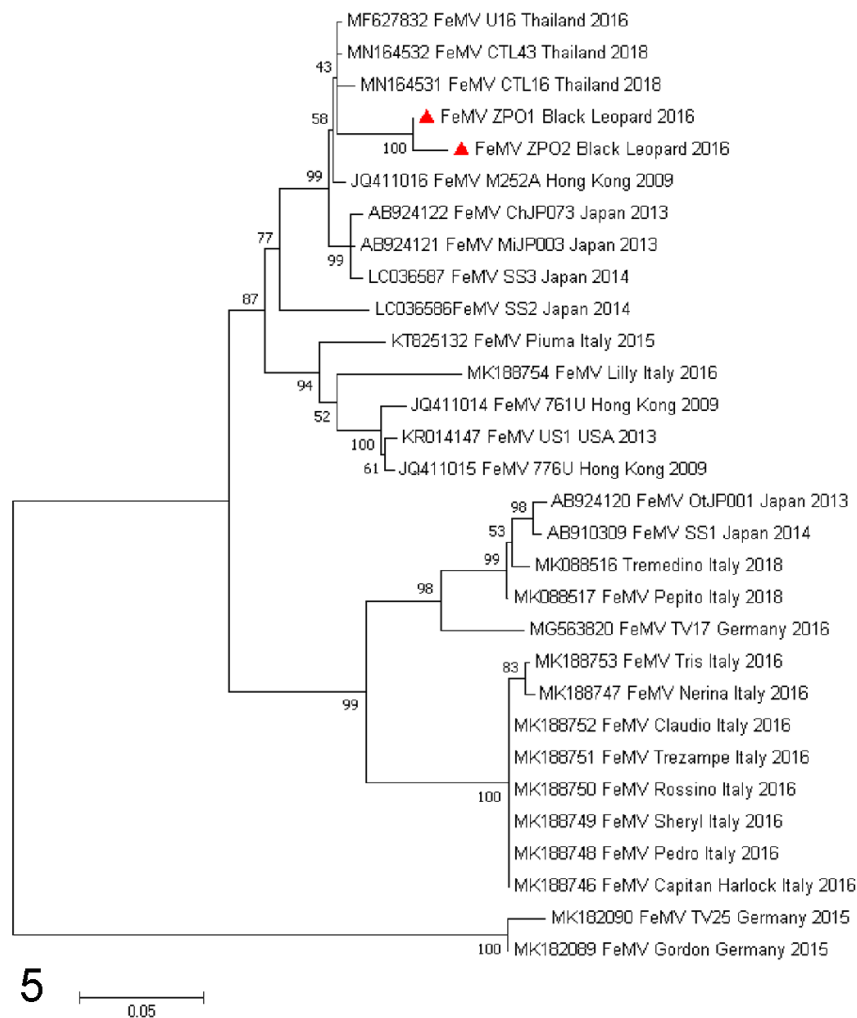


**Figure V-5** Phylogeny of feline morbillivirus genome sequences compared with reference FeMV viruses in the NCBI database.



Tree construction was performed by ML using the GTR nucleotide substitution, invariable sites and gamma distribution models (GTR+ G+I) for tree construction, as determined by BIC, with 1,000 bootstrapping replicates. Bootstrap values (%) are shown at each node. GenBank accession numbers are shown on the tree. The FeMV genomes detected in the leopard case 1 (ZPO1) and 2 (ZPO2) are indicated by red triangles. The bar indicates the estimated numbers of nucleotide substitutions per site.

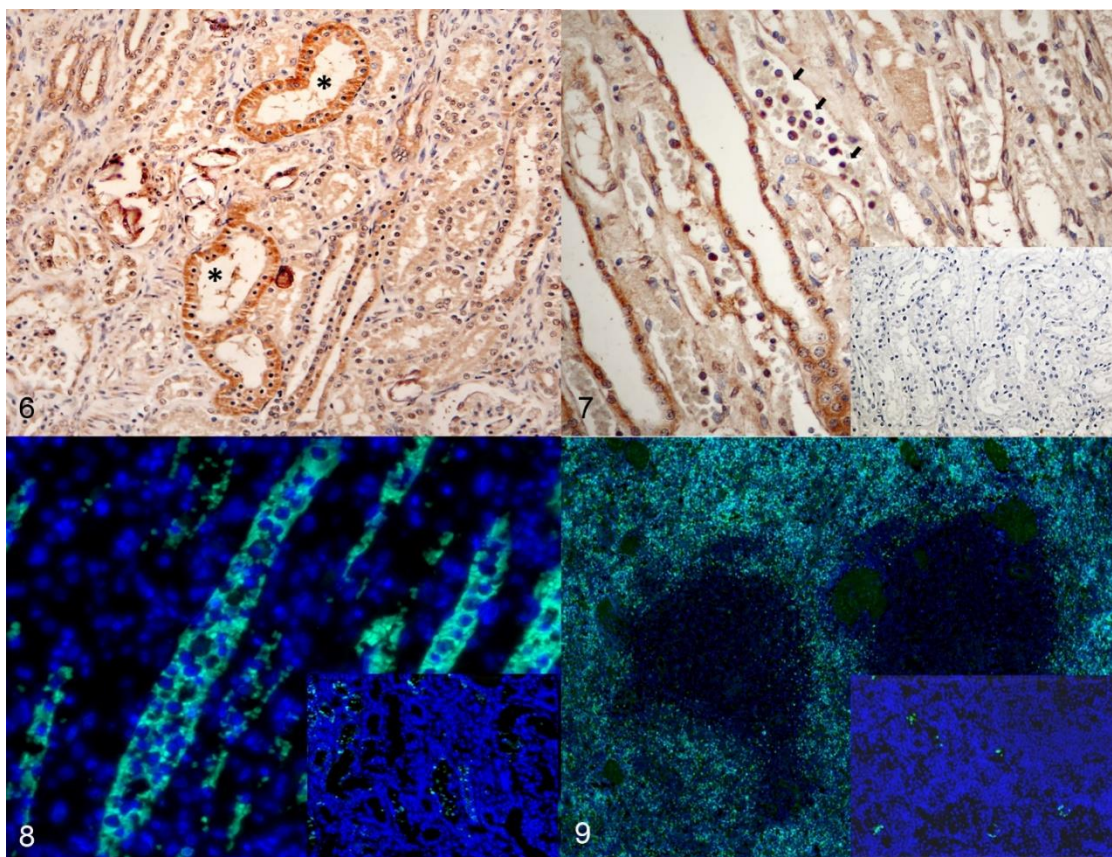


**Figure V-6** Feline morbillivirus infection, kidney, black leopard. Case 1 (IHC).

There is strongly positive immunolabeling (dark brown) within the cytoplasm of renal tubular cells of the renal cortex (asterisk). Immunohistochemistry for feline morbillivirus.

**Figure V-7** Kidney. black leopard. Case 2 (IHC).

Immunolabeling within the cytoplasm of renal tubular epithelial cells and infiltrating lymphocytes in the tubular interstitium (arrows). No immunoreactivity was observed in the negative control (inset). Immunohistochemistry for feline morbillivirus.

**Figure V-8** Kidney. Black leopard. Case 1 (IF).

Strong immunofluorescence (bright green) in the cytoplasm of renal tubular epithelial cells. Immunofluorescence for feline morbillivirus. DAPI staining (bright blue colour) was used to identify the nuclei and to evaluate gross cell morphology. No positive-immunolabelled signal was detected in negative control (inset).

**Figure V-9** Spleen, black leopard, case 2 (IF).

Diffuse immunofluorescence (bright green colour) within the red pulp. Immunofluorescence for feline morbillivirus. DAPI staining (bright blue) was used to identify the nuclei and to evaluate gross cell morphology. No positive signal was detected in negative control (inset).

## Discussion

In recent years, the FeMV isolates have been discovered in domestic cats in association with, and as the proposed cause of, renal disease (Woo et al., 2012). Even though the proposed cause of renal disease in domestic cats by FeMV infection is yet to be confirmed, due to inconsistent results in recent publications (Park et al., 2016; Darold et al., 2017; Yilmaz et al., 2017), the evidence of FeMV localization in renal tubular epithelial cells in cats with renal disease warrants further clarification as to whether FeMV isolates are associated with the disease.

The CDV, as the FeMV counterpart, has been reported as a pathogen causing fatal outbreaks in various carnivores throughout wild felids (Loots et al., 2017; Piewbang et al., 2020a), supporting the possible role of morbillivirus infection across a diverse range of hosts. Thus, we therefore were interested in investigating whether FeMV was associated with disease in wild felids.

In this study, we describe the detection and characterization of FeMV, which was detected in the urine, kidney, and spleen samples of two black leopards showing evidence of tubulointerstitial nephritis. Although the postmortem examinations revealed evidence of renal failure without specific infection, both the genetic detection, using several pan-conventional PCRs in combination with genetic sequencing, and IHC analyses of the tissue samples of both black leopards revealed no other viruses except for FeMV. Moreover, the FeMV antigen was also found in the kidney and spleen FFPE tissues by PCR, IHC, and IF analyses.

Since the black leopard FeMVs were genetically similar to the FeMV isolated from cats in Thailand, the possible role of FeMV transmission between domestic cats and leopards should be considered and needs further investigation. In this study, the whole genome of the black leopard FeMV was not determined because of the limited amount of sample. The identification of FeMV antigen in the tissues supports an association of FeMV infection with tubulointerstitial nephritis. A retrospective study of FeMV nucleic acid detection in tissue samples of two other wild felid species showed no evidence of FeMV infection, suggesting that FeMV infection is not common in these species. However, there were no FFPE sections available from these animals to examine the kidney lesions and only a relatively small number of animals were tested and from different temporal periods and different species. Therefore, definitive conclusions on the association of FeMV infection and tubulointerstitial nephritis in black leopards cannot be drawn.

To understand the role of FeMV-associated renal disease in these black leopards, viral antigen was identified in tissues with histological lesions of fatal tubulointerstitial nephritis. Here, the FeMV antigens were generally localized in the cytoplasm of renal tubular epithelial cells and in the mononuclear cells that had infiltrated the renal interstitial lesions. Thus, this study demonstrated FeMV localization in the tubular epithelial cells, where the most pathological changes (i.e. tubular



degeneration) were observed. This finding is similar to those in FeMV-infected domestic cats (Park et al., 2016; Sutummaporn et al., 2019). Furthermore, FeMV antigen was identified in the lymphocytes, which corresponds to the lymphotropic nature of other morbilliviruses and evidence from in vitro studies of FeMV infection (De Vries et al., 2015; Sakaguchi et al., 2015). However, the incongruous results for FeMV identification using PCR and IHC of the spleen of case 1 may result from low amounts of extracted FeMV-1 RNA from FFPE tissue that can impact subsequent ancillary diagnostics.

Recently, CDV has been detected in large felids and associated with fatal diseases in large groups of felines (Appel et al., 1994; Roelke-Parker et al., 1996; Seimon et al., 2013; Sulikhan et al., 2018). The discovery of FeMV in two black leopards, which is listed as a vulnerable species by the International Union for Conservation of Nature Red List raises concerns about a new, potentially fatal disease that can develop in other endangered *Felidae* species. The transmission and pathogenesis of FeMV infection in leopards and other non-domestic cats warrants further investigation.

In this study, we identified the presence of FeMV at post-mortem in two black leopards in Thailand that showed clinical evidence of chronic kidney disease. This is the first report of FeMV in a non-domestic felid species. Additional testing to further characterize the virus and determine if it is identical to FeMV-1 is needed. The molecular identification of FeMV localization in tissues was confirmed by IHC and IF analyses, in conjunction with pathological changes in the kidney and spleen, suggesting a possible role of FeMV in this disease. A causative association between FeMV and fatal tubulointerstitial nephritis in black leopards could not be determined but remains possible.

## Acknowledgements

Chutchai Piewbang was funded by a grant from the Ratchadaphisek Somphot Fund for Postdoctoral Fellowship, Chulalongkorn University. Surangkanang Chaiyasak was supported by the 100<sup>th</sup> Anniversary Chulalongkorn University Fund for Doctoral Scholarship. We are grateful to Asst. Prof. Dr. Theerawat Tharasanit and Mr. Rattapoom Thaiwong for technical assistance.



## CHAPTER VI

### DISCUSSION AND CONCLUSION

#### General discussion

Since genus *Morbillivirus*, family *Paramyxoviridae*, play a key role in many important fatal diseases in human and animals (Anderson, 1995; Barrett, 1999; Guardo et al., 2005; De Vries et al., 2015), Feline morbillivirus (FeMV) is a relatively new discovered in morbilliviruses (Woo et al., 2012). FeMV research has widely gained attention and consecutively approached in domestic cat population worldwide. Those studies indicated that FeMV might have significant impact beyond the felid health (Choi et al., 2020). However, FeMV pathogenesis is incoherently clarified due to the insufficiency of FeMV infected cases, clinical data, and the unsuccessful *in vitro* cultivation. To overcome these burdens, the various viral infective stages and continuous follow-up FeMV-infected cases will be needed. Thus, we performed the FeMV studies in Thailand since 2016-2019 in the aspects of molecular characterization, serological test, histopathology, and virus localization. These studies provided the insightful data and raised new understandings of FeMV-infected animals, not only domestic cats but also in black leopards (*Panthera pardus*).

#### Genetic-based surveillance of FeMV infection in Thai domestic cats

This is the first report of the molecular identification and epidemiology of FeMV genotype 1 (FeMV-1) in Thailand, revealing the existence of FeMV in Thai cats. The identified Thai FeMV strains had a genetic homology amongst themselves and were classified as FeMV-1A without any evidence of genetic recombination. The prevalence of FeMV in the present study (11.9%) was quite similar to that reported from Hong Kong (12.3%) (Woo et al., 2012), but higher than those reported in some other regions,

such as Turkey (5.4%) (Yilmaz et al., 2017) and Japan (6.1%) (Furuya et al., 2014), or lower than that in Malaysia (39.4%) (Mohd Isa et al., 2019). This discrepancy in the FeMV prevalence may result from various factors, such as the cat's colony and the testing groups (Furuya et al., 2014; Yilmaz et al., 2017).

Interesting, FeMV that positive in their urine were associated with abnormal urine characteristics, such as hematuria, pyuria, proteinuria, and aciduria. Even though this association was not statistically significant, it might raise a note of FeMV infection in cats showing urinary tract infections (UTIs), since a small number of recent publications have demonstrated urinalysis results in cats with FeMV (Darold et al., 2017; Yilmaz et al., 2017; Stranieri et al., 2019). However, other potential pathogens contributing to the feline UTIs, which are bacteria, FIV, leptospirosis and bartonellosis (Jepson, 2016), were not excluded from this study.

The genetic variations of the H and F genes of the FeMVs have been focused and interpreted in this study. Contrast to the CDV, we observed that the F gene of the FeMVs revealed more hypervariable portion than the H gene. The effects of amino acid mutations in the F and H genes, which are hypothesized to be associated with the viral infectivity and virulence, needs further investigation in a future study. In addition, we also proposed distinct deduced amino acid residues in the F and H genes that can potentially differentiate isolates within the FeMV clades.

RNA viruses possess a high mutation rate as a result of viral RNA polymerases lack a proof-reading property, then allowing rapid adaptations to various selection pressures (Yuan et al., 2017; Piewbang and Techangamsuwan, 2019). To understanding the evolutionary of FeMVs, the algorithms were used in the study. The recent studies have shown evidence of other morbilliviruses undergoing selective pressure, such as the negative and positive selective pressure for canine distemper virus and measles virus, respectively (Ke et al., 2015; Piewbang et al., 2019b). In this study, we found that

overall the FeMV evolution has undergone a negative selective pressure, but positive selection sites were observed, with the highest frequency in the P gene, followed by in the H, N and F genes. This finding may suggest that these FeMV genes may play a role in FeMV evolution and emphasize the importance of P gene, the non-structural gene of morbillivirus, in the aspect of immunopathogenesis in particular hosts as already mentioned previously in rinderpest virus (RPV) and measles virus (MeV) (Chinnakannan et al., 2013). However, the data used in this study were restricted to the 23 currently available full-length FeMV genomes. More analyzed sequences would likely allow a more clear understanding of FeMV evolution.

#### **FeMV antibody against matrix protein in Thai domestic cat**

Along the molecular study, to complete the epidemiology surveillance of FeMV infection, The recombinant matrix protein of FeMV was properly constructed by bacterial expression system. Among the unglycosylation protein (N, P, M and L), we have attempted to use the M protein in this study because of 1) M protein is the virus inner membrane, attached to other integral glycoprotein such F and H genes and (Mahapatra et al., 2006) 2) M protein has more identity of amino acid sequence among feline morbillivirus clades (Chaiyasak et al., 2020) and incline to have more sensitivity in serological testing when compare to other protein of FeMV has been used (Arikawa et al., 2017). This study investigated two categories of cats derived from the sheltered and hospitalized cats in Thailand. Both colonies were different result of prevalence of FeMV RNA positive blood. The shelter colony had significantly higher prevalence (19.6%, 11/56) than the hospitalized colony (0%, 0/80) ( $p < 0.001$ ). This data support to other previous research that sheltered cats had more circulated FeMV transmission (De Luca et al., 2020). Although, the hospitalized cat bloods were negative to molecular study, but the immunoblotting result of the FeMV antibody against M protein are recognized with significantly higher than sheltered cats ( $p < 0.001$ ) at that

time. However, this study has performed in sheltered and hospitalized cats which was indicating the high prevalence of FeMV infection in Thai domestic cats.

Comparison between real time-RT-PCR and immunoblotting, the positive FeMV RNA blood samples do not correlate to the positive cat sera. Whereas the pitfall of this study is not detected FeMV in urine sample that might enhancing to completely identify the status of FeMV infection in these cats. Possibility, the reason of uncorrelation between viremia and antibody production may cause by FeMV has short viremia in the host (Mohd Isa et al., 2019).

This study showed relatively higher prevalence of FeMV antibody detection than previous studies (Woo et al., 2012; Sakaguchi et al., 2014; Park et al., 2016; Arikawa et al., 2017; De Luca et al., 2020) might be due to M protein has more amino acid identity in between the FeMV genotypes (Chaiyasak et al., 2020). In addition, the cut off value in this study (CO=0.244) is lower than previous study (CO=0.43) (Arikawa et al., 2017) that might lead to have more FeMV positive sera. By the way, we have another pitfall that have no testing for the antibody against other morbilliviruses such as canine distemper (CDV) antibody in dog sera, which previous research have been reported that cat sera had neutralizing anti-CDV antibodies (Appel et al., 1974; Ikeda et al., 2001). The result might be false positive from the cross reaction between rHis-FeMV\_M and CDV antibody in cat serum. The cross reaction performing is needed in further study.

Another reason supporting that FeMV has short viremia, this study showed the lower rate of RNA+/Ab+ (4.4%) and highest rate was in RNA-/Ab+ (62.5%) indicated that cats have been infected with FeMV without viremia phage were more than cats showed up with viremia and immune response. This preliminary study of i-ELISA based rHis-FeMV\_M is susceptible agreement related with western blotting. However, in

serological test, the viral neutralizing assay is further needed to validate the ELISA based rHis-FeMV<sub>M</sub>.

This study revealed that serological test in FeMV, such i-ELISA using matrix protein as an antigen, is useful to detect FeMV infected cat. Nevertheless, the FeMV pathogenesis is still unclear, thus the antigen and antibody-based techniques will be ready to perform in viral infection in larger scale of cases. However, this study is initially started with small scale of Thai domestic cat, thus larger scale of cat population in various colonies will raise the understanding of FeMV infection.

#### **Localization of FeMV antigen in cats with active FeMV infection**

A number of viruses causing CKD are documented such as feline immunodeficiency virus (FIV), feline leukemia virus (FeLV), feline infectious peritonitis virus (FIPV) (Brown et al., 2016), feline paramyxovirus (FPaV) (Sieg et al., 2015), and FeMV (Woo et al., 2012; Sutummaporn et al., 2019; Crisi et al., 2020). However, the association of FeMV with kidney injury remained argumentative. To raise understanding of relation between FeMV and CKD, the study of variety stages of FeMV infected cat is need.

In this study, two naturally moribund cats suffering from acute hemorrhagic cystitis with unknown previous illness history were infected with FeMV-1A genotype which clarified by ultrastructural, molecular and IHC assays. By pathological study, the lesion of CKD or TIN such as mononuclear interstitial nephritis or renal fibrosis was not evidenced in renal tissues. This implied that both FeMV-infected cats were not involved with kidney inflammation, which in agreement with previous investigations (Sakaguchi et al., 2014; Darold et al., 2017; Yilmaz et al., 2017; McCallum et al., 2018; Mohd Isa et al., 2019; Stranieri et al., 2019).

Since the discovery of FeMV in 2012, the ultrastructural morphology of this virus was displayed only *in vitro* cell culture system (Woo et al., 2012). Multiple attempts had been conducted to persuade the existence of FeMV in urinary tract system either by genetic detection (Sakaguchi et al., 2014; Sieg et al., 2015; Park et al., 2016; Donato et al., 2019; Sieg et al., 2019; Stranieri et al., 2019; Chaiyasak et al., 2020; De Luca et al., 2020) or immunoreactive reaction (Woo et al., 2012; Park et al., 2016; Sharp et al., 2016; Yilmaz et al., 2017; De Luca et al., 2018; Donato et al., 2019; Sieg et al., 2019; Sutummaporn et al., 2019; De Luca et al., 2020). However, there was no *in situ* confirmation of FeMV. The round to oval intracytoplasmic eosinophilic hyalinized globules, especially in renal epithelial cells of proximal convoluted tubules at corticomedullary junction and renal pelvis in both cats, prompted us to perform further ultrastructural investigation. We, therefore, reported here as the first evidence of the typical herringbone appearance of viral ribonucleocapsid in paramyxovirus in non-kidney diseased cats. These findings implemented that FeMV could be dormant inside host without stimulating the host immune response. The viral property and pathogenesis of FeMV-induced disease are needed to clarify in future study.

Morbilliviruses possess the property of lymphotropism and epitheliotropism by invading host cells via specific cellular receptors including signaling lymphocytic activation molecule (SLAM) and nectin-4, respectively (Pratakpiriya et al., 2017). We demonstrated here the cellular localization of FeMV in infected cats by IHC technique, which are in accordance with previous research (Woo et al., 2012; De Luca et al., 2018; De Luca et al., 2020). FeMV-1A genotype identified in this study also had *in vitro* tropism for various epithelial cells of trachea, bronchi, bronchioles, kidneys, and urinary bladder, suggesting the epitheliotropic of FeMV, while the FeMV immunoreactivity was also evident in the cytoplasm of lymphoid cells, suggesting the nature of lymphotropic of FeMV that was recently described (Piewbang et al., 2020a). Moreover, the viral infectivity also expanded to residing glial cells in brain and infiltrating mononuclear



cells in spleen and lymph node. Even the neither definitive role of FeMV presentation with the association of the cause of death nor the role of hematuria in these cats were summarized, the immunoreactive results were in agreement with the Ct value derived from RT-qPCR assays, suggesting systemic viral infection.

This study provided another supportive evidence of FeMV infection in non-kidney diseased cats and indicated the dormant existence of FeMV in kidney in the absence of host immune response and pathological changes but remained the active FeMV infection. Significantly, we proposed that FeMV is renal epitheliotropic virus in cats by existing viral inclusions. Further a large scale of histopathological investigation should be warranted to elucidate the viral inclusion bodies in other organs.

#### **Molecular and pathological aspect in non-domestic cat**

In recent years, the FeMV isolates have been discovered in domestic cats in association with, and as the proposed cause of, renal disease (Woo et al., 2012). Even though the proposed cause of renal disease in domestic cats by FeMV infection is yet to be confirmed, due to inconsistent results in recent publications (Park et al., 2016; Darold et al., 2017; Yilmaz et al., 2017) the evidence of FeMV localization in renal tubular epithelial cells in cats with renal disease warrants further clarification as to whether FeMV isolates are associated with the disease. The CDV, as the FeMV counterpart, has been reported as a pathogen causing fatal outbreaks in various carnivores throughout wild felids (Loots et al., 2017; Piewbang et al., 2020a), supporting the possible role of morbillivirus infection across a diverse range of hosts. Thus, we therefore were interested in investigating whether FeMV was associated with disease in wild felids.

In this study, we describe the detection and characterization of FeMV, which was detected in the urine, kidney, and spleen samples of two black leopards showing evidence of tubulointerstitial nephritis. Although the postmortem examinations

revealed evidence of renal failure without specific infection, both the genetic detection, using several pan-conventional PCRs in combination with genetic sequencing, and IHC analyses of the tissue samples of both black leopards revealed no other viruses except for FeMV. Moreover, the FeMV antigen was also found in the kidney and spleen FFPE tissues by PCR, IHC, and IF analyses.

Since the black leopard FeMVs were genetically similar to the FeMV isolated from cats in Thailand, the possible role of FeMV transmission between domestic cats and leopards should be considered and needs further investigation. In this study, the whole genome of the black leopard FeMV was not determined because of the limited amount of sample. The identification of FeMV antigen in the tissues supports an association of FeMV infection with tubulointerstitial nephritis. A retrospective study of FeMV nucleic acid detection in tissue samples of two other wild felid species showed no evidence of FeMV infection, suggesting that FeMV infection is not common in these species. However, there were no FFPE sections available from these animals to examine the kidney lesions and only a relatively small number of animals were tested and from different temporal periods and different species. Therefore, definitive conclusions on the association of FeMV infection and tubulointerstitial nephritis in black leopards cannot be drawn.

To understand the role of FeMV-associated renal disease in these black leopards, viral antigen was identified in tissues with histological lesions of fatal tubulointerstitial nephritis. Here, the FeMV antigens were generally localized in the cytoplasm of renal tubular epithelial cells and in the mononuclear cells that had infiltrated the renal interstitial lesions. Thus, this study demonstrated FeMV localization in the tubular epithelial cells, where the most pathological changes (i.e. tubular degeneration) were observed. This finding is similar to those in FeMV-infected domestic cats (Park et al., 2016; Sutummaporn et al., 2019). Furthermore, FeMV antigen was identified in the lymphocytes, which corresponds to the lymphotropic nature of other

morbilliviruses and evidence from *in vitro* studies of FeMV infection (De Vries et al., 2015; Sakaguchi et al., 2015). However, the incongruous results for FeMV identification using PCR and IHC of the spleen of case 1 may result from low amounts of extracted FeMV-1 RNA from FFPE tissue that can impact subsequent ancillary diagnostics.

Recently, CDV has been detected in large felids and associated with fatal diseases in large groups of felines (Appel et al., 1994; Roelke-Parker et al., 1996; Seimon et al., 2013; Sulikhan et al., 2018). The discovery of FeMV in two black leopards, which is listed as a vulnerable species by the International Union for Conservation of Nature Red List raises concerns about a new, potentially fatal disease that can develop in other endangered *Felidae* species. The transmission and pathogenesis of FeMV infection in leopards and other non-domestic cats warrants further investigation.

In this study, we identified the presence of FeMV at post-mortem in two black leopards in Thailand that showed clinical evidence of chronic kidney disease. This is the first report of FeMV in a non-domestic felid species. Additional testing to further characterize the virus and determine if it is identical to FeMV-1 is needed. The molecular identification of FeMV localization in tissues was confirmed by IHC and IF analyses, in conjunction with pathological changes in the kidney and spleen, suggesting a possible role of FeMV in this disease. A causative association between FeMV and fatal tubulointerstitial nephritis in black leopards could not be determined but remains possible.

### **Limitation of the study**

#### **Molecular study and Immunohistochemistry**

Animal scale of the study is limited in both live and dead animals and FeMV Thai strain is difficult to propagate on CRFK cells.

### **Serology**

Along the serological assay, only blood sample have tested for FeMV RNA by qRT-PCR without testing in urine samples which leading to the lower prevalence of FeMV status in those cats. This study did not perform for other morbilliviruses such as canine distemper (CDV). The cross reaction is needed in further study.

### **Suggestion of the study**

The Further study have to obtain larger scale of felid population of both domestic and non-domestic cats. The other techniques such as viral neutralizing assay development, viral isolation in FeMV Thai strains in various cell types and cross reaction study of FeMV-M protein and Pab-FeMV-M to other morbilliviruses or feline viral pathogen are needed.

### **Conclusions**

This thesis provided the solid evidence and new knowledges regarding FeMV infection in both domestic and non-domestic felids. Kidney is the viral tropism organ which can be finally promoted further kidney diseases in the susceptible hosts, as well as, FeMV could shed via urine without clinical significance. Thus, we suggest that FeMV is playing role as an integral candidate virus that need to be tested in urologic associated cats. Moreover, since FeMV possesses the genetic diversity, comprehensive research on FeMV will be very useful to the cat health and close-related species. The FeMV study would be not accomplished unless its pathogenesis is well elucidated.

## APPENDIX

## Supplemental data of Chapter II

**Supplementary Table S1.** Primers for the RT-PCR amplification of the FeMV F and H gene.

Primer name	Primer sequence (5'-3')	Nucleotide position (based on MF627832)	Product size (bp)
CFW-F1	ATACCAATGGTCTCTTCAAGATTA	4374-4397	753
CRV-F1	TTGGAACCATCTTTATAACCAT	5104-5126	
CFW-F2	GGRGTTATAAGTACTAAGCA	5044-5063	714
CRV-F2	CAAATCAGTCATATCTGCAT	5738-5757	
CFW-F3	AATGGTAATCTTCAGGCA	5641-5658	893
CRV-F3	AGCGGTTCAATTGAAGTA	6516-6533	
CFW-H1	GTTAGAGCAATCAGATAAGATT	6354-6375	926
CRV-H1	GTAGGAATATGAAGTCCTA	7261-7279	
CFW-H2	ACTTAGGAATCCATGTTAAT	6929-6948	768
CRV-H2	ACTCGATATTGAACATCAGT	7677-7696	
CFW-H3	TCAGCAATCAACGTATAACATT	7600-7621	664
CRV-H3	AGAGAATTATGAGATGGAGCT	8243-8263	
CFW-H4	GACAACTCTGAGAATTACTGTA	8097-8118	816
CRV-H4	TTGGTAGTCTGACTGCTC	8895-8912	

**Supplementary Table S2.** Urinalysis and FeMV RT-PCR results from 100 cats's urine samples.

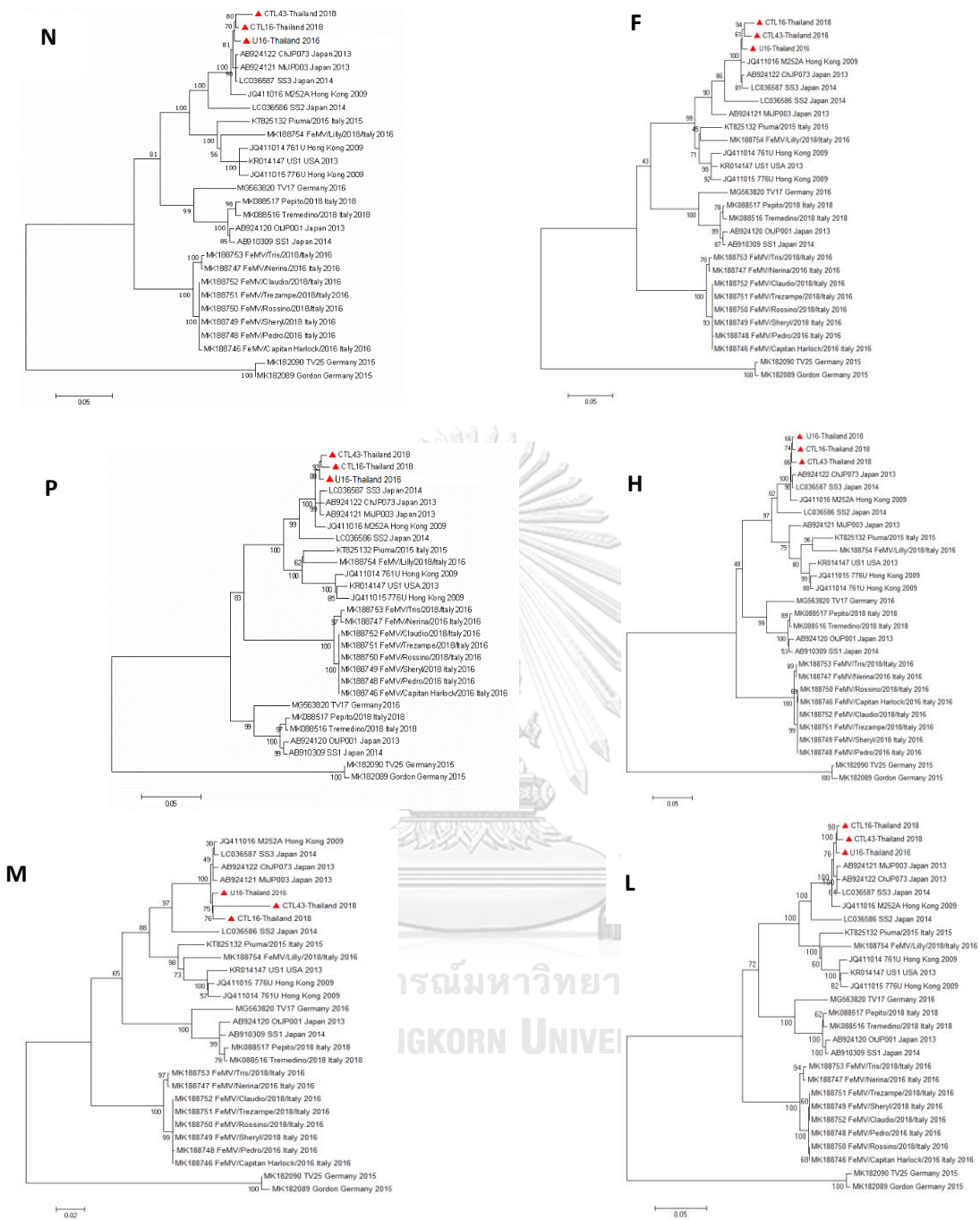
Urinalysis	FeMV-positive	FeMV-negative	P-value
<i>- Clarity</i>			
Turbid	4	33	0.6179
Clear	9	54	
<i>- Specific gravity</i>			
Hyposthenuria	1	13	0.528
Isosthenuria	9	46	
Hypersthenuria	3	28	
<i>- pH</i>			
Aciduria	9	61	0.9483
Alkalinuria	4	26	
<i>- Hematuria</i>			
Positive	11	56	0.1476
Negative	2	31	
<i>- Pyuria</i>			
Positive	10	57	0.4146
Negative	3	30	
<i>- Proteinuria</i>			
Positive	9	43	0.1825
Negative	4	44	
<i>- Crystalluria</i>			
Positive	2	20	0.537
Negative	11	67	
<i>- Bilirubinuria</i>			
Positive	0	2	0.583
Negative	13	86	
<i>- Glucosuria</i>			
Positive	1	3	0.4664
Negative	12	84	
<i>- Ketonuria</i>			
Positive	0	3	0.4966
Negative	13	84	
<i>- Urologic disease</i>			
Yes	13	78	0.6007
No	0	9	

**Supplementary Table S3.** Nucleotide identity of the full-length genome between FeMV-Thai strains and other genotypes and clades.

FeMV-Thai strains	Nucleotide identity (%)												
	FeMV-1A			FeMV-1B			FeMV-1C			FeMV-1D		FeMV-2	
	SS3	M252	US1	Pluma/2015	TV17	OUTP001	Tris/2018	Shery/2018	TV25	Gordon			
U16-2016	98.5	98.3	91.9	92.0	88.2	88.3	87.4	87.4	81.8	81.9			
CTL16-2018	98.4	98.08	91.8	91.9	88.1	88.2	87.2	87.2	81.8	81.9			
CTL43-2018	97.8	97.53	91.3	91.5	87.7	87.8	86.9	86.9	81.6	81.7			

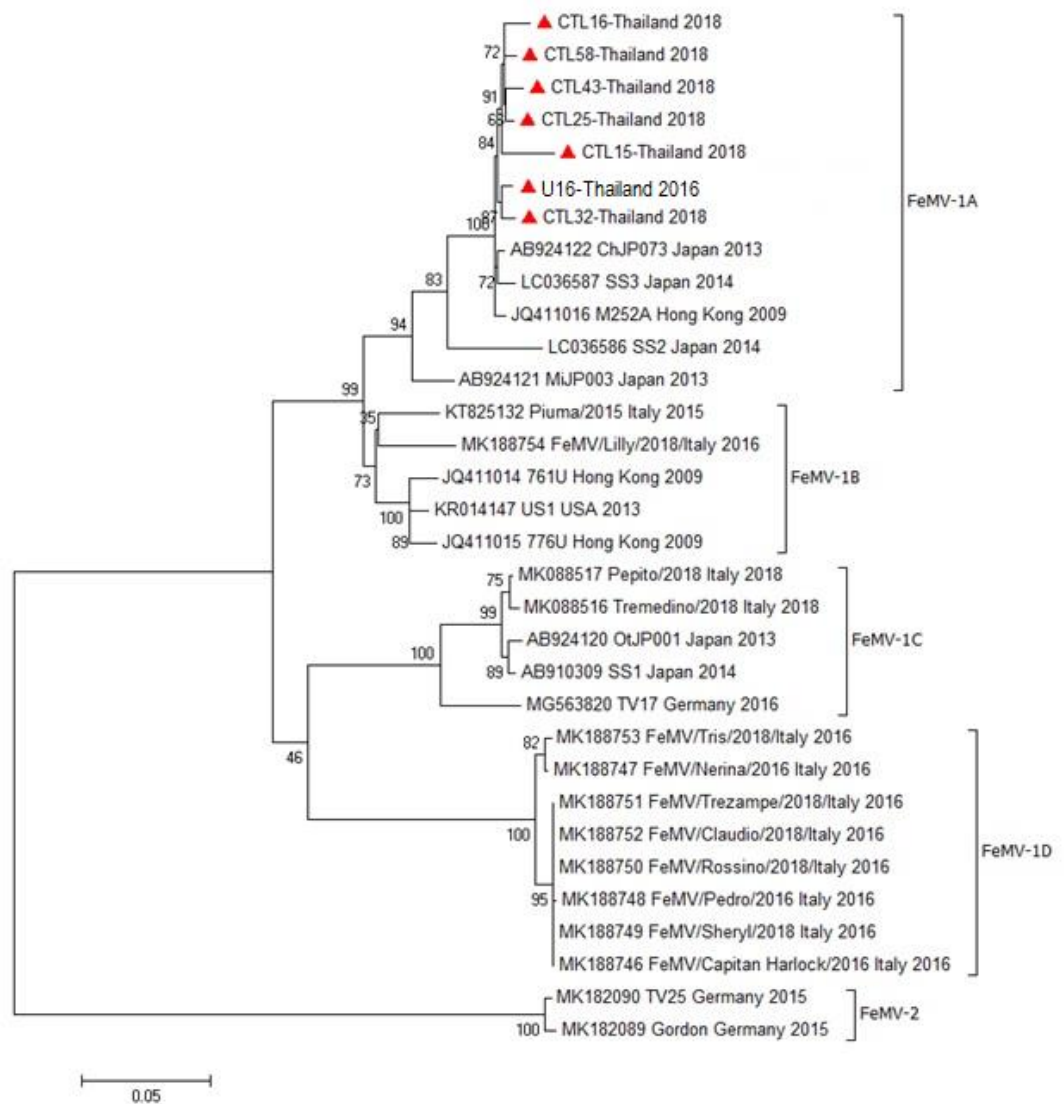
**Supplementary Table S4.** Nucleotide and amino acid identities of each gene between the FeMV-Thai strains (FeMV-1) and the Gordon strain (FeMV-2).

FeMV-Thai strains	Nucleotide and amino acid identities (%)																					
	N gene			P gene			M gene			F gene		H gene		L gene								
	nt	aa	nt	aa	nt	aa	nt	aa	nt	aa	nt	aa	nt	aa								
U16-2016	81.9	90.2	80.6	80.6	74.5	74.5	83.2	83.2	92.0	92.0	81.4	81.4	89.1	89.1	80.6	80.6	86.2	86.2	82.5	82.5	90.8	90.8
CTL16-2018	81.8	89.8	80.4	80.4	69.2	69.2	82.8	82.8	91.1	91.1	81.1	81.1	87.9	87.9	80.6	80.6	86.4	86.4	82.5	82.5	90.6	90.6
CTL43-2018	81.0	88.8	80.6	80.6	73.9	73.9	80.5	80.5	85.2	85.2	80.9	80.9	87.9	87.9	80.2	80.2	85.2	85.2	82.4	82.4	90.6	90.6

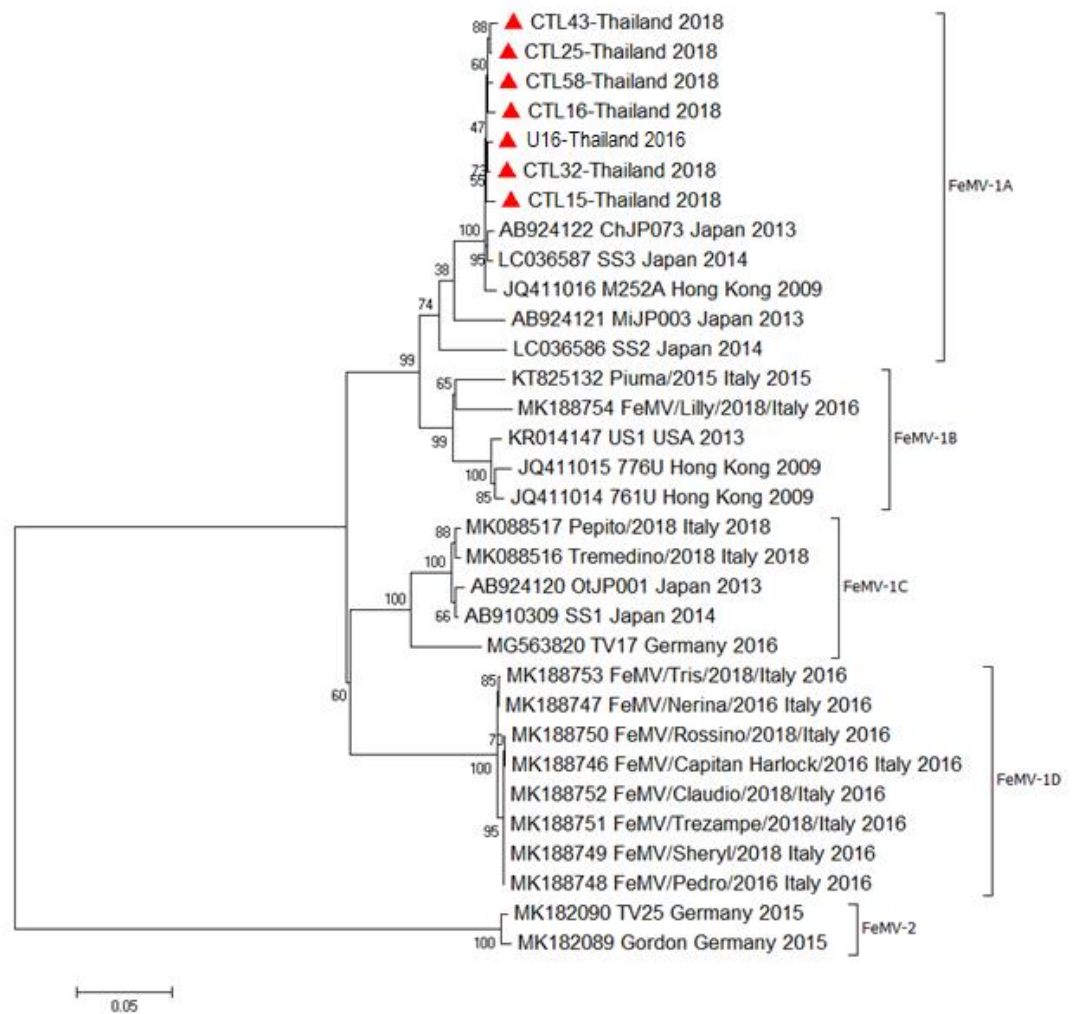


Supplementary Figure S1. Phylogenetic analysis of the codon region sequence of the six genes in FeMV strains.





**Supplementary Figure S2.** Phylogenetic tree of the codon region of the F gene among FeMVs. Scale bar is the substitution rate per site. The ML method with a GTR model and 1000 bootstrap replicates (shown as a %) were performed in the Mega 7 software.



**Supplementary Figure S3.** Phylogenetic tree of the codon region of the H gene among FeMVs. Scale bar is the substitution rate per site. The ML method with a GTR model and 1000 bootstrap replicates (shown as a %) were performed in the Mega 7 software.

## Supplemental data of Chapter III

Supplemental table 1. The results of serological and molecular assay, and clinical sign

Sheltered-no.	OD	i-ELISA	WB	RT-PCR	Clinical signs
1	0.4565	Pos	Pos	Neg	pale mm, mild gingivitis
2	0.242	Pos	Pos	Neg	gingivitis
3	0.445	Pos	Pos	Neg	gingivitis
4	0.1175	Neg	Neg	Neg	mild dental tartar
5	0.46	Pos	Pos	Neg	mild gingivitis, submandibular lymph node enlargement
6	0.4055	Pos	Pos	Neg	gingivitis, hypersalivation
7	0.1025	Neg	Neg	Neg	Chronic kidney disease (CKD)
8	0.1125	Neg	Neg	Neg	mild gingivitis
9	0.086	Neg	Neg	Neg	severe gingivitis, faucitis, submandibular lymph node enlargement
10	0.1	Neg	Neg	Neg	normal appearance
11	0.508	Pos	Pos	Pos	normal appearance
12	0.568	Pos	Pos	Neg	tonsilitis
13	0.131	Neg	Neg	Neg	normal appearance
14	0.298	Pos	Pos	Neg	severe gingivitis
15	0.292	Pos	Neg	Neg	normal appearance
16	0.038	Neg	Neg	Neg	serous nasal discharge, tonsilitis
17	0.159	Neg	Neg	Neg	normal appearance
18	0.194	Neg	Neg	Pos	mild gingivitis
19	0.218	Neg	Neg	Neg	normal appearance
20	0.2215	Neg	Neg	Neg	normal appearance
21	0.2395	Neg	Pos	Pos	chronic corneal ulcerative
22	0.148	Neg	Neg	Neg	mild icteric mm
23	0.2585	Pos	Pos	Pos	mild gingivitis
24	0.1095	Neg	Neg	Neg	normal appearance
25	0.2105	Neg	Neg	Pos	right eye blind and ocular secretion
26	0.233	Neg	Pos	Neg	icteric mm
27	0.224	Neg	Neg	Pos	normal appearance
28	0.173	Neg	Neg	Neg	submandibular lymph node enlargement, gingivitis
29	0.311	Pos	Pos	Neg	icteric mm
30	0.2155	Neg	Neg	Pos	dental tartar
31	0.304	Pos	Pos	Neg	normal appearance
32	0.3715	Pos	Pos	Neg	dental tartar
33	0.202	Neg	Pos	Neg	normal appearance
34	0.3825	Pos	Pos	Neg	pale mm
35	0.1965	Neg	Neg	Neg	normal appearance

36	0.262	Neg	Pos	Neg	mild dental tartar
37	0.091	Neg	Neg	Neg	icteric mm
38	0.1065	Neg	Neg	Neg	submandibular lymph node enlargement , gingivitis, pale mm
39	0.2925	Pos	Pos	Neg	normal appearance
40	0.2195	Neg	Pos	Neg	pale mm
41	0.2225	Neg	Pos	Neg	normal appearance
42	0.3215	Pos	Pos	Neg	tonsilitis, gingivitis
43	0.1025	Neg	Neg	Neg	submandibular lymph node enlargement , gingivitis, popliteal lymph node enlargement
44	0.0635	Neg	Neg	Neg	hematuria
45	0.781	Pos	Pos	Pos	OD: glaucoma (cataract induced)
46	0.377	Pos	Pos	Neg	gingivitis
47	0.7315	Pos	Pos	Neg	serous ocular discharge
48	0.135	Neg	Neg	Pos	mild gingivitis
49	0.453	Pos	Pos	Neg	normal appearance
50	0.089	Neg	Neg	Neg	normal appearance
51	0.3585	Pos	Pos	Pos	Pale-icteric mm., submandibular lymph node enlargement
52	0.336	Pos	Neg	Neg	normal appearance
53	0.1525	Neg	Neg	Neg	submandibular lymph node enlargement , tonsilitis
54	0.129	Neg	Neg	Neg	normal appearance
55	0.1015	Neg	Neg	Neg	normal appearance
56	0.6755	Pos	Pos	Pos	normal appearance
Hospitalized no.	OD	i-ELISA	WB	RT-PCR	Clinical signs
1	0.281	Pos	Neg	Neg	Feline eosinophilic granuloma complex
2	0.3075	Pos	Neg	Neg	CKD, feline respiratory disease complex
3	0.123	Neg	Neg	Neg	FeLV, Dyspnea
4	0.5565	Pos	Pos	Neg	Healthy
5	0.7825	Pos	Pos	Neg	Healthy
6	0.6255	Pos	Pos	Neg	Healthy
7	1.032	Pos	Pos	Neg	CKD
8	0.403	Pos	Pos	Neg	No observe
9	0.3865	Pos	Pos	Neg	none
10	0.2935	Pos	Pos	Neg	ventral hernia
11	0.281	Pos	Pos	Neg	CKD
12	0.2335	Neg	Pos	Neg	Healthy
13	0.5515	Pos	Pos	Neg	Healthy
14	0.0685	Neg	Neg	Neg	Jaundice
15	0.294	Pos	Pos	Neg	Hit by car
16	0.0745	Neg	Neg	Neg	CKD, FRDC

---

17	0.2705	Pos	Pos	Neg	CKD
18	0.3475	Pos	Pos	Neg	CKD
19	0.2505	Pos	Pos	Neg	Squamous cell carcinoma
20	0.613	Pos	Pos	Neg	FeLV
21	0.053	Neg	Neg	Neg	FeLV (Mediastinal lymphoma)
22	0.618	Pos	Pos	Neg	CKD
23	0.279	Pos	Pos	Neg	Bite wound
24	1.0335	Pos	Pos	Neg	Healthy
25	0.344	Pos	Pos	Neg	Bite wound
26	0.2545	Pos	Pos	Neg	CKD
27	0.194	Neg	Pos	Neg	vomit, fever
28	0.3175	Pos	Neg	Neg	Healthy
29	0.318	Pos	Neg	Neg	CKD
30	0.315	Pos	Neg	Neg	Healthy
31	0.193	Neg	Neg	Neg	CKD
32	0.196	Neg	Neg	Neg	Polycystic kidney disease
33	0.3555	Pos	Neg	Neg	FRDC
34	0.2575	Pos	Pos	Neg	CKD
35	0.2965	Pos	Pos	Neg	Stomatitis
36	0.394	Pos	Pos	Neg	Otitis, opened wound
37	0.308	Pos	Pos	Neg	CKD, FRDC
38	0.182	Neg	Pos	Neg	Urethral prolapse
39	0.283	Pos	Pos	Neg	CKD, stomatitis
40	0.3125	Pos	Pos	Neg	AKD
41	0.729	Pos	Pos	Neg	Stomatitis
42	0.8425	Pos	Pos	Neg	FLUTD
43	0.2515	Pos	Pos	Neg	FeLV, Dyspnea
44	0.362	Pos	Pos	Neg	Healthy
45	0.67	Pos	Pos	Neg	Healthy
46	0.467	Pos	Neg	Neg	AKD
47	0.3235	Pos	Pos	Neg	No observe
48	0.272	Pos	Pos	Neg	No observe
49	0.3125	Pos	Pos	Neg	No observe
50	0.258	Pos	Pos	Neg	No observe
51	0.007	Neg	Neg	Neg	No observe
52	0.7265	Pos	Pos	Neg	No observe
53	0.321	Pos	Pos	Neg	No observe
54	0.434	Pos	Pos	Neg	No observe
55	0.3625	Pos	Pos	Neg	No observe
56	0.3605	Pos	Pos	Neg	No observe
57	0.334	Pos	Pos	Neg	No observe
58	0.266	Pos	Pos	Neg	No observe

---

---

59	0.5415	Pos	Pos	Neg	No observe
60	0.3955	Pos	Pos	Neg	No observe
61	0.3825	Pos	Pos	Neg	No observe
62	0.2575	Pos	Pos	Neg	No observe
63	0.4565	Pos	Pos	Neg	No observe
64	0.53	Pos	Pos	Neg	No observe
65	0.555	Pos	Pos	Neg	No observe
66	0.9145	Pos	Pos	Neg	No observe
67	0.306	Pos	Pos	Neg	No observe
68	0.5935	Pos	Pos	Neg	No observe
69	0.353	Pos	Pos	Neg	No observe
70	0.281	Pos	Neg	Neg	No observe
71	0.346	Pos	Pos	Neg	No observe
72	0.3315	Pos	Pos	Neg	No observe
73	0.3265	Pos	Pos	Neg	No observe
74	0.5025	Pos	Pos	Neg	No observe
75	0.944	Pos	Pos	Neg	No observe
76	0.4755	Pos	Pos	Neg	No observe
77	0.8775	Pos	Pos	Neg	No observe
78	0.3385	Pos	Pos	Neg	No observe
79	0.312	Pos	Pos	Neg	No observe
80	0.453	Pos	Neg	Neg	No observe

---

Pos=Positive, Neg=Negative

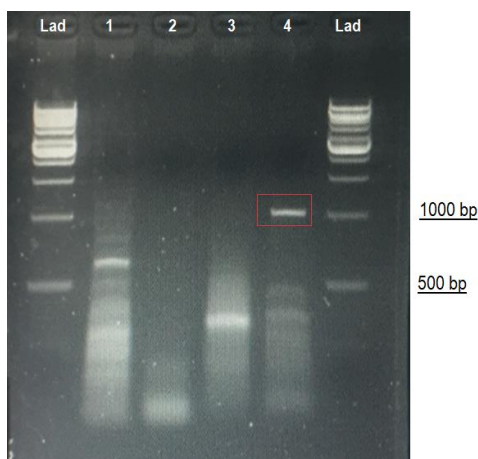


**Figure S1.** Amplification of whole matrix gene of FeMV strain Thai-U16. Lad= ladder, lane 1= Partial N gene (Fraction of N3), lane 2= whole N gene (no expected product), lane 3=partial M gene (Fraction of M3), lane 4= whole M gene (product=1011 bp, red square)



**Figure S2.** Figure showed M-band (1011 bp) of samples after digestion. Lad= ladder, lane 1-8= the selected single colony no. 17-24 have double digested with EcoRI and XhoI restriction enzyme in samples harboring in pET24a vector.

**Figure S3.** Alignment of recombinant FeMV-M protein harboring in pET24a vector with FeMV strain Thi-U16 (BLAST<sup>®</sup>, free software of NCBI)

**Feline morbillivirus isolate FmoPV-Thai-U16, complete genome**  
 Sequence ID: [MF627832.1](#) Length: 16050 Number of Matches: 1

Range 1: 3388 to 4399 [GenBank](#) [Graphics](#) [▼ Next Match](#) [▲ Previous Match](#)

Score	Expect	Identities	Gaps	Strand
1847 bits(1000)	0.0	1009/1013(99%)	1/1013(0%)	Plus/Minus
Query 381	TTTAAATCTTGAAGAGACCAATGGTATTGTCAATAATGACATCATCATATACTTTAAATTC	448		
Sbjct 4399	TTTAAATCTTGAAGAGACCAATGGTATTGTCAATAATGACATCATCATATACTTTAAATTC	4348		
Query 441	ATTTGGAACAGATGGCTGTAAGACTGCTTGAACCTTCTCTATTCTACATTCATTTCTCCA	508		
Sbjct 4339	ATTTGGAACAGATGGCTGTAAGACTGCTTGAACCTTCTCTATTCTACATTCATTTCTCCA	4288		
Query 501	CAGTGTTTTATTTAGCCCTTCATTTACATACATCAGGGGGTAAACATAAAGTCCTTTTGAA	568		
Sbjct 4279	CAGTGTTTTATTTAGCCCTTCATTTACATACATCAGGGGGTAAACATAAAGTCCTTTTGAA	4228		
Query 561	TCCTAAGTAGGCCTGTAGTCGTTTGCTCATCTTACCTGTGCATCTAATATGTAAGCTTGT	628		
Sbjct 4219	TCCTAAGTAGGCCTGTAGTCGTTTGCTCATCTTACCTGTGCATCTAATATGTAAGCTTGT	4168		
Query 621	GCCACCAATTGCACCTAATGAGAATATCAAACCAAGCCCTCATTATTTTCTCTTGACGTA	688		
Sbjct 4159	GCCACCAATTGCACCTAATGAGAATATCAAACCAAGCCCTCATTATTTTCTCTTGACGTA	4108		
Query 681	TTCCGGTGAATAAGATTTATTACTCTCCGTTTGAAGTTCCTCAATATGAATCATAAATGT	748		
Sbjct 4099	TTCCGGTGAATAAGATTTATTACTCTCCGTTTGAAGTTCCTCAATATGAATCATAAATGT	4048		
Query 741	AATCACAGTTTCCCAGTATTTCTTAATCGAGAGTCTTGGATTGGTCAAGTAAATTTGT	808		
Sbjct 4039	AATCACAGTTTCCCAGTATTTCTTAATCGAGAGTCTTGGATTGGTCAAGTAAATTTGT	3988		
Query 801	ACCCATTGATAGATGCACAAGGATGTTGAATGCAACAGAATTTGACGATTTGAAATCTTG	868		
Sbjct 3979	ACCCATTGATAGATGCACAAGGATGTTGAATGCAACAGAATTTGACGATTTGAAATCTTG	3928		
Query 861	AATCATCTTTGGTATCTGATAATAGCCATCATCAGATAATTTTGTAAACAGTCAAATATAC	928		
Sbjct 3919	AATCATCTTTGGTATCTGATAATAGCCATCATCAGATAATTTTGTAAACAGTCAAATATAC	3868		
Query 921	AGGCCAAAACTTTGTGGAATATCTATTGGTATAGAGCTTGTATCACTGCAGACCTGATT	988		
Sbjct 3859	AGGCCAAAACTTTGTGGAATATCTATTGGTATAGAGCTTGTATCACTGCAGACCTGATT	3808		
Query 981	AGCATTAAAGATGCTTCCATATGCCAACACCTTTTCCAGGGAGTCAGTAAATGTATAGG	1048		
Sbjct 3799	AGCATTAAAGATGCTTCCATATGCCAACACCTTTTCCAGGGAGTCAGTAAATGTATAGG	3748		
Query 1041	TGTGGTATTATAATAAACTAACTTCTCATTAAATCCAGCAGTCTACGAGTCACGATATT	1108		
Sbjct 3739	TGTGGTATTATAATAAACTAACTTCTCATTAAATCCAGCAGTCTACGAGTCACGATATT	3688		
Query 1101	GAGAGTTAATATTTCTTAAACAAATCTTCTGGGTTTTTCAGTTGATTGACCCACTCCTAA	1168		
Sbjct 3679	GAGAGTTAATATTTCTTAAACAAATCTTCTGGGTTTTTCAGTTGATTGACCCACTCCTAA	3628		
Query 1161	TGGGAATGCCCAAATGCTCTCCCTTTGGACTAATCATGTTCTCGCTGTCTTCTATGAC	1228		
Sbjct 3619	TGGGAATGCCCAAATGCTCTCCCTTTGGACTAATCATGTTCTCGCTGTCTTCTATGAC	3568		
Query 1221	ACCATGGGAGAAAGTAGATACATATATCCCCACTCTTGCATCTCCTAGGCCCGGATCGA	1288		
Sbjct 3559	ACCATGG-AGAAAGTAGATACATATATCCCCACTCTTGCATCTCCTAGGCCCGGATCGA	3508		
Query 1281	TAACCCGAACTTTGGGCACAAGTCTCCCATCAGAATAGATATCAGGTGTTAGCGGATCAA	1348		
Sbjct 3508	TAACCCGAACTTTGGGCACAAGTCTCCCATCAGGATAGATATCAGGTGTTAGCGGATCAA	3448		
Query 1341	GCGTTCCTTTGATTGACCATGAGCTCTCATCAAGAGTGAATATCTCAGTCATG	1393		
Sbjct 3448	GTGTTCCTTTGATTGACCATGAGCTTTTCATCAAGAGTGAATATCTCAGTCATG	3388		



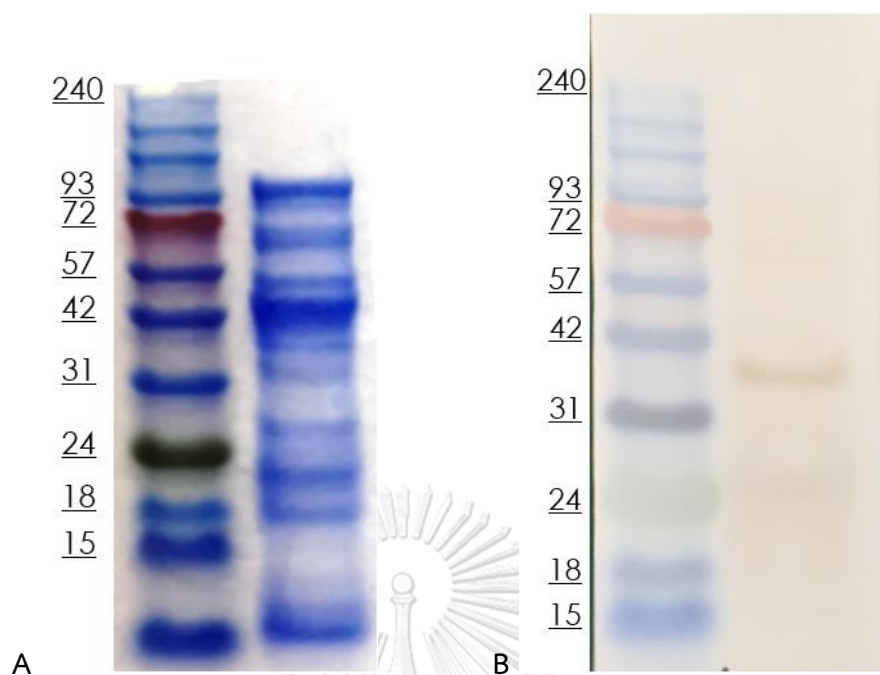


**Figure S4.** Detecting of 36 kDa MW of rFeMV-M protein using SDS-Page (A).  
Antigenicity testing of rFeMV-M protein incubated with Ni-NTA HRP conjugated (B).

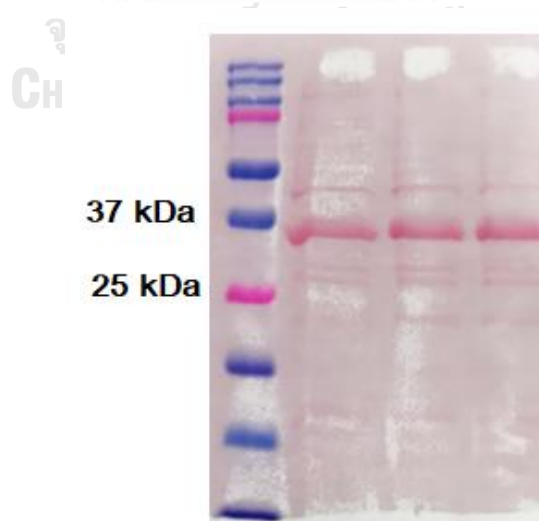


**Figure S5.** Ponceau S staining after rFeMV-M proteins (all lanes) were completely transferred on PVDF membrane.

## Supplemental data of Chapter IV

Supplementary Table 1 Macroscopic findings of two FeMV-positive necropsied cats

Organs	Case number	
	1 (19P244N)	2 (19P314K)
Brain	Mild congestion	Moderate congestion
Mucous membrane	Pale mucous membrane	No remarkable lesion (NRL)
Respiratory tract		
• Trachea	Frothy exudate	NRL
• Lung	Edema	NRL
Heart	Thickening of left ventricle myocardium	Thickening of left ventricle myocardium
Gastrointestinal tract		
• Esophagus	NRL	NRL
• Stomach	Two tapeworms with patchy submucosal hemorrhage	NRL
• Small intestine	Moderate submucosal hemorrhage at duodenum	NRL
• Large intestine	NRL	NRL
Liver	Congestion	Congestion
Spleen	Old lesion of splenic body rupture	Focal fibrosis at splenic tail
Mesenteric lymph node	NRL	Mild hemorrhage
Adrenal gland	Multifocal hemorrhage at right cortical adrenal gland	NRL
Urinary tract		
• Kidney	Moderate congestion at corticomedullary junction	Moderate congestion at corticomedullary junction
• Urinary bladder	Severe distension of bladder with red urine and multifocal to coalescing hemorrhage at mucosal and serosal surface	Severe distention of bladder with red urine and diffuse patchy hemorrhage at mucosal surface
• Urethra	Urethral plug at the tip of penis with black discoloration	NRL
Other lesions	Mild peritoneal effusion	

**Supplementary Table 2** Histopathological findings of two FeMV-positive necropsied cats

Organs	Case number	
	1 (19P244N)	2 (19P314K)
Brain	There is increased number and prominence of neuron associated glial cells consistent with satellitosis. Many cerebral blood vessels within the neuropil are variably engorged.	There are multifocal areas of hemorrhage, and many blood vessels of cerebral cortex, meninges, are markedly diffusely engorged. In one region, the meninges along the cerebral sulci is expanded, and is filled with large fibrin accumulations intermixed with pools of neutrophils, and the subjacent neuropil is rarefied, and vacuolated, and occasional neurons contain discrete vacuole.
Lung	The pulmonary parenchyma is diffusely congested, has areas of hemorrhage, and the alveoli are locally extensively replaced by abundant eosinophilic proteinaceous edema, variable numbers of foamy histiocytes, and few scattered erythrocytes.	Pulmonary parenchyma is diffusely congested accompanied by increased numbers of circulatory neutrophils and other leukocytes. Alveoli are filled abundant eosinophilic proteinaceous edema and contain few scattered foamy histiocytes in some areas. Rare pulmonary vessels contain variable fibrin often intermixed with neutrophils.
Heart	There is a focus of hemorrhage, and cardiac myofibers are thicker 1-2 times than normal and are haphazardly arranged in some areas.	There is foci of myocardial disarray and many myocardial cells exhibit variability of tinctorial staining and size with occasional loss of cross striation and nuclear pyknosis. In the lumen of the right ventricle, there is a large accumulation of organizing fibrin intermixed with dense pools of neutrophils.
Small intestine	The intestinal mucosa is necrotic as evidenced by remaining enterocytes being hypereosinophilic and pyknotic intermixed with numerous 4-7 $\mu\text{m}$ rod shaped bacterial bacilli, variable aggregates of eosinophilic and pyknotic debris.	There are increased numbers of goblet cells, and there is abundant eosinophilic acellular material intermixed with large clumps of bacterial bacilli and desquamating enterocytes. In some section, the superficial villous epithelial cells are hypereosinophilic and pyknotic. There are mild to moderate numbers of lymphocytes, plasma cells, and few neutrophils within the mucosal lamina propria, and small numbers of these lymphocytes are scattered within the superficial villous

		epithelium as individuals and rare nests. Occasional crypts contain eosinophilic debris.
Liver	Liver is diffusely congested. There are mildly increased numbers of circulating leukocytes including neutrophils and small lymphocytes. Kupffer cells are diffusely hypertrophied, and hepatocytes are often arranged in irregular cords. Occasional central veins are thickened by thin bands of fibrosis. Several portal tracts are in close proximity to one another resulting in lobular collapse.	Liver is diffusely congested, and there are mildly increased numbers of circulating leukocytes including neutrophils and lymphocytes. Many hepatocytes are diffusely rounded and dissociated or contain occasional discrete vacuole.
Spleen	No remarkable lesion	Many lymphoid follicles are expanded, but numbers of lymphocytes are depleted and replaced by abundant eosinophilic material, karyorrhectic debris, and increased numbers and prominence of reticuloendothelial cells. In another section of spleen, the red pulp is diffusely congested, and contains high numbers of erythropoietic precursors including megakaryocytes.
Lymph node	Lymphoid follicles are variably expanded by edema, but the numbers of lymphocytes within the follicles are depleted with increased prominence of histiocytes. Moreover, subcapsular and medullary sinuses contain numerous erythrocytes and high numbers of erythrophages.	Mild congestion by showing erythrocytes occupy in the medullary sinuses.
Kidney	Many renal tubules are degenerate and diffusely contain discrete vacuole while some renal tubular epithelial cells are plump cuboidal or tall columnar and contain 2-4 $\mu\text{m}$ round to oval intracytoplasmic eosinophilic hyalinized globule. Many glomeruli have segmental thickening of capillary wall by moderate hyalinized material. The renal interstitium at the renal corticomedullary junction and medulla is markedly engorged. Rare renal tubules contain mineralized material.	Renal tubules are diffusely markedly vacuolated, occasional tubular epithelial cells become tall columnar with vesiculated round nuclei, and rare epithelial cells are hypereosinophilic and pyknotic. In addition, many tubular epithelial cells contain variable amounts of yellow brown granular hemosiderin or lipofuscin pigment while occasional cells contain 2-4 $\mu\text{m}$ round to oval intracytoplasmic eosinophilic hyalinized globule. Changes of several glomeruli are characterized by global thickening of capillary wall by moderate hyalinized material with associated increased numbers of proliferative mesangial cells, and

Urinary bladder

There is marked expansion of the substantial propria by large pools of erythrocytes with extensive loss of urothelium. Such massive hemorrhage also sometimes extends into the subjacent tunica muscularis in some areas.

glomerular spaces are often filled with eosinophilic proteinaceous material. All glomeruli and interstitial stroma at the level of corticomedullary junction are markedly congested. In one focus, there is an interstitial aggregate of lymphocytes and plasma cells. Other changes include foci of renal tubular loss with replacement by dense fibrosis and rare tubular mineralization noted in medullary region.

There is extensive loss of urothelium with associated segmental expansion of the substantial propria by large pools of hemorrhage intermixed with fibrin and karyorrhectic debris. Such extensive pools of hemorrhage accompanied by high numbers of infiltrative neutrophils extend through the whole width of bladder wall and adjacent omental adipose tissue and dissect around variably loosely edematous supporting stroma, muscular bundles, and surrounding adipocytes in many areas. Endothelial cells of several blood vessels are necrotic or reactive and walls of such vessels are expanded by fibrin accumulations intermixed karyorrhectic debris (fibrinoid necrosis).

**Supplementary Table 3** Cellular tropism and tissue localization of two FeMV-positive necropsied cases

Cell tropism	Case number	
	1 (19P244N)	2 (19P314K)
Epithelial cells (Cytoplasm)		
1. Tracheal epithelial cells	++	++
2. Bronchial epithelial cells	++	++
3. Bronchiolar epithelial cells	++	++
4. Transitional cells	++	++
5. Renal tubular epithelial cells (cytoplasmic hyalinized globules)	++	++
Spleen		
● Histiocytes	+	+
● Lymphoid cells	+	+
Mesenteric lymph node		
● Histiocytes	+	+
● Lymphoid cells	+	+
Cerebrum and cerebellum		
● Neuroglial in white matter	++	++

- (no immunopositive cells); + ( $\leq$  25% immunopositive cells); ++ (26–50% immunopositive cells); +++ (51–75% immunopositive cells); ++++ ( $\geq$  76% immunopositive cells)

Sequence	1	2	3	4	5	6	7	8	9	10	11	12	13	14	15	16	17	18	19	20	21	22	23	24	25	26	27	28	29	30
1 MTJ38572 24HK-2019 Thailand 2019	0.982	0.972	0.937	0.972	0.953	0.948	0.924	0.952	0.939	0.933	0.926	0.944	0.924	0.928	0.931	0.893	0.891	0.869	0.891	0.918	0.893	0.895	0.895	0.895	0.895	0.893	0.909	0.909	0.911	0.854
2 MTJ38573 34HK-2019 Thailand 2019	0.982	0.976	0.959	0.972	0.972	0.968	0.941	0.972	0.953	0.933	0.944	0.966	0.942	0.944	0.948	0.911	0.909	0.907	0.909	0.918	0.893	0.895	0.895	0.895	0.891	0.911	0.909	0.911	0.871	0.872
3 MN164531 CTL16-Thailand 2018	0.962	0.976	0.982	0.972	0.965	0.961	0.941	0.972	0.952	0.953	0.944	0.966	0.942	0.944	0.948	0.911	0.909	0.907	0.909	0.918	0.893	0.895	0.895	0.895	0.891	0.911	0.909	0.911	0.871	0.872
4 MN164532 CTL43-Thailand 2018	0.965	0.977	0.982	0.984	0.965	0.961	0.941	0.972	0.952	0.953	0.944	0.966	0.942	0.944	0.948	0.911	0.909	0.907	0.909	0.918	0.893	0.895	0.895	0.895	0.891	0.911	0.909	0.911	0.871	0.872
5 HK627032 U16-2016 Thailand 2016	0.965	0.977	0.982	0.984	0.965	0.961	0.941	0.972	0.952	0.953	0.944	0.966	0.942	0.944	0.948	0.911	0.909	0.907	0.909	0.918	0.893	0.895	0.895	0.895	0.891	0.911	0.909	0.911	0.871	0.872
6 MTJ38574 24HK-2019 Thailand 2019	0.982	0.972	0.937	0.972	0.953	0.948	0.924	0.952	0.939	0.933	0.926	0.944	0.924	0.928	0.931	0.893	0.891	0.869	0.891	0.918	0.893	0.895	0.895	0.895	0.895	0.893	0.909	0.909	0.911	0.854
7 LCO38586 SCS 2014	0.925	0.926	0.939	0.944	0.945	0.947	0.957	0.961	0.959	0.953	0.952	0.957	0.942	0.946	0.957	0.916	0.917	0.917	0.916	0.924	0.917	0.917	0.917	0.917	0.916	0.924	0.924	0.924	0.887	
8 AB924122 CH0073 Jaen 2013	0.965	0.978	0.982	0.985	0.969	0.969	0.949	0.961	0.959	0.952	0.965	0.987	0.963	0.965	0.968	0.935	0.933	0.933	0.933	0.933	0.933	0.935	0.935	0.935	0.935	0.934	0.934	0.934	0.887	
9 AB924121 M3P003 Jaen 2013	0.931	0.943	0.946	0.946	0.956	0.952	0.943	0.959	0.959	0.972	0.963	0.968	0.961	0.966	0.968	0.935	0.933	0.933	0.933	0.933	0.933	0.935	0.935	0.935	0.935	0.934	0.934	0.934	0.887	
10 KRQ14447 US1 USA 2013	0.911	0.921	0.925	0.926	0.933	0.932	0.93	0.936	0.932	0.944	0.958	0.959	0.976	0.974	0.977	0.944	0.942	0.939	0.939	0.948	0.939	0.937	0.937	0.937	0.935	0.939	0.937	0.937	0.893	
11 KTR325132 Pim2015 Italy 2015	0.908	0.918	0.922	0.924	0.933	0.932	0.928	0.932	0.932	0.944	0.958	0.959	0.976	0.974	0.977	0.944	0.942	0.939	0.939	0.948	0.939	0.937	0.937	0.937	0.935	0.939	0.937	0.937	0.893	
12 JQ411016 PCS2A Hong Kong 2009	0.964	0.977	0.982	0.985	0.968	0.967	0.95	0.962	0.955	0.933	0.933	0.933	0.933	0.933	0.933	0.933	0.933	0.933	0.933	0.933	0.933	0.933	0.933	0.933	0.933	0.933	0.933	0.933	0.887	
13 JQ411017 PCS2B Hong Kong 2009	0.964	0.977	0.982	0.985	0.968	0.967	0.95	0.962	0.955	0.933	0.933	0.933	0.933	0.933	0.933	0.933	0.933	0.933	0.933	0.933	0.933	0.933	0.933	0.933	0.933	0.933	0.933	0.933	0.887	
14 JQ411015 7610 Hong Kong 2009	0.906	0.917	0.919	0.927	0.927	0.927	0.927	0.927	0.927	0.927	0.927	0.927	0.927	0.927	0.927	0.927	0.927	0.927	0.927	0.927	0.927	0.927	0.927	0.927	0.927	0.927	0.927	0.927	0.887	
15 JQ411014 7610 Hong Kong 2009	0.911	0.921	0.924	0.927	0.923	0.923	0.923	0.923	0.923	0.923	0.923	0.923	0.923	0.923	0.923	0.923	0.923	0.923	0.923	0.923	0.923	0.923	0.923	0.923	0.923	0.923	0.923	0.923	0.887	
16 MK088517 Aepno2/2018 Italy 2018	0.87	0.881	0.888	0.885	0.89	0.89	0.882	0.892	0.89	0.89	0.89	0.889	0.889	0.889	0.889	0.889	0.889	0.889	0.889	0.889	0.889	0.889	0.889	0.889	0.889	0.889	0.889	0.889	0.889	0.889
17 MK088515 Tremedino/2018 Italy 2018	0.868	0.878	0.883	0.888	0.887	0.887	0.878	0.889	0.888	0.889	0.889	0.887	0.887	0.886	0.889	0.889	0.889	0.889	0.889	0.889	0.889	0.889	0.889	0.889	0.889	0.889	0.889	0.889	0.889	0.889
18 AB924120 CH0001 Jaen 2013	0.877	0.881	0.881	0.886	0.889	0.889	0.879	0.891	0.89	0.89	0.894	0.889	0.889	0.886	0.889	0.889	0.889	0.889	0.889	0.889	0.889	0.889	0.889	0.889	0.889	0.889	0.889	0.889	0.889	0.889
19 AB924120 CH0001 Jaen 2013	0.877	0.881	0.881	0.886	0.889	0.889	0.879	0.891	0.89	0.89	0.894	0.889	0.889	0.886	0.889	0.889	0.889	0.889	0.889	0.889	0.889	0.889	0.889	0.889	0.889	0.889	0.889	0.889	0.889	0.889
20 MK188752 FcM/Trieste/2016 Italy 2016	0.858	0.869	0.875	0.878	0.883	0.879	0.877	0.879	0.876	0.878	0.881	0.879	0.878	0.876	0.879	0.879	0.879	0.879	0.879	0.879	0.879	0.879	0.879	0.879	0.879	0.879	0.879	0.879	0.879	0.879
21 MK188753 FcM/Trieste/2016 Italy 2016	0.86	0.87	0.875	0.878	0.883	0.879	0.877	0.879	0.876	0.878	0.881	0.879	0.878	0.876	0.879	0.879	0.879	0.879	0.879	0.879	0.879	0.879	0.879	0.879	0.879	0.879	0.879	0.879	0.879	0.879
22 MK188752 FcM/Clusone/2018 Italy 2018	0.86	0.87	0.875	0.878	0.883	0.879	0.877	0.879	0.876	0.878	0.881	0.879	0.878	0.876	0.879	0.879	0.879	0.879	0.879	0.879	0.879	0.879	0.879	0.879	0.879	0.879	0.879	0.879	0.879	0.879
23 MK188751 FcM/Treviso/2018 Italy 2018	0.86	0.87	0.875	0.878	0.883	0.879	0.877	0.879	0.876	0.878	0.881	0.879	0.878	0.876	0.879	0.879	0.879	0.879	0.879	0.879	0.879	0.879	0.879	0.879	0.879	0.879	0.879	0.879	0.879	0.879
24 MK188750 FcM/Rossini/2018 Italy 2018	0.86	0.87	0.875	0.878	0.883	0.879	0.877	0.879	0.876	0.878	0.881	0.879	0.878	0.876	0.879	0.879	0.879	0.879	0.879	0.879	0.879	0.879	0.879	0.879	0.879	0.879	0.879	0.879	0.879	0.879
25 MK188749 FcM/Sere/2018 Italy 2018	0.86	0.87	0.875	0.878	0.883	0.879	0.877	0.879	0.876	0.878	0.881	0.879	0.878	0.876	0.879	0.879	0.879	0.879	0.879	0.879	0.879	0.879	0.879	0.879	0.879	0.879	0.879	0.879	0.879	0.879
26 MK188748 FcM/Pesaro/2016 Italy 2016	0.859	0.869	0.873	0.877	0.881	0.881	0.879	0.881	0.877	0.879	0.881	0.881	0.881	0.881	0.881	0.881	0.881	0.881	0.881	0.881	0.881	0.881	0.881	0.881	0.881	0.881	0.881	0.881	0.881	0.881
27 MK188747 FcM/Verona/2016 Italy 2016	0.86	0.87	0.875	0.878	0.883	0.879	0.877	0.879	0.876	0.878	0.881	0.879	0.878	0.876	0.879	0.879	0.879	0.879	0.879	0.879	0.879	0.879	0.879	0.879	0.879	0.879	0.879	0.879	0.879	0.879
28 MK188746 FcM/Caserta/2015 Italy 2015	0.86	0.87	0.875	0.878	0.883	0.879	0.877	0.879	0.876	0.878	0.881	0.879	0.878	0.876	0.879	0.879	0.879	0.879	0.879	0.879	0.879	0.879	0.879	0.879	0.879	0.879	0.879	0.879	0.879	0.879
29 MK182099 TV25 Germany 2015	0.794	0.805	0.81	0.807	0.811	0.815	0.814	0.814	0.814	0.819	0.824	0.812	0.825	0.828	0.808	0.808	0.808	0.808	0.808	0.81	0.815	0.814	0.814	0.814	0.814	0.814	0.814	0.814	0.814	0.814
30 MK182099 Gordon Germany 2015	0.792	0.803	0.808	0.805	0.81	0.813	0.818	0.813	0.811	0.819	0.821	0.81	0.824	0.819	0.806	0.806	0.806	0.806	0.806	0.808	0.815	0.814	0.814	0.814	0.814	0.814	0.814	0.814	0.814	0.814

Supplemental figure S1. F gene sequence similarity of the feline morbillivirus from this study along with other reference strains. Upper half shows amino acid similarity; lower half shows nucleotide similarity.







## Supplemental data of Chapter V

### Immunohistochemistry-Morbilliviruses Protocol

This protocol is suitable to use in the study of Feline morbillivirus (FeMV) and other morbilliviruses; Canine distemper (CDV) and New castle disease

Primary Antibody: Polyclonal ab against rM-FmoPV...Pab-rMFmoPV,

Monoclonal ab against CDV (H gene) Mab-CDV

Secondary Antibody: Envision polymer-Mouse and Rabbit, DAKO EnVision system™

#### *Materials and reagents*

1. Deparaffinized and dehydrated kit (Graded alc. and Xylene)
2. Chamber and tissue paper (fined touch)
3. Autoclave
4. Rack and jar
5. Stirrer and magnetic stirrer
6. Up-down shaker (If has)
7. DW Type II
8. PBS 1X (PBS diluted in DW type II)
9. Skim milk (Lab grade is considered)
10. H<sub>2</sub>O<sub>2</sub> 3% (H<sub>2</sub>O<sub>2</sub> 30%)
11. Absolute Methanol
12. Mounting medium

Slide: Positive control slide (FeMV, CDV),

Negative control slide: normal tissue and/or substitution slide (omitted primary ab or Ab anti-other IgG)

Step	Check
1 Incubate slide 60°C, 30 min	
2 Deparaffinization: Xylene I,II,III (5 min) → Xylene alc (2 min) → Abs.alc I,II (2 min) → 95% alc (2 min) → 80% alc (2 min) → 70% alc (2 min) → Running water (5 min) → DW type II (5 min) → 1X PBS (5 min)	
3 Pretreated slides with DW 121°C, 5 min in autoclave	
4 Wash 1X PBS 5 min x3	
5 Block endogenous peroxidase with 3% H2O2 10 min, RT (15ml 30% H2O2 + 150 ml Abs methanol) 1 jar	
6 Wash 1X PBS 5 min x3	
7 Blocking slide, for non-specific reaction, with 1% BSA or 5% skim milk (2-5%) 30 min, RT or 37C (1.25 g skim milk in 25 ml 1X PBS for 10 slides)	
8 Wash 1X PBS 5 min x3	
9 Add 100-200 ul-I ab (Mab-CDV/Pab-rM FeMV) 1:200/1:500 overnight, 4C (10/5 ul Mab/Pab in 1990/1995 ul 2% skim milk or IHC diluent or PBS for 10 slides)	
10 Wash 1X PBS 5 min x3	
11 100-200 ul Envision polymer (Rabbit/ mouse DAKO) per slide 45 min, RT	
12 Wash 1X PBS 5 min x3 (then dip in DW quickly before AEC solution)	
13 100-200 ul DAB substrate -Brown (1:100/ substrate: substrate buffer) AEC (single solution) - Red  Until color develop (approximately 1min)	
14 Stop reaction in DW type II	
15 Counterstain with hematoxylin 45 sec	
16 Wash in running water 5 min	
17 Dehydrate slide and mount	

## Western Blot analysis

### 12% Separating gel (15 ml) 2 gels

	Total 15 ml	Designed volume _____
DW Type II	4.9 ml	
30% acrylamide mix	6 ml	
1.5M Tris (pH 8.8)	3.8 ml	
10% SDS	150 $\mu$ l	
10% APS	150 $\mu$ l	
TEMED	6 $\mu$ l	

### 5% Stacking gel (5 ml) 2 gels

	Total 5 ml	Designed volume _____
DW Type II	2.77 ml	
30% acrylamide mix	830 $\mu$ l	
0.5M Tris (pH 6.8)	1260 $\mu$ l	
10% SDS	50 $\mu$ l	
10% APS	50 $\mu$ l	
TEMED	5 $\mu$ l	

### 2X Sample Buffer (10ml)

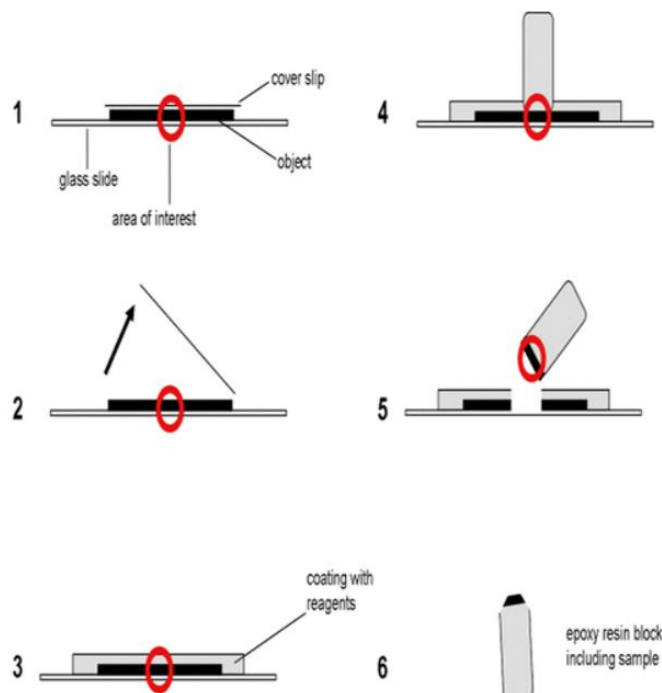
	Total 10 ml	Designed volume _____
0.5M Tris-HCl (pH 6.8)	2 ml	
10% SDS	4 ml	
Glycerol	2 ml	
DW Type II	800 $\mu$ l	
1% PBP	5 drops or more	

Step	Check
1. After SDS Page Run and before running in wet model, submerge filter paper in transfer buffered (Methanol) for 20 min and submerge PVDF membrane in methanol 20 min	
2. Prepare layer of transferring: 3-lower filter 3 → PVDF → gel** → 3-upper filter  (electrode charge was considered)  (250 mAP, 3h)	
3. After transferring, polyacrylamide gel was proved completely transferred to membrane by staining with Coomassie Brilliant Blue for 1 h, de-stain 20 min x2, then shaking overnight	
4. As well, PVDF membrane will be stained with Ponceau S for 5-10 min in RT → quick dip in DW II → pink band was recorded then label and cut membrane into strip for each sample → TBST 5 min several times until no longer band visible	
5. Blocking with 5% skim milk (diluted in TBST) in 4°C, overnight	
7. Wash with TBST 5 min x3 shaking	
8. Primary Ab= cat serum (1:1000, diluted in 2% skimmed mik-TBST) in 4°C, overnight (total solution covers each strip is 1.5 ml)  Marker (PTC): Ni-NTA 1:1000 in TBST	
9. Wash with TBST 5 min x3 shaking	
10. Add Mab anti-Cat IgG 1:8,000 (diluted in TBST) on membrane having cat serum in RT, 1 h	
11. Wash with TBST 5 min x3 shaking	
12. Prepare chromogen by using DAB kit (TBST 10,000+ DAB 25 ul) 3-5 min	
13. Stop reaction with DW II	

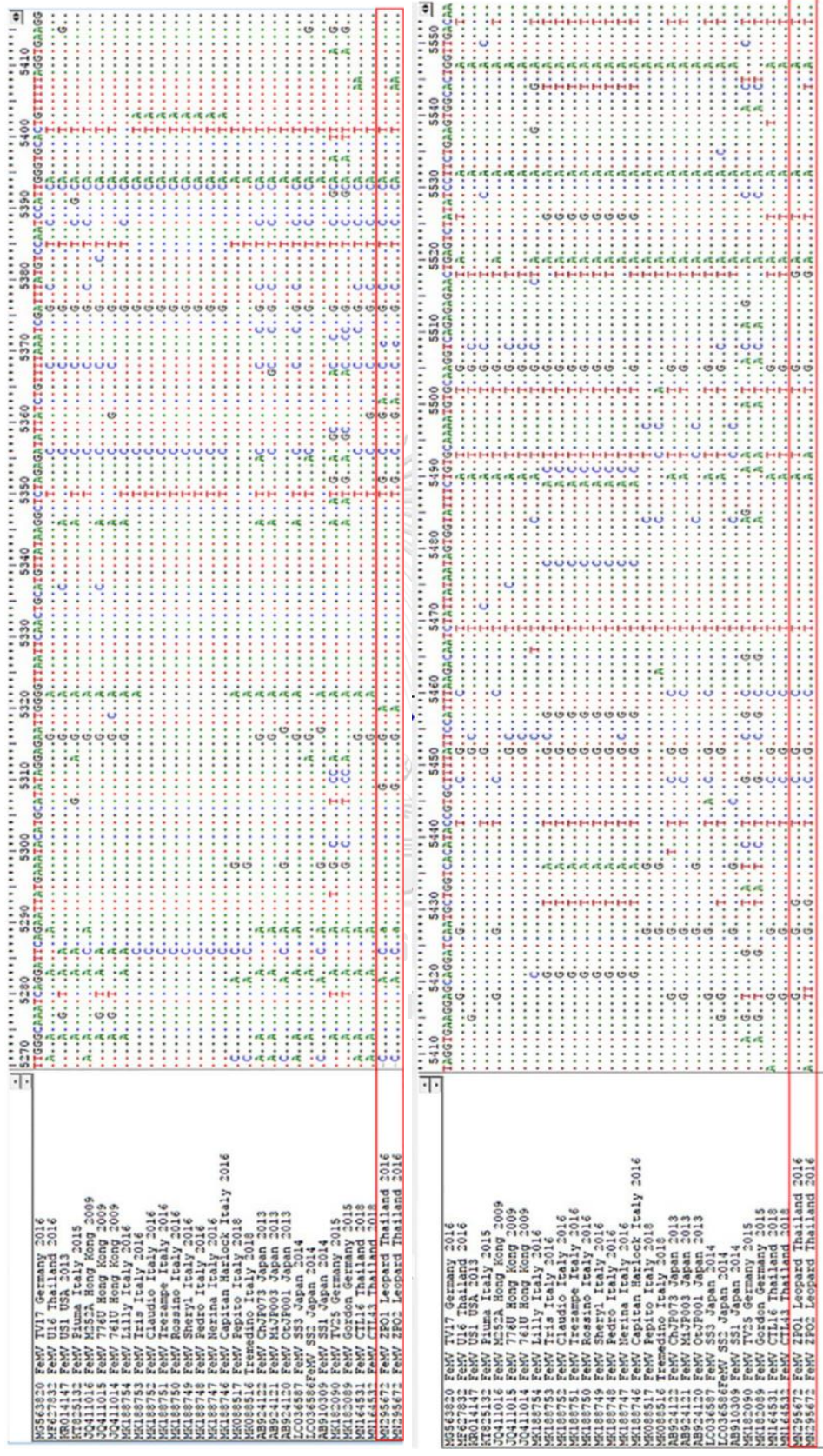
## Pop-off Technique

### HE/IHC stained

1. Incubate with xylene 1 day or up to 7 days until cover slip removed.
2. Rinse twice with 100% ethanol for 5 min and incubate in propylene oxide and 100% ethanol (1:1) for 2 min
3. Coat with pure propylene oxide and immediately cover with propylene oxide and epoxy resin (1:1) for 20 min
4. Fill a gelatin capsule with epoxy resin, then place the gelatin capsule upside down on top of the marked area. The epoxy resin will be polymerized for 1 hr at 35°C, and follow by 1 hr at 45°C and overnight at 85°C.
5. After polymerization, the epoxy resin blocks will be removed from the glass slide by dipping in liquid nitrogen.
6. The blocks will be trimmed for the interest area under visible control for ultra-sectioning. The 70-nm thick ultrathin section will be prepared and mounted on 200 mesh copper grids then investigate sample under a transmission electron microscopy



**Supplemental Figure S1.** Sequence alignment of leopard FeMV sequences. The partial FeMV L genes detected in Thailand (red-lined box) were aligned with various FeMV strains retrieved from GenBank.







	5830	5840	5850	5860	5870	5880	5890	5900	5910	5920	5930	5940	5950	5960	5970	5980	5990	6000
MS63820 FcWV TWT Germany 2016	T	A	T	A	T	A	T	A	T	A	T	A	T	A	T	A	T	A
MF27893 FcWV U16 Thailand 2016	T	A	T	A	T	A	T	A	T	A	T	A	T	A	T	A	T	A
KR01417 FcWV US1 USA 2013	T	A	T	A	T	A	T	A	T	A	T	A	T	A	T	A	T	A
KR25132 FcWV Puma Italy 2015	T	A	T	A	T	A	T	A	T	A	T	A	T	A	T	A	T	A
QJ411016 FcWV M55A Hong Kong 2009	T	A	T	A	T	A	T	A	T	A	T	A	T	A	T	A	T	A
QJ411018 FcWV 716D Hong Kong 2009	T	A	T	A	T	A	T	A	T	A	T	A	T	A	T	A	T	A
QJ411019 FcWV 716D Hong Kong 2009	T	A	T	A	T	A	T	A	T	A	T	A	T	A	T	A	T	A
MS18274 FcWV Lilly Hong Kong 2016	T	A	T	A	T	A	T	A	T	A	T	A	T	A	T	A	T	A
MS18273 FcWV Isis Italy 2016	T	A	T	A	T	A	T	A	T	A	T	A	T	A	T	A	T	A
MS18272 FcWV Claudio Italy 2016	T	A	T	A	T	A	T	A	T	A	T	A	T	A	T	A	T	A
MS18271 FcWV Treasapo Italy 2016	T	A	T	A	T	A	T	A	T	A	T	A	T	A	T	A	T	A
MS18270 FcWV Rossino Italy 2016	T	A	T	A	T	A	T	A	T	A	T	A	T	A	T	A	T	A
MS18275 FcWV Sheryl Italy 2016	T	A	T	A	T	A	T	A	T	A	T	A	T	A	T	A	T	A
MS18278 FcWV Pedro Italy 2016	T	A	T	A	T	A	T	A	T	A	T	A	T	A	T	A	T	A
MS18277 FcWV Nerina Italy 2016	T	A	T	A	T	A	T	A	T	A	T	A	T	A	T	A	T	A
MS18276 FcWV Pakistan Italy 2016	T	A	T	A	T	A	T	A	T	A	T	A	T	A	T	A	T	A
MS082517 FcWV Pakistan Italy 2016	T	A	T	A	T	A	T	A	T	A	T	A	T	A	T	A	T	A
MS082516 FcWV Treasapo Italy 2016	T	A	T	A	T	A	T	A	T	A	T	A	T	A	T	A	T	A
AB24123 FcWV ChJF03 Japan 2013	T	A	T	A	T	A	T	A	T	A	T	A	T	A	T	A	T	A
AB24121 FcWV MJJF03 Japan 2013	T	A	T	A	T	A	T	A	T	A	T	A	T	A	T	A	T	A
AB24120 FcWV OJF001 Japan 2013	T	A	T	A	T	A	T	A	T	A	T	A	T	A	T	A	T	A
LC034587 FcWV SS3 Japan 2014	T	A	T	A	T	A	T	A	T	A	T	A	T	A	T	A	T	A
LC034586 FcWV SS3 Japan 2014	T	A	T	A	T	A	T	A	T	A	T	A	T	A	T	A	T	A
MS182020 FcWV Zeta Germany 2015	T	A	T	A	T	A	T	A	T	A	T	A	T	A	T	A	T	A
MS182019 FcWV Zeta Germany 2015	T	A	T	A	T	A	T	A	T	A	T	A	T	A	T	A	T	A
MS182098 FcWV Gazdon Germany 2015	T	A	T	A	T	A	T	A	T	A	T	A	T	A	T	A	T	A
MS184531 FcWV CT116 Thailand 2018	T	A	T	A	T	A	T	A	T	A	T	A	T	A	T	A	T	A
MS184530 FcWV CT143 Thailand 2018	T	A	T	A	T	A	T	A	T	A	T	A	T	A	T	A	T	A
MS184531 FcWV CT143 Thailand 2018	T	A	T	A	T	A	T	A	T	A	T	A	T	A	T	A	T	A
MS184531 FcWV ZFO1 Leopard Thailand 2016	T	A	T	A	T	A	T	A	T	A	T	A	T	A	T	A	T	A
MS184531 FcWV ZFO1 Leopard Thailand 2016	T	A	T	A	T	A	T	A	T	A	T	A	T	A	T	A	T	A







## REFERENCES



จุฬาลงกรณ์มหาวิทยาลัย  
**CHULALONGKORN UNIVERSITY**

- Anderson E. 1995. Morbillivirus infections in wildlife (in relation to their population biology and disease control in domestic animals). *Veterinary Microbiology*. 44(2-4): 319-332.
- Appel M, Sheffy B, Percy D and Gaskin J. 1974. Canine distemper virus in domesticated cats and pigs. *American Journal of Veterinary Research*. 35(6): 803-806.
- Appel MJ and Summers BA. 1995. Pathogenicity of morbilliviruses for terrestrial carnivores. *Veterinary microbiology*. 44(2-4): 187-191.
- Appel MJ, Yates RA, Foley GL, Bernstein JJ, Santinelli S, Spelman LH, Miller LD, Arp LH, Anderson M, Barr M and et al. 1994. Canine distemper epizootic in lions, tigers, and leopards in North America. *J Vet Diagn Invest*. 6(3): 277-288.
- Arikawa K, Wachi A, Imura Y, Sutummaporn K, Kai C, Park ES, Morikawa S, Uematsu Y, Yamaguchi T and Furuya T. 2017. Development of an ELISA for serological detection of feline morbillivirus infection. *Arch Virol*. 162(8): 2421-2425.
- Baazizi R, Mahapatra M, Clarke BD, Ait-Oudhia K, Khelef D and Parida S. 2017. Peste des petits ruminants (PPR): A neglected tropical disease in Maghreb region of North Africa and its threat to Europe. *PLoS One*. 12(4): e0175461.
- Balamurugan V, Venkatesan G, Sen A, Annamalai L, Bhanuprakash V and Singh RK. 2010. Recombinant protein-based viral disease diagnostics in veterinary medicine. *Expert Rev Mol Diagn*. 10(6): 731-753.
- Barrett T. 1999. Morbillivirus infections, with special emphasis on morbilliviruses of carnivores. *Veterinary microbiology*. 69(1-2): 3-13.
- Barrett T, Visser IK, Mamaev L, Goatley L, van Bresse MF and Osterhaust AD. 1993. Dolphin and porpoise morbilliviruses are genetically distinct from phocine distemper virus. *Virology*. 193(2): 1010-1012.
- Beineke A, Baumgartner W and Wohlsein P. 2015. Cross-species transmission of canine distemper virus-an update. *One Health*. 1: 49-59.
- Beineke A, Puff C, Seehusen F and Baumgartner W. 2009. Pathogenesis and immunopathology of systemic and nervous canine distemper. *Vet Immunol Immunopathol*. 127(1-2): 1-18.

- Brown CA, Elliott J, Schmiedt CW and Brown SA. 2016. Chronic Kidney Disease in Aged Cats: Clinical Features, Morphology, and Proposed Pathogenesis. *Vet Pathol.* 53(2): 309-326.
- Chaiyasak S, Piewbang C, Rungsipat A and Techangamsuwan S. 2020. Molecular epidemiology and genome analysis of feline morbillivirus in household and shelter cats in Thailand. *BMC Vet Res.* 16(1): 240.
- Chaiyasak S and Techangamsuwan S. 2017. First evidence of Feline morbillivirus detected in sheltered cats in Thailand. *Thai J Vet Med Suppl.* 47: 127-128.
- Chinnakannan SK, Nanda SK and Baron MD. 2013. Morbillivirus v proteins exhibit multiple mechanisms to block type 1 and type 2 interferon signalling pathways. *PLoS One.* 8(2): e57063.
- Choi EJ, Ortega V and Aguilar HC. 2020. Feline Morbillivirus, a New Paramyxovirus Possibly Associated with Feline Kidney Disease. *Viruses.* 12(5).
- Crisi PE, Dondi F, De Luca E, Di Tommaso M, Vasylyeva K, Ferlizza E, Savini G, Luciani A, Malatesta D, Lorusso A and Boari A. 2020. Early Renal Involvement in Cats with Natural Feline Morbillivirus Infection. *Animals (Basel).* 10(5).
- da Fontoura Budaszewski R and von Messling V. 2016. Morbillivirus Experimental Animal Models: Measles Virus Pathogenesis Insights from Canine Distemper Virus. *Viruses.* 8(10).
- Dandekar S, Beebe AM, Barlough J, Phillips T, Elder J, Torten M and Pedersen N. 1992. Detection of feline immunodeficiency virus (FIV) nucleic acids in FIV-seronegative cats. *J Virol.* 66(7): 4040-4049.
- Darold GM, Alfieri AA, Muraro LS, Amude AM, Zanatta R, Yamauchi KC, Alfieri AF and Lunardi M. 2017. First report of feline morbillivirus in South America. *Arch. Virol.* 162(2): 469-475.
- De Luca E, Crisi PE, Di Domenico M, Malatesta D, Vincifori G, Di Tommaso M, Di Guardo G, Di Francesco G, Petrini A, Savini G, Boari A and Lorusso A. 2018. A real-time RT-PCR assay for molecular identification and quantitation of feline morbillivirus RNA from biological specimens. *J. Virol. Methods.* 258: 24-28.
- De Luca E, Crisi PE, Marcacci M, Malatesta D, Di Sabatino D, Cito F, D'Alterio N, Puglia I, Berjaoui S, Colaianni ML, Tinelli A, Ripa P, Vincifori G, Di Teodoro G, Dondi F,

- Savini G, Boari A and Lorusso A. 2020. Epidemiology, pathological aspects and genome heterogeneity of feline morbillivirus in Italy. *Vet. Microbiol.* 240: 108484.
- De Vries RD, Duprex WP and De Swart RL. 2015. Morbillivirus infections: an introduction. Multidisciplinary Digital Publishing Institute.
- Deem SL, Spelman LH, Yates RA and Montali RJ. 2000. Canine distemper in terrestrial carnivores: A review. *Journal of Zoo and Wildlife Medicine.* 31(4): 441-451.
- Delpeut S, Noyce RS and Richardson CD. 2014. The Tumor-Associated Marker, PVRL4 (Nectin-4), Is the Epithelial Receptor for Morbilliviruses. *Viruses-Basel.* 6(6): 2268-2286.
- Denzin N, Herwig V and van der Grinten E. 2013. Occurrence and geographical distribution of Canine Distemper Virus infection in red foxes (*Vulpes vulpes*) of Saxony-Anhalt, Germany. *Vet Microbiol.* 162(1): 214-218.
- Donato G, De Luca E, Crisi PE, Pizzurro F, Masucci M, Marcacci M, Cito F, Di Sabatino D, Boari A, D'Alterio N, Pennisi MG and Lorusso A. 2019. Isolation and genome sequences of two Feline Morbillivirus genotype 1 strains from Italy. *Vet. ital.* 55(2): 179-182.
- Fukuhara H, Ito Y, Sako M, Kajikawa M, Yoshida K, Seki F, Mwaba MH, Hashiguchi T, Higashibata MA, Ose T, Kuroki K, Takeda M and Maenaka K. 2019. Specificity of Morbillivirus Hemagglutinins to Recognize SLAM of Different Species. *Viruses.* 11(8).
- Furuse Y and Oshitani H. 2017. Global Transmission Dynamics of Measles in the Measles Elimination Era. *Viruses-Basel.* 9(4).
- Furuya T, Sassa Y, Omatsu T, Nagai M, Fukushima R, Shibutani M, Yamaguchi T, Uematsu Y, Shirota K and Mizutani T. 2014. Existence of feline morbillivirus infection in Japanese cat populations. *Arch. Virol.* 159(2): 371-373.
- Greene JP, Lefebvre SL, Wang M, Yang M, Lund EM and Polzin DJ. 2014. Risk factors associated with the development of chronic kidney disease in cats evaluated at primary care veterinary hospitals. *J Am Vet Med Assoc.* 244(3): 320-327.

- Griot C, Vandeveld M, Schobesberger M and Zurbriggen A. 2003. Canine distemper, a re-emerging morbillivirus with complex neuropathogenic mechanisms. *Anim Health Res Rev.* 4(1): 1-10.
- Gualandi-Signorini AM and Giorgi G. 2001. Insulin formulations--a review. *Eur Rev Med Pharmacol Sci.* 5(3): 73-83.
- Guardo GD, Marruchella G, Agrimi U and Kennedy S. 2005. Morbillivirus infections in aquatic mammals: a brief overview. *Journal of Veterinary Medicine Series A.* 52(2): 88-93.
- Ikeda Y, Nakamura K, Miyazawa T, Chen MC, Kuo TF, Lin JA, Mikami T, Kai C and Takahashi E. 2001. Seroprevalence of canine distemper virus in cats. *Clin Diagn Lab Immunol.* 8(3): 641-644.
- Jepson RE. 2016. Current Understanding of the Pathogenesis of Progressive Chronic Kidney Disease in Cats. *Vet Clin North Am Small Anim Pract.* 46(6): 1015-1048.
- Ke GM, Ho CH, Chiang MJ, Sanno-Duanda B, Chung CS, Lin MY, Shi YY, Yang MH, Tyan YC, Liao PC and Chu PY. 2015. Phylodynamic analysis of the canine distemper virus hemagglutinin gene. *BMC Vet. Res.* 11: 164.
- Koide R, Sakaguchi S and Miyazawa T. 2015. Basic biological characterization of feline morbillivirus. *J Vet Med Sci.* 77(5): 565-569.
- Ksiazek TG, Erdman D, Goldsmith CS, Zaki SR, Peret T, Emery S, Tong S, Urbani C, Comer JA, Lim W, Rollin PE, Dowell SF, Ling AE, Humphrey CD, Shieh WJ, Guarner J, Paddock CD, Rota P, Fields B, DeRisi J, Yang JY, Cox N, Hughes JM, LeDuc JW, Bellini WJ, Anderson LJ and Group SW. 2003. A novel coronavirus associated with severe acute respiratory syndrome. *N Engl J Med.* 348(20): 1953-1966.
- Lamb RA. 2001. Paramyxoviridae: the viruses and their replication. *Fields virology.*
- Lehmbecker A, Rittinghausen S, Rohn K, Baumgartner W and Schaudien D. 2014. Nanoparticles and pop-off technique for electron microscopy: a known technique for a new purpose. *Toxicol Pathol.* 42(6): 1041-1046.
- Lempp C, Spitzbarth I, Puff C, Cana A, Kegler K, Techangamsuwan S, Baumgartner W and Seehusen F. 2014. New aspects of the pathogenesis of canine distemper leukoencephalitis. *Viruses.* 6(7): 2571-2601.

- Loots AK, Mitchell E, Dalton DL, Kotze A and Venter EH. 2017. Advances in canine distemper virus pathogenesis research: a wildlife perspective. *J Gen Virol.* 98(3): 311-321.
- Lorusso A, Di Tommaso M, Di Felice E, Zaccaria G, Luciani A, Marcacci M, Aste G, Boari A and Savini G. 2015. First report of feline morbillivirus in Europe. *Vet Ital.* 51(3): 235-237.
- Ludes-Wehrmeister E, Dupke C, Harder TC, Baumgartner W, Haas L, Teilmann J, Dietz R, Jensen LF and Siebert U. 2016. Phocine distemper virus (PDV) seroprevalence as predictor for future outbreaks in harbour seals. *Vet Microbiol.* 183: 43-49.
- Mahapatra M, Parida S, Baron M and Barrett T. 2006. Matrix protein and glycoproteins F and H of Peste-des-petits-ruminants virus function better as a homologous complex. *Journal of General Virology.* 87(7): 2021-2029.
- Marcacci M, De Luca E, Zaccaria G, Di Tommaso M, Mangone I, Aste G, Savini G, Boari A and Lorusso A. 2016. Genome characterization of feline morbillivirus from Italy. *J. Virol. Methods.* 234: 160-163.
- Martin DP, Murrell B, Golden M, Khoosal A and Muhire B. 2015. RDP4: Detection and analysis of recombination patterns in virus genomes. *Virus Evol.* 1(1): vev003.
- Martinez-Gutierrez M and Ruiz-Saenz J. 2016. Diversity of susceptible hosts in canine distemper virus infection: a systematic review and data synthesis. *BMC Vet Res.* 12: 78.
- McCallum KE, Stubbs S, Hope N, Mickleburgh I, Dight D, Tiley L and Williams TL. 2018. Detection and seroprevalence of morbillivirus and other paramyxoviruses in geriatric cats with and without evidence of azotemic chronic kidney disease. *J. Vet. Intern.* 32(3): 1100-1108.
- McCarthy AJ, Shaw MA and Goodman SJ. 2007. Pathogen evolution and disease emergence in carnivores. *Proc Biol Sci.* 274(1629): 3165-3174.
- Metz CE. 1978. Basic principles of ROC analysis. *Seminars in nuclear medicine.* P 283-298.

- Mochizuki M, Horiuchi M, Hiragi H, San Gabriel MC, Yasuda N and Uno T. 1996. Isolation of canine parvovirus from a cat manifesting clinical signs of feline panleukopenia. *J Clin Microbiol.* 34(9): 2101-2105.
- Mohd Isa NH, Selvarajah GT, Khor KH, Tan SW, Manoraj H, Omar NH, Omar AR and Mustaffa-Kamal F. 2019. Molecular detection and characterisation of feline morbillivirus in domestic cats in Malaysia. *Vet. Microbiol.* 236: 108382.
- Ohishi K, Suzuki R, Maeda T, Tsuda M, Abe E, Yoshida T, Endo Y, Okamura M, Nagamine T, Yamamoto H, Ueda M and Maruyama T. 2014. Recent host range expansion of canine distemper virus and variation in its receptor, the signaling lymphocyte activation molecule, in carnivores. *J Wildl Dis.* 50(3): 596-606.
- Overton TW. 2014. Recombinant protein production in bacterial hosts. *Drug Discov Today.* 19(5): 590-601.
- Park ES, Suzuki M, Kimura M, Maruyama K, Mizutani H, Saito R, Kubota N, Furuya T, Mizutani T, Imaoka K and Morikawa S. 2014. Identification of a natural recombination in the F and H genes of feline morbillivirus. *Virology.* 468-470: 524-531.
- Park ES, Suzuki M, Kimura M, Mizutani H, Saito R, Kubota N, Hasuike Y, Okajima J, Kasai H, Sato Y, Nakajima N, Maruyama K, Imaoka K and Morikawa S. 2016. Epidemiological and pathological study of feline morbillivirus infection in domestic cats in Japan. *BMC Vet. Res.* 12(1): 228.
- Piewbang C, Chaiyasak S, Kongmakee P, Sanannu S, Khotapat P, Ratthanophart J, Banlunara W and Techangamsuwan S. 2020a. Feline Morbillivirus Infection Associated With Tubulointerstitial Nephritis in Black Leopards (*Panthera pardus*). *Vet Pathol.* 300985820948820.
- Piewbang C, Chansaenroj J, Kongmakee P, Banlunara W, Poovorawan Y and Techangamsuwan S. 2020b. Genetic Adaptations, Biases, and Evolutionary Analysis of Canine Distemper Virus Asia-4 Lineage in a Fatal Outbreak of Wild-Caught Civets in Thailand. *Viruses.* 12(4).
- Piewbang C, Jo WK, Puff C, Ludlow M, van der Vries E, Banlunara W, Rungsipipat A, Kruppa J, Jung K, Techangamsuwan S, Baumgartner W and Osterhaus A. 2018.



- Canine Bocavirus Type 2 Infection Associated With Intestinal Lesions. *Vet Pathol.* 55(3): 434-441.
- Piewbang C, Kasantikul T, Pringproa K and Techangamsuwan S. 2019a. Feline bocavirus-1 associated with outbreaks of hemorrhagic enteritis in household cats: potential first evidence of a pathological role, viral tropism and natural genetic recombination. *Sci. Rep.* 9(1): 16367.
- Piewbang C, Radtanakantikanon A, Puenpa J, Poovorawan Y and Techangamsuwan S. 2019b. Genetic and evolutionary analysis of a new Asia-4 lineage and naturally recombinant canine distemper virus strains from Thailand. *Sci Rep.* 9(1): 3198.
- Piewbang C, Rungsipipat A, Poovorawan Y and Techangamsuwan S. 2017. Development and application of multiplex PCR assays for detection of virus-induced respiratory disease complex in dogs. *J Vet Med Sci.* 78(12): 1847-1854.
- Piewbang C and Techangamsuwan S. 2019. Phylogenetic evidence of a novel lineage of canine pneumovirus and a naturally recombinant strain isolated from dogs with respiratory illness in Thailand. *BMC Vet Res.* 15(1): 300.
- Pond SL and Frost SD. 2005. Datamonkey: rapid detection of selective pressure on individual sites of codon alignments. *Bioinformatics.* 21(10): 2531-2533.
- Pratakpiriya W, Ping Teh AP, Radtanakantikanon A, Pirarat N, Thi Lan N, Takeda M, Techangamsuwan S and Yamaguchi R. 2017. Expression of canine distemper virus receptor nectin-4 in the central nervous system of dogs. *Sci Rep.* 7(1): 349.
- Pratakpiriya W, Seki F, Otsuki N, Sakai K, Fukuhara H, Katamoto H, Hirai T, Maenaka K, Techangamsuwan S, Lan NT, Takeda M and Yamaguchi R. 2012. Nectin4 is an epithelial cell receptor for canine distemper virus and involved in neurovirulence. *J Virol.* 86(18): 10207-10210.
- Pusoonthornthum R, Pusoonthornthum P and Krishnamra N. 2010. Calcium-phosphorus homeostasis and changes in parathyroid hormone secretion in cats with various stages of spontaneous chronic renal failure. *Comparative clinical pathology.* 19(3): 287-293.

- Radtanakatikanon A, Keawcharoen J, Charoenvisal NT, Poovorawan Y, Prompetchara E, Yamaguchi R and Techangamsuwan S. 2013. Genotypic lineages and restriction fragment length polymorphism of canine distemper virus isolates in Thailand. *Vet Microbiol.* 166(1-2): 76-83.
- Rima BK and Duprex WP. 2006. Morbilliviruses and human disease. *J Pathol.* 208(2): 199-214.
- Roelke-Parker ME, Munson L, Packer C, Kock R, Cleaveland S, Carpenter M, O'Brien SJ, Pospischil A, Hofmann-Lehmann R, Lutz H, Mwamengele GL, Mgasa MN, Machange GA, Summers BA and Appel MJ. 1996. A canine distemper virus epidemic in Serengeti lions (*Panthera leo*). *Nature.* 379(6564): 441-445.
- Sakaguchi S, Koide R and Miyazawa T. 2015. In vitro host range of feline morbillivirus. *J. Vet. Med. Sci.* 77(11): 1485-1487.
- Sakaguchi S, Nakagawa S, Yoshikawa R, Kuwahara C, Hagiwara H, Asai K, Kawakami K, Yamamoto Y, Ogawa M and Miyazawa T. 2014. Genetic diversity of feline morbilliviruses isolated in Japan. *J Gen Virol.* 95(Pt 7): 1464-1468.
- Sato H, Yoneda M, Honda T and Kai C. 2012. Morbillivirus receptors and tropism: multiple pathways for infection. *Front Microbiol.* 3: 75.
- Schobesberger M, Summerfield A, Doherr MG, Zurbriggen A and Griot C. 2005. Canine distemper virus-induced depletion of uninfected lymphocytes is associated with apoptosis. *Vet Immunol Immunopathol.* 104(1-2): 33-44.
- Seimon TA, Miquelle DG, Chang TY, Newton AL, Korotkova I, Ivanchuk G, Lyubchenko E, Tupikov A, Slabe E and McAloose D. 2013. Canine distemper virus: an emerging disease in wild endangered Amur tigers (*Panthera tigris altaica*). *mBio.* 4(4).
- Shaila MS, Shamaki D, Forsyth MA, Diallo A, Goatley L, Kitching RP and Barrett T. 1996. Geographic distribution and epidemiology of peste des petits ruminants virus. *Virus Res.* 43(2): 149-153.
- Sharp CR, Nambulli S, Acciardo AS, Rennick LJ, Drexler JF, Rima BK, Williams T and Duprex WP. 2016. Chronic Infection of Domestic Cats with Feline Morbillivirus, United States. *Emerg. Infect. Dis.* 22(4): 760-762.

- Sieg M, Busch J, Eschke M, Bottcher D, Heenemann K, Vahlenkamp A, Reinert A, Seeger J, Heilmann R, Scheffler K and Vahlenkamp TW. 2019. A New Genotype of Feline Morbillivirus Infects Primary Cells of the Lung, Kidney, Brain and Peripheral Blood. *Viruses*. 11(2).
- Sieg M, Heenemann K, Ruckner A, Burgener I, Oechtering G and Vahlenkamp TW. 2015. Discovery of new feline paramyxoviruses in domestic cats with chronic kidney disease. *Virus Genes*. 51(2): 294-297.
- Sieg M, Vahlenkamp A, Baums CG and Vahlenkamp TW. 2018. First Complete Genome Sequence of a Feline Morbillivirus Isolate from Germany. *Genome Announc*. 6(16).
- Singethan K, Muller N, Schubert S, Luttge D, Kremmentsov DN, Khurana SR, Krohne G, Schneider-Schaulies S, Thali M and Schneider-Schaulies J. 2008. CD9 clustering and formation of microvilli zippers between contacting cells regulates virus-induced cell fusion. *Traffic*. 9(6): 924-935.
- Singethan K, Topfstedt E, Schubert S, Duprex WP, Rima BK and Schneider-Schaulies J. 2006. CD9-dependent regulation of Canine distemper virus-induced cell-cell fusion segregates with the extracellular domain of the haemagglutinin. *J Gen Virol*. 87(Pt 6): 1635-1642.
- Stranieri A, Lauzi S, Dallari A, Gelain ME, Bonsembiante F, Ferro S and Paltrinieri S. 2019. Feline morbillivirus in Northern Italy: prevalence in urine and kidneys with and without renal disease. *Vet. Microbiol*. 233: 133-139.
- Sulikhan NS, Gilbert M, Blidchenko EY, Naidenko SV, Ivanchuk GV, Gorpenchenko TY, Alshinetskiy MV, Shevtsova EI, Goodrich JM, Lewis JCM, Goncharuk MS, Uphyrkina OV, Rozhnov VV, Shedko SV, McAloose D, Miquelle DG and Seimon TA. 2018. Canine Distemper Virus in a Wild Far Eastern Leopard ( *Panthera Pardus Orientalis*). *J Wildl Dis*. 54(1): 170-174.
- Sutummaporn K, Suzuki K, Machida N, Mizutani T, Park ES, Morikawa S and Furuya T. 2019. Association of feline morbillivirus infection with defined pathological changes in cat kidney tissues. *Vet. Microbiol*. 228: 12-19.

- Takeda M, Seki F, Yamamoto Y, Nao N and Tokiwa H. 2020. Animal morbilliviruses and their cross-species transmission potential. *Current Opinion in Virology*. 41: 38-45.
- Tandon R, Cattori V, Gomes-Keller MA, Meli ML, Golder MC, Lutz H and Hofmann-Lehmann R. 2005. Quantitation of feline leukaemia virus viral and proviral loads by TaqMan real-time polymerase chain reaction. *J Virol Methods*. 130(1-2): 124-132.
- Tatsuo H, Ono N and Yanagi Y. 2001. Morbilliviruses use signaling lymphocyte activation molecules (CD150) as cellular receptors. *J Virol*. 75(13): 5842-5850.
- Techangamsuwan S, Banlunara W, Radtanakantikanon A, Sommanustweechai A, Siritaroonrat B, Lombardini ED and Rungsipipat A. 2015. Pathologic and Molecular Virologic Characterization of a Canine Distemper Outbreak in Farmed Civets. *Vet Pathol*. 52(4): 724-731.
- Tong S, Chern SW, Li Y, Pallansch MA and Anderson LJ. 2008. Sensitive and broadly reactive reverse transcription-PCR assays to detect novel paramyxoviruses. *J Clin Microbiol*. 46(8): 2652-2658.
- VanDevanter DR, Warrener P, Bennett L, Schultz ER, Coulter S, Garber RL and Rose TM. 1996. Detection and analysis of diverse herpesviral species by consensus primer PCR. *J Clin Microbiol*. 34(7): 1666-1671.
- Vandevelde M and Zurbriggen A. 2005. Demyelination in canine distemper virus infection: a review. *Acta Neuropathol*. 109(1): 56-68.
- von Messling V, Zimmer G, Herrler G, Haas L and Cattaneo R. 2001. The hemagglutinin of canine distemper virus determines tropism and cytopathogenicity. *J Virol*. 75(14): 6418-6427.
- Woo PC, Lau SK, Wong BH, Fan RY, Wong AY, Zhang AJ, Wu Y, Choi GK, Li KS, Hui J, Wang M, Zheng BJ, Chan KH and Yuen KY. 2012. Feline morbillivirus, a previously undescribed paramyxovirus associated with tubulointerstitial nephritis in domestic cats. *PNAS USA*. 109(14): 5435-5440.
- Yanagi Y, Takeda M and Ohno S. 2006. Measles virus: cellular receptors, tropism and pathogenesis. *J Gen Virol*. 87(Pt 10): 2767-2779.

- Yang WC, Wu BJ, Sierra E, Fernandez A, Groch KR, Catao-Dias JL, West K and Chan KW. 2016. A simultaneous diagnosis and genotyping method for global surveillance of cetacean morbillivirus. *Sci Rep.* 6: 30625.
- Yilmaz H, Tekelioglu BK, Gurel A, Bamac OE, Ozturk GY, Cizmecigil UY, Altan E, Aydin O, Yilmaz A, Berriatua E, Helps CR, Richt JA and Turan N. 2017. Frequency, clinicopathological features and phylogenetic analysis of feline morbillivirus in cats in Istanbul, Turkey. *J. Feline. Med. Surg.* 19(12): 1206-1214.
- Yuan C, Liu W, Wang Y, Hou J, Zhang L and Wang G. 2017. Homologous recombination is a force in the evolution of canine distemper virus. *PLoS One.* 12(4): e0175416.



## VITA

**NAME** Surangkanang Chaiyasak

**DATE OF BIRTH** 05 April 1986

**PLACE OF BIRTH** Maha Sarakham

**INSTITUTIONS ATTENDED** M.Sc. (Pathobiology) Chulalongkorn University  
D.V.M. Khonkaen University

**HOME ADDRESS** 92 Moo 10 Thakhonyang, Kantarawichai, Maha Sarakham 44150

**PUBLICATION** (Poster presentation) Incidence of feline morbillivirus in Hematuric cats, FECAVA 2019  
(Poster presentation) Development of Indirect ELISA for Detection of Feline Morbillivirus, CUVC 2018  
(Poster presentation) The Detection of Feline morbillivirus antibody based on Matrix Recombinant Protein by indirect ELISA in Thailand , ASVP 2017  
(Poster presentation) First evidence of feline morbillivirus detected in shelter cats in Thailand, CUVC 2017  
(Publication) Molecular epidemiology and genome analysis of feline morbillivirus in household and shelter cats in Thailand, Journal: BMC Veterinary Research  
(Publication) Feline morbillivirus infection associated with tubulointerstitial nephritis in black leopards (Panthera pardus), Journal: Veterinary Pathology

**AWARD RECEIVED** (Poster presentation) 2017: Honorable mention prize in the field of microbiology awarded to the topic "First evidence of feline morbillivirus detected in shelter cats in Thailand"